Smoking-gun signatures of little Higgs models

Tao Han[1,2]**, Heather E. Logan**[1] **and Lian-Tao Wang**[1,3]

[1] *Department of Physics, University of Wisconsin, Madison, Wisconsin 53706 USA*

[2] *Institute of Theoretical Physics, Academia Sinica, Beijing 100080, China*

[3] *Jefferson Laboratory of Physics, Harvard University, Cambridge, Massachusetts 02138 USA*

E-mail: than@physics.wisc.edu, logan@physics.wisc.edu, liantaow@schwinger.harvard.edu

ABSTRACT: Little Higgs models predict new gauge bosons, fermions and scalars at the TeV scale that stabilize the Higgs mass against quadratically divergent one-loop radiative corrections. We categorize the many little Higgs models into two classes based on the structure of the extended electroweak gauge group and examine the experimental signatures that identify the little Higgs *mechanism* in addition to those that identify the particular little Higgs *model*. We find that by examining the properties of the new heavy fermion(s) at the LHC, one can distinguish the structure of the top quark mass generation mechanism and test the little Higgs mechanism in the top sector. Similarly, by studying the couplings of the new gauge bosons to the light Higgs boson and to the Standard Model fermions, one can confirm the little Higgs mechanism and determine the structure of the extended electroweak gauge group.

Contents

1. Introduction

Elucidating the mechanism of electroweak symmetry breaking (EWSB) is the central goal of particle physics today. A full understanding of EWSB will include a solution to the hierarchy or naturalness problem – that is, why the weak scale is so much lower than the Planck scale. Whatever is responsible for EWSB and its hierarchy, it must manifest experimentally at or below the TeV energy scale.

A wide variety of models have been introduced over the past three decades to address EWSB and the hierarchy problem: supersymmetry, extra dimensions, strong dynamics leading to a composite Higgs boson, and the recent "little Higgs" models [1, 2, 3, 4, 5, 6, 7, 8, 9] in which the Higgs is a pseudo-Goldstone boson. In this paper we consider this last possibility.

In the little Higgs models, the Standard Model (SM) Higgs doublet appears as a pseudo-Goldstone boson of an approximate global symmetry that is spontaneously broken at the TeV scale. The low energy degrees of freedom are described by nonlinear sigma models, with a cutoff at an energy scale one loop factor above the spontaneous symmetry breaking scale. Thus the little Higgs models require an ultraviolet (UV) completion [10, 11] at roughly the 10 TeV scale.

The explicit breaking of the global symmetry, by gauge, Yukawa and scalar interactions, gives the Higgs a mass and non-derivative interactions, as required of the SM Higgs doublet. The little Higgs models are constructed in such a way that no *single* interaction breaks *all* of the symmetry forbidding a mass term for the SM Higgs doublet. This collective symmetry breaking guarantees the cancellation of the one-loop quadratically divergent radiative corrections to the Higgs boson mass. Quadratic sensitivity of the Higgs mass to the cutoff scale then arises only at the *two*-loop level, so that a Higgs mass at the 100 GeV scale, two loop factors below the 10 TeV cutoff, is natural. Little Higgs models can thus stabilize the "little hierarchy" between the electroweak scale and the 10 TeV scale at which strongly-coupled new physics is allowed by electroweak precision constraints.

Little Higgs models contain new gauge bosons, a heavy top-like quark, and new scalars, which cancel the quadratically divergent one-loop contributions to the Higgs boson mass from the SM gauge bosons, top quark, and Higgs self-interaction, respectively. Thus the "smoking gun" feature of the little Higgs mechanism is the existence of these new gauge bosons, heavy top-like quark, and new scalars, with the appropriate couplings to the Higgs boson to cancel the one-loop quadratic divergence.

Since the little Higgs idea was introduced [1], many explicit models [2, 3, 4, 5, 6, 7, 8, 9] have been constructed. Since the little Higgs idea could be implemented in a number of ways, it is crucial to pick out the experimental signatures that identify the little Higgs *mechanism* in addition to those that identify the particular little Higgs *model*. Detailed phenomenological [12, 13, 14] and experimental [15, 16] studies of little Higgs physics at the CERN Large Hadron Collider (LHC) have so far been carried out only within the "Littlest Higgs" model [3].[1] Fortunately, this effort need not be repeated for each of the many little Higgs models, because the models can be grouped into two classes that share many phenomenological features, including the crucial "smoking gun" signatures that identify the little Higgs mechanism.

In this paper we categorize the little Higgs models into two classes based on the structure of the extended electroweak gauge group: models in which the SM $SU(2)_L$ gauge group arises from the diagonal breaking of two or more gauge groups, called "product group" models [1, 2, 3, 4, 6, 8], and models in which the SM $SU(2)_L$ gauge group arises from the breaking of a single larger gauge group down to an $SU(2)$ subgroup, called "simple group" models [5, 7, 9]. (This categorization and nomenclature was introduced in Ref. [5].) These two classes of models also exhibit an important difference in the implementation of the little Higgs mechanism in the fermion sector. As representatives of the two classes, we study the Littlest Higgs model [3] and the $SU(3)$ simple group model [5, 9], respectively. We find that by examining the properties of the new heavy fermion(s), one can distinguish the structure of the top quark mass generation mechanism and test the little Higgs mechanism in the top sector. Furthermore, by measuring the couplings of the new TeV-scale gauge bosons to the Higgs, SM gauge bosons, and fermions, one can determine the gauge structure of the extended theory and test the little Higgs mechanism in the gauge sector. To emphasize the "smoking gun" nature of the signals, we also compare our results with other models that give rise to similar signatures. For the heavy top partner, we compare the little Higgs signatures with the signatures of a fourth generation top-prime and of the top quark see-saw model. For the TeV-scale gauge bosons, we compare with the Z' signatures in E_6, left-right symmetric, and sequential Z' models. In each case, we point out the features of the little Higgs model that distinguish it from competing interpretations.

The rest of this paper is organized as follows. In the next section we describe the basic features of the two representative models. Specific little Higgs models that fall into each of the two classes are surveyed in Appendix A. In Sec. 3, we discuss the top quark mass generation and the quadratic divergence cancellation mechanism in the two classes of models, describe the resulting differences in phenomenology, and show how to test the little

---

[1]The LHC phenomenology of the Littlest Higgs model with T-parity [17, 18, 19] was studied in Ref. [20]; models with T-parity will be briefly discussed in Sec. 2.

Higgs mechanism in the top sector. We also comment on the phenomenological differences between little Higgs models and other models with extended top sectors. In Sec. 4, we discuss the gauge sectors in the two classes of models and identify features common to the models in each class. We discuss techniques for determining the structure of the extended gauge sector and for testing the little Higgs mechanism in the gauge sector. In Sec. 5 we collect some additional features of the phenomenology of the SU(3) simple group model. We conclude in Sec. 6. Technical details of the SU(3) simple group model are given in Appendix B.

2. Two classes of little Higgs models

If the little Higgs mechanism is realized in nature, it will be of ultimate importance to verify it at the LHC, by discovering the predicted new particles and determining their specific couplings to the SM fields that guarantee the cancellation of the Higgs mass quadratic divergence. The most important characteristics of implementations of the little Higgs idea are (i) the structure of the extended gauge symmetry and its breaking pattern, and (ii) the treatment of the new heavy fermion sector necessary to cancel the Higgs mass quadratic divergence coming from the top quark. As we will see, the distinctive features of both the gauge and top sectors of little Higgs models separate naturally into the product group and simple group classes.

The majority of little Higgs models are product group models. In addition to the Littlest Higgs, these include the theory space models (the Big Moose [1] and the Minimal Moose [2]), the SU(6)/Sp(6) model of Ref. [4], and two extensions of the Littlest Higgs with built-in custodial SU(2) symmetry [6, 8]. The product group models have the following generic features. First, the models all contain a set of SU(2) gauge bosons at the TeV scale, obtained from the diagonal breaking of two or more gauge groups down to $SU(2)_L$, and thus contain free parameters in the gauge sector from the independent gauge couplings. Second, since the collective symmetry breaking in the gauge sector is achieved by multiple gauged subgroups of the global symmetry, models can be built in which the SM Higgs doublet is embedded within a single non-linear sigma model field; many product group models make this simple choice. Third, the fermion sector of this class of models can usually be chosen to be very simple, involving only a single new vector-like quark.

The simplest incarnation of the product group class is the so-called Littlest Higgs model [3], which we briefly review here. It features a $[SU(2) \times U(1)]^2$ gauge symmetry[2] embedded in an SU(5) global symmetry. The gauge symmetry is broken by a single vacuum condensate $f \sim$ TeV down to the SM $SU(2)_L \times U(1)_Y$ gauge symmetry. The SM Higgs doublet is contained in the resulting Goldstone bosons, whose interactions are parameterized by a nonlinear sigma model. The gauge and Yukawa couplings radiatively generate a Higgs potential and trigger EWSB.

---

[2]Strictly speaking, it is not necessary to gauge two factors of U(1) in order to stablize the little hierarchy, because the hypercharge gauge coupling is rather small and does not contribute significantly to the Higgs mass quadratic divergence below a scale of several TeV. Thus, there is an alternate version of the Littlest Higgs model [21] in which only $SU(2)^2 \times U(1)_Y$ is gauged.

The new heavy quark sector in the Littlest Higgs model consists of a pair of vectorlike SU(2)-singlet quarks that couple to the top sector. The Lagrangian is

$$\mathcal{L}_Y = \frac{i}{2}\lambda_1 f \epsilon_{ijk}\epsilon_{xy}\chi_i \Sigma_{jx}\Sigma_{ky}u_3'^c + \lambda_2 f \tilde{t}\tilde{t}'^c + \text{h.c.,} \tag{2.1}$$

where $\chi_i = (b_3, t_3, i\tilde{t})$ and the factors of i in Eq. (2.1) and χ_i are inserted to make the masses and mixing angles real. The summation indices are $i, j, k = 1, 2, 3$ and $x, y = 4, 5$, and ϵ_{ijk}, ϵ_{xy} are antisymmetric tensors. The vacuum expectation value (vev) $\langle\Sigma\rangle \equiv \Sigma_0$ marries $\tilde{t}$ to a linear combination of $u_3'^c$ and $\tilde{t}'^c$, giving it a mass of order $f \sim$ TeV. The resulting new charge $2/3$ quark T is an isospin singlet up to its small mixing with the SM top quark (generated after EWSB). The orthogonal linear combination of $u_3'^c$ and $\tilde{t}'^c$ becomes the right-handed top quark and marries t_3. The scalar interactions of the up-type quarks of the first two generations can be chosen to take the same form as Eq. (2.1), except that there is no need for an extra $\tilde{t}$, $\tilde{t}'^c$ since the contribution to the Higgs mass quadratic divergence from quarks other than top is numerically insignificant below the nonlinear sigma model cutoff $\Lambda \sim 4\pi f \sim 10$ TeV.

In contrast, the simple group models share two features that distinguish them from the product group models. First, the simple group models all contain an SU(N)×U(1) gauge symmetry that is broken down to SU(2)$_L$×U(1)$_Y$, yielding a set of TeV-scale gauge bosons. The two gauge couplings of the SU(N)×U(1) are fixed in terms of the two SM SU(2)$_L$×U(1)$_Y$ gauge couplings, leaving no free parameters in the gauge sector once the symmetry-breaking scale is fixed. This gauge structure also forbids mixing between the SM $W^\pm$ bosons and the TeV-scale gauge bosons, again in contrast to the product group models. Second, in order to implement the collective symmetry breaking, simple-group models require at least two sigma-model multiplets. The SM Higgs doublet is embedded as a linear combination of the Goldstone bosons from these multiplets. This introduces at least one additional model parameter, which can be chosen as the ratio of the vevs of the sigma-model multiplets. Moreover, due to the enlarged SU(N) gauge symmetry, all SM fermion representations have to be extended to transform as fundamental (or antifundamental) representations of SU(N), giving rise to additional heavy fermions in all three generations. The existence of multiple sigma-model multiplets generically results in a more complicated structure for the fermion couplings to scalars. On the other hand, the existence of heavy fermion states in all three generations as required by the enlarged gauge symmetry provides extra experimental observables that in principle allow one to disentangle this more complicated structure.

The simplest incarnation of the simple group class is the SU(3) simple group model [5, 9]. We briefly review its construction here; additional details are presented in Appendix B. The electroweak gauge structure is SU(3)×U(1)$_X$. There are two sigma-model fields, Φ_1 and Φ_2, transforming as **3**s under SU(3). Vacuum condensates $\langle\Phi_{1,2}\rangle = (0, 0, f_{1,2})^T$ break SU(3)×U(1)$_X$ down to the SM SU(2)$_L$×U(1)$_Y$. The TeV-scale gauge sector consists of an SU(2)$_L$ doublet (Y^0, X^-) of gauge bosons corresponding to the broken off-diagonal generators of SU(3), and a Z' gauge boson corresponding to the broken linear combination

of the T^8 generator of SU(3) and the U(1)$_X$. The model also contains a singlet pseudoscalar η.

The top quark mass is generated by the Lagrangian

$$\mathcal{L}_Y = i\lambda_1^t u_1^c \Phi_1^\dagger Q_3 + i\lambda_2^t u_2^c \Phi_2^\dagger Q_3, \tag{2.2}$$

where $Q_3^T = (t, b, iT)$ and the factors of i in Eq. (2.2) and Q_3 are again inserted to make the masses and mixing angles real. The Φ vevs marry T to a linear combination of u_1^c and u_2^c, giving it a mass of order $f \sim$ TeV. The new charge 2/3 quark T is a singlet under SU(2)$_L$ up to its small mixing with the SM top quark (generated after EWSB). The orthogonal linear combination of u_1^c and u_2^c becomes the right-handed top quark. For the rest of the quarks, the scalar interactions depend on the choice of their embedding into SU(3). The most straightforward choice is to embed all three generations in a universal way, $Q_m^T = (u, d, iU)_m$, so that each quark generation contains a new heavy charge 2/3 quark. This embedding leaves the SU(3) and U(1)$_X$ gauge groups anomalous; the anomalies can be canceled by adding new spectator fermions at the cutoff scale $\Lambda \sim 4\pi f$. An alternate, anomaly-free embedding [22] puts the quarks of the first two generations into antifundamentals of SU(3), $Q_m^T = (d, -u, iD)_m$, with $m = 1, 2$, so that the first two quark generations each contain a new heavy charge $-1/3$ quark. Interestingly, an anomaly-free embedding of the SM fermions into SU(3)$_c$×SU(3)×U(1)$_X$ is only possible if the number of generations is a multiple of three [22, 23].[3]

Electroweak precision observables provide strong constraints on any extensions of the SM. The constraints on the little Higgs models have been studied extensively [21, 25, 26, 27, 28, 29, 30]. Of course, any phenomenological study of a particular model must take these constraints into account. However, in this paper we study the generic phenomenology of classes of little Higgs models, using specific models only as prototypes. We focus on features of the phenomenology that are expected to persist in all models within a given class, in spite of variations in the model that can give rise to very different constraints from electroweak precision observables. For exmaple, variations of the model that improve the electroweak fit will not in general change the generic features of the new heavy top-partner phenomenology. Thus, in order to maintain applicability to a wide range of models in each class, we will not limit our presentation of results to the parameter space allowed by electroweak precision fits in the specific models under consideration.

For completeness, we now briefly summarize the results of electroweak precision fits in the models under consideration. The most up-to-date studies are Refs. [28, 29, 30], which include LEP-2 data above the Z pole. In most little Higgs models, particularly the product group models, the electroweak data mostly set lower bounds on the masses of the heavy vector bosons due to their contributions to four-Fermi operators and their mixing with the W and Z bosons. On the other hand, the most important contributions to the Higgs mass quadratic divergence cancellation come from the top quark partner T, which should be as light as possible to minimize the fine-tuning. These competing desires dictate the favored parameter regions of the little Higgs models.

---

[3]This rule can be violated in models containing fermion generations with non-SM quantum numbers, e.g., mirror families [24].

- *Littlest Higgs model:* The Littlest Higgs model with $[\mathrm{SU}(2)\times\mathrm{U}(1)]^2$ gauged contains a new U(1) boson, A_H, which is relatively light and tends to give rise to large corrections to electroweak precision observables. Assigning the fermions to transform under $\mathrm{SU}(2)_1$ and $\mathrm{U}(1)_1$ only, Ref. [29] finds a stringent constraint $f \geq 5$ TeV. However, allowing the fermions to transform under both U(1) groups (as required in order to write down gauge invariant Yukawa couplings in a straightforward way) tends to reduce this constraint; Refs. [21, 25], which do not include LEP-2 data in their fit, found the constraint on f reduced from 4 TeV to about 1 TeV; similarly, Ref. [29] found the constraint reduced from 5 TeV to about 2–3 TeV. Gauging only $\mathrm{SU}(2)^2\times\mathrm{U}(1)_Y$, Ref. [28] found that $f > \max(6.5c^2, 3.7c)$ TeV [c is defined below Eq. (4.1)]. Thus, for example, $f > 1$ TeV for $c \sim 1/3$; this yields a lower bound on the heavy gauge boson mass of $M_{W_H} = M_{Z_H} \geq 2$ TeV. The mass of the T quark is constrained to be $M_T \geq \sqrt{2}f$, or in this most favorable case $M_T \geq 1.4$ TeV.

- *SU(3) simple group model:* Reference [30] expands on the analysis of Ref. [29] for this model by including the effect of the TeV-scale fermions in the universal fermion embedding. For our choice of parameterization, the constraint on $f \equiv \sqrt{f_1^2 + f_2^2}$ is relaxed by going to $t_\beta \equiv f_2/f_1 > 1$ [31]. For $t_\beta = 3$, $f \geq 3.9$ TeV [31], corresponding to $M_{Z'} \geq 2.2$ TeV. The mass of the T quark in this model is bounded by $M_T \geq f \sin 2\beta$; this constraint then translates into $M_T \geq 2.3$ TeV. Reference [9] found that the anomaly-free fermion embedding is somewhat favored over the universal embedding by electroweak precision constraints.

Finally, we mention briefly a different approach to alleviating the electroweak precision constraints on little Higgs models. Because the little Higgs mechanism for canceling the quadratically divergent radiative corrections to the Higgs mass operates at one-loop, it is possible to impose an additional symmetry, dubbed T-parity [17, 18, 19], under which the new gauge bosons and scalars are odd. This eliminates tree-level contributions of the new particles to electroweak precision observables, thereby essentially eliminating the electroweak precision constraints[4]. It also changes the collider phenomenology drastically, by eliminating signals from single production of the new particles that are odd under T-parity: in particular, the heavy gauge bosons can only be produced in pairs, eliminating the distinctive Drell-Yan signal. The heavy top-partners remain even under T-parity, however, so that their signals are robust. It was shown in Ref. [19] how to add T-parity to any product group little Higgs model. Ref. [19] also concluded that in simple group models, one cannot find a consistent definition of T-parity under which all heavy gauge bosons are odd.

---

[4]Although T-parity suppresses the contributions of heavy gauge bosons and heavy top partners to electroweak oblique parameters, there is a contribution to four fermion operators through a box diagram involving mirror fermions and Goldstone bosons that is not suppressed by the same mechanism and does not decouple as the mirror fermions become heavy. The mirror fermions must be kept light (i.e., be introduced into the low energy spectrum) in order to suppress the relevant couplings [18, 20].

3. The heavy quark sector

The SM top quark gives rise to the largest quadratically divergent correction to the Higgs mass. A characteristic feature of all little Higgs models is the existence of new TeV-scale quark state(s) with specific couplings to the Higgs so that the loops involving the TeV-scale quark(s) cancel the quadratic divergence from the SM top quark loop. Therefore, we begin with a study of the extended top sector of little Higgs models.

3.1 Top sector masses and parameters

The masses of the top quark t and its heavy partner T are given in terms of the model parameters by

$$
m_t = \lambda_t v =
\begin{cases}
\dfrac{\lambda_1 \lambda_2}{\sqrt{\lambda_1^2 + \lambda_2^2}} v & \text{in the Littlest Higgs model,} \\[4mm]
\dfrac{\lambda_1 \lambda_2}{\sqrt{2}\sqrt{\lambda_1^2 c_\beta^2 + \lambda_2^2 s_\beta^2}} v & \text{in the SU(3) simple group model;}
\end{cases}
$$

$$
M_T =
\begin{cases}
\sqrt{\lambda_1^2 + \lambda_2^2}\, f = (x_\lambda + x_\lambda^{-1})\dfrac{m_t}{v} f & \text{in the Littlest Higgs model,} \\[4mm]
\sqrt{\lambda_1^2 c_\beta^2 + \lambda_2^2 s_\beta^2}\, f = \sqrt{2}\,\dfrac{t_\beta^2 + x_\lambda^2}{(1 + t_\beta^2)x_\lambda}\dfrac{m_t}{v}\, f & \text{in the SU(3) simple group model.}
\end{cases}
$$

Fixing the top quark mass m_t leaves two free parameters in the Littlest Higgs model, which can be chosen to be f and $x_\lambda \equiv \lambda_1/\lambda_2$. We see that the SU(3) simple group model contains one additional parameter, $t_\beta \equiv \tan\beta = f_2/f_1$. In the SU(3) simple group model, we define $f \equiv \sqrt{f_1^2 + f_2^2}$.

To reduce fine-tuning in the Higgs mass, the top-partner T should be as light as possible. The lower bound on M_T is obtained for certain parameter choices:

$$
M_T \geq
\begin{cases}
2\dfrac{m_t}{v} f \approx \sqrt{2} f & \text{for } x_\lambda = 1 \text{ in the Littlest Higgs model,} \\[4mm]
2\sqrt{2} s_\beta c_\beta \dfrac{m_t}{v} f \approx f \sin 2\beta & \text{for } x_\lambda = t_\beta \text{ in the SU(3) simple group model,}
\end{cases}
$$

where in the last step we used $m_t/v \approx 1/\sqrt{2}$. The T mass can be lowered in the SU(3) model for fixed f by choosing $t_\beta \neq 1$, thereby introducing a mild hierarchy between f_1 and f_2. With our parameter definitions, the choice $t_\beta > 1$ reduces the mixing between the light SM fermions and their TeV-scale partners, thereby reducing constraints from W coupling universality.

3.2 Heavy T couplings to Higgs and gauge bosons

The couplings of the Higgs doublet to the t and T mass eigenstates can be written in terms of an effective Lagrangian,

$$
\mathcal{L}_Y \supset \lambda_t H t^c t + \lambda_T H T^c t + \frac{\lambda_T'}{2M_T} H H T^c T + \text{h.c.,} \tag{3.1}
$$

where the four-point coupling arises from the expansion of the nonlinear sigma model field. This effective Lagrangian leads to three diagrams contributing to the Higgs mass corrections at one-loop level, shown in Fig. 1: (a) the SM top quark diagram, which depends on the well-known SM top Yukawa coupling λ_t; (b) the diagram involving a top quark and a top-partner T, which depends on the HTt coupling λ_T; and (c) the diagram involving a T loop coupled to the Higgs doublet via the dimension-five $HHTT$ coupling. The couplings in the three diagrams of Fig. 1 must satisfy the following relation [14] in order for the quadratic divergences to cancel:

$$\lambda_T' = \lambda_t^2 + \lambda_T^2. \tag{3.2}$$

This equation embodies the cancellation of the Higgs mass quadratic divergence in any little Higgs theory. It is of course satisfied by the couplings in both the Littlest Higgs and the SU(3) simple group models, as can be seen by plugging in the explicit couplings given in Table 1. Note that in the SU(3) simple group model, λ_T vanishes when $x_\lambda = 1$. If the little Higgs mechanism is realized in nature, it will be of fundamental importance to establish the relation in Eq. (3.2) experimentally.
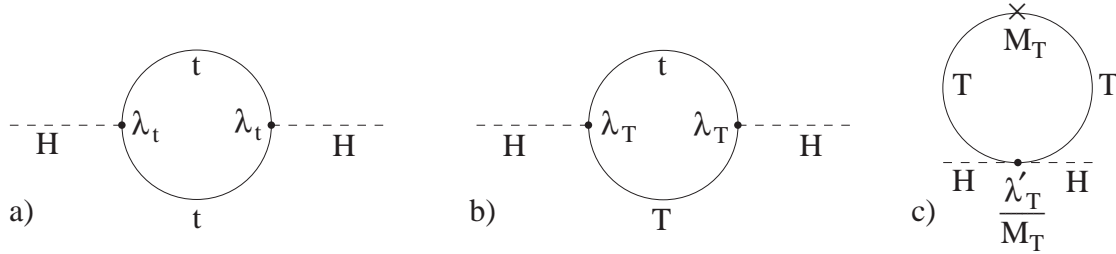
Figure 1: Quadratically divergent one-loop contributions to the Higgs boson mass-squared from the top sector in little Higgs models.

	Littlest Higgs	SU(3) simple group
$\lambda_t =$	$m_t/v = \frac{\lambda_1\lambda_2}{\sqrt{\lambda_1^2+\lambda_2^2}}$	$m_t/v = \frac{\lambda_1\lambda_2}{\sqrt{2}\sqrt{\lambda_1^2 c_\beta^2 + \lambda_2^2 s_\beta^2}}$
$\lambda_T =$	$x_\lambda m_t/v$	$s_\beta c_\beta(x_\lambda - x_\lambda^{-1})m_t/v$
$\lambda_T' =$	$(x_\lambda^2 + 1)m_t^2/v^2$	$\left[s_\beta^2 c_\beta^2(x_\lambda - x_\lambda^{-1})^2 + 1\right] m_t^2/v^2$
$Ht_R\bar{t}_L$:	$i\lambda_t$	$i\lambda_t$
$HT_R\bar{t}_L$:	$i\lambda_T$	$i\lambda_T$
$HHT_R\bar{T}_L$:	$i\lambda_T'/M_T$	$i\lambda_T'/M_T$
$W_\mu^+\overline{T}b:\ i\delta_T\frac{g}{\sqrt{2}}\gamma_\mu P_L;\ \ \delta_T =$	$\lambda_T v/M_T = x_\lambda m_t/M_T$	$\lambda_T v/M_T = s_\beta c_\beta(x_\lambda - x_\lambda^{-1})m_t/M_T$
$Z_\mu\overline{T}t:\ i\delta_T\frac{g}{2c_w}\gamma_\mu P_L;\ \ \delta_T =$	same as above	same as above

Table 1: Heavy T couplings and Feynman rules in the Littlest Higgs and SU(3) simple group models.

After EWSB, the coupling λ_T induces a small mixing of electroweak doublet into T,

$$T = T_0 - \delta_T t_0, \quad \delta_T = \lambda_T \frac{v}{M_T}, \tag{3.3}$$

where T_0, t_0 stand for the electroweak eigenstates before the mass diagonalization at the order of v/f. This mixing gives rise to the couplings of T to the SM states bW and tZ with the same form as the corresponding SM couplings of the top quark except suppressed by the mixing factor δ_T. The Feynman rules are given in Table 1.

3.3 Additional heavy quark couplings in the SU(3) simple group model

Expanding the $SU(2)_L$ gauge symmetry to $SU(3)$ forces the introduction of a heavy partner associated with each $SU(2)_L$ fermion doublet of the SM. The first two generations of quarks are therefore enlarged to contain two new TeV-scale quarks $Q_{1,2}$. We consider both the universal and the anomaly-free fermion embeddings, as discussed in more detail in Sec. B.2. The universal embedding gives rise to two charge $2/3$ quarks, U and C, while the anomaly-free embedding gives rise to two charge $-1/3$ quarks, D and S.

The masses of the two heavy quarks $Q_{1,2}$ are given, for either fermion embedding, by

$$M_{Q_m} = s_\beta \lambda_{Q_m} f \qquad (m = 1, 2), \tag{3.4}$$

where we have neglected the masses of the quarks of the first two generations and chosen λ_{Q_m} to be the Yukawa coupling involving Φ_2 (see Sec. B.2.3 and B.2.6 for further details). The heavy quark couplings to the Higgs boson are proportional to the Yukawa couplings λ_{Q_m} as expected, and can be rewritten in terms of the heavy quark mass M_Q (see Table 2).

After EWSB, the Yukawa couplings λ_{Q_m} lead to mixing between the heavy quarks Q and the corresponding SM quarks of like charge given by $Q = Q_0 - \delta_q q_0$, where as usual Q_0, q_0 denote the electroweak eigenstates of each generation. The mixing angle δ_q is given to order v/f by

$$\delta_q = \pm \frac{v}{\sqrt{2} f t_\beta} \equiv \mp \delta_\nu, \tag{3.5}$$

where the upper sign is for the anomaly-free embedding $(Q = D, S)$ and the lower sign is for the universal embedding $(Q = U, C)$.

The mixing between SM quarks and their heavy counterparts causes isospin violation at order δ_ν^2 in processes involving only SM fermions. This isospin violation can be suppressed by choosing $t_\beta \gtrsim 1$. As in the top sector, the mixing due to δ_q gives rise to the couplings of Q to $q'W$ and qZ; the Feynman rules are given in Table 2.

Although the new heavy quarks $Q_{1,2}$ of the first two generations do not play a significant role in the cancellation of the Higgs mass quadratic divergence (they take part in the cancellation of the numerically insignificant Higgs mass quadratic divergence from their SM partners in the first two generations), they share the common parameters f and t_β with the top sector, providing additional experimental observables that can be used to test the little Higgs structure of the couplings. The new heavy quarks of the first two generations introduce two further parameters, which can be chosen as their masses M_{Q_m} or

	SU(3) simple group
$H\overline{U}_R u_L$:	$-ic_\beta \lambda_U/\sqrt{2} = -iM_U/\sqrt{2}ft_\beta$
$W_\mu^+ \overline{U}d$:	$i\delta_\nu \frac{g}{\sqrt{2}}\gamma_\mu P_L$
$Z_\mu \overline{U}u$:	$i\delta_\nu \frac{g}{2c_w}\gamma_\mu P_L$
$H\overline{D}_R d_L$:	$ic_\beta \lambda_D/\sqrt{2} = iM_D/\sqrt{2}ft_\beta$
$W_\mu^- \overline{D}u$:	$-i\delta_\nu \frac{g}{\sqrt{2}}\gamma_\mu P_L$
$Z_\mu \overline{D}d$:	$-i\delta_\nu \frac{g}{2c_w}\gamma_\mu P_L$
$X_\mu^- \overline{b}T$:	$\frac{g}{\sqrt{2}}\gamma_\mu P_L$
$Y_\mu^0 \overline{t}T$:	$\frac{g}{\sqrt{2}}\gamma_\mu P_L$
$\eta \overline{t}T$:	$-m_t/vP_L$
$X_\mu^- \overline{d}U$:	$\frac{g}{\sqrt{2}}\gamma_\mu P_L$
$Y_\mu^0 \overline{u}U$:	$\frac{g}{\sqrt{2}}\gamma_\mu P_L$
$X_\mu^- \overline{D}u$:	$-\frac{g}{\sqrt{2}}\gamma_\mu P_L$
$Y_\mu^0 \overline{D}d$:	$-\frac{g}{\sqrt{2}}\gamma_\mu P_L$
$X_\mu^- \overline{e}N$:	$\frac{g}{\sqrt{2}}\gamma_\mu P_L$
$Y_\mu^0 \overline{\nu}N$:	$\frac{g}{\sqrt{2}}\gamma_\mu P_L$
$Z'\overline{T}T$:	$-\frac{ig}{c_W\sqrt{3-4s_W^2}}[(-1+\frac{5}{3}s_W^2)P_L + \frac{2}{3}s_W^2 P_R]$
$Z'\overline{U}U$:	$-\frac{ig}{c_W\sqrt{3-4s_W^2}}[(-1+\frac{5}{3}s_W^2)P_L + \frac{2}{3}s_W^2 P_R]$
$Z'\overline{D}D$:	$-\frac{ig}{c_W\sqrt{3-4s_W^2}}[(-1+\frac{5}{3}s_W^2)P_L - \frac{1}{3}s_W^2 P_R]$
$Z'\overline{N}N$:	$-\frac{ig}{c_W\sqrt{3-4s_W^2}}(-1+s_W^2)P_L$

Table 2: Feynman rules for T and Q in the SU(3) simple group model. Note that $U = U, C$ in the universal embedding and $D = D, S$ in the anomaly-free embedding. δ_ν is defined in Eq. (3.5). The extra is in the couplings of X, Y are due to our phase choice.

equivalently their Yukawa couplings λ_{Q_m}, as related by Eq. (3.4). The couplings between the new heavy quarks and the TeV-scale gauge bosons are fixed by the gauge symmetry; they are summarized in Table 2. We will not comment on them further here since they will not play a significant role in our phenomenological analysis.

3.4 Heavy quark production and decay at the LHC

3.4.1 T production and decay

The top-partner T can be pair-produced via QCD interactions at the LHC; however, because the final state contains two heavy particles, the pair-production cross section falls quickly with increasing M_T. Instead, single T production via Wb fusion yields a larger cross section in both the Littlest Higgs model and the SU(3) simple group model, as shown in Figs. 2 and 3, respectively.

In the Littlest Higgs model, the single T production cross section at fixed M_T depends on only one model parameter, x_λ, as shown in Fig. 2. In particular, the cross section is proportional to x_λ^2, as can be seen by examining the $W^+\overline{T}b$ coupling in Table 1 while
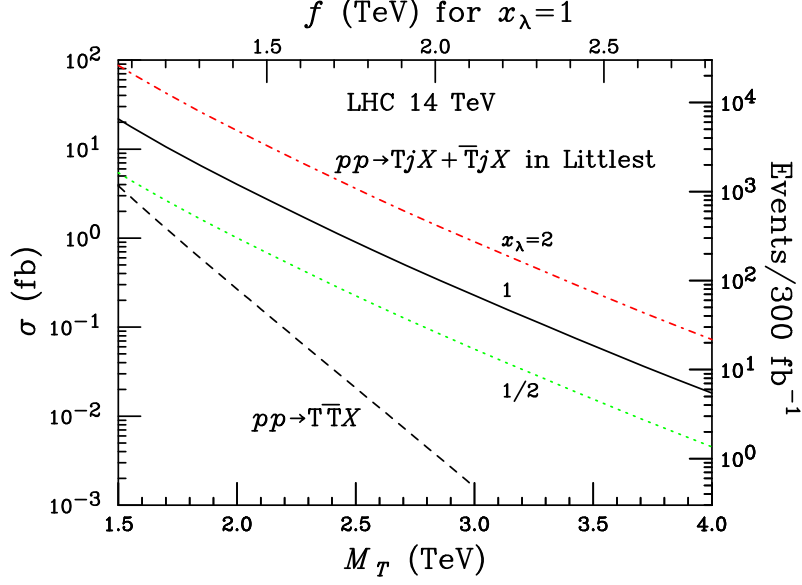
Figure 2: Production cross sections for T in the Littlest Higgs model. The top axis shows the value of f corresponding to M_T for $x_\lambda = 1$.
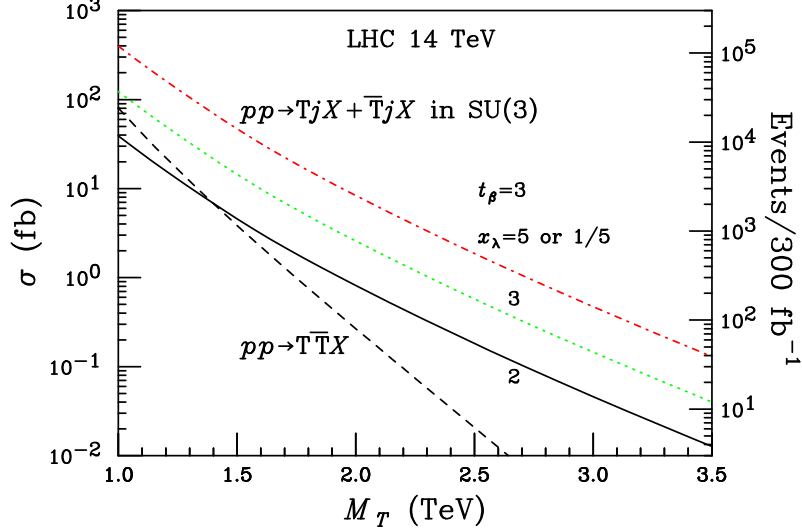
Figure 3: Production cross sections for T in the SU(3) simple group model. Single T production is plotted for $t_\beta = 3$ and various values of x_λ. The single T production cross section is invariant under $x_\lambda \to 1/x_\lambda$ and vanishes at $x_\lambda = 1$.

holding M_T fixed. We see that the cross section is typically in the range 0.01–100 fb for $M_T = 1.5$–3.5 TeV.

In the SU(3) simple group model, the single T production cross section at fixed M_T depends on two model parameters, x_λ and t_β. From the $W^+ \overline{T} b$ coupling in Table 1 one can see that at fixed M_T, the cross section scales with λ_T^2:

$$\sigma \propto \lambda_T^2 \propto s_\beta^2 c_\beta^2 (x_\lambda - x_\lambda^{-1})^2. \tag{3.6}$$

The cross section is invariant under $t_\beta \leftrightarrow 1/t_\beta$ and under $x_\lambda \leftrightarrow 1/x_\lambda$. It reaches a maximum at $t_\beta = 1$, and vanishes at $x_\lambda = 1$. Away from unity, it falls like t_β^{-2} (t_β^2) for large (small) t_β, and grows like x_λ^2 (x_λ^{-2}) for large (small) x_λ. The cross section is shown in Fig. 3 for $t_\beta = 3$ and various values of x_λ. We see that the cross section is similar in size to that in the Littlest Higgs model, depending on the parameter values in either model.

The dominant decay modes of T in all little Higgs models are tH, tZ and bW. The partial widths of T to these final states are all controlled by the same coupling λ_T,

$$\Gamma(T \to tH) = \Gamma(T \to tZ) = \frac{1}{2}\Gamma(T \to bW) = \frac{\lambda_T^2}{32\pi}M_T = 9.9\lambda_T^2 \left(\frac{M_T}{\text{TeV}}\right)\text{GeV}, \qquad (3.7)$$

where we neglect final-state masses compared to M_T. If these are the only decays of T, then its total width is $40\lambda_T^2(M_T/\text{TeV})$ GeV. The branching fractions of T into these final states are then given by

$$\text{BR}(T \to tH) = \text{BR}(T \to tZ) = 1/4, \qquad \text{BR}(T \to bW) = 1/2. \qquad (3.8)$$

This simple relation between the branching fractions is easily understood in terms of the Goldstone boson equivalence theorem: the decay modes at high energies (large M_T) are just those into the four components of the SM Higgs doublet, i.e., the three Goldstone degrees of freedom and the physical Higgs boson.

Phenomenological studies of these T decays have been performed at the level of somewhat realistic detector simulations in Ref. [15]. The T mass can be reconstructed from each of these three channels; $T \to Zt \to \ell^+\ell^-b\ell\,\rlap{/}{E}_T$ provides the cleanest mass peak [15].

If the only significant decays of T are into tH, tZ and bW, then the branching fractions of T are predicted independent of any model parameters by Eq. (3.8). A measurement of the rate for single T production with decays into any one of the three final states is sufficient to determine the production cross section, and thus extract λ_T. The measurement of the characteristic pattern of branching fractions also provides a test of the model (see Sec. 3.6.1).

In the SU(3) simple group model, T has additional possible decay modes due to the additional particles in the spectrum. In particular, T can also decay to $t\eta$, tY^0, and bX^+ final states, depending on the relative masses of T, η, and X, Y. In order to measure the single T production cross section, and hence λ_T, one needs to know the branching fraction(s) of the decay mode(s) in which T is observed. Assuming the SU(3) simple group model structure, these can be predicted as follows. The T mass can be reconstructed in, e.g., $T \to Zt \to \ell^+\ell^-b\ell\,\rlap{/}{E}_T$ as discussed above. The X, Y gauge boson masses are fixed in terms of $M_{Z'}$, which will be easily measurable from its decays to dileptons (see Sec. 4). The T partial widths to tY and bX can then be calculated in terms of the gauge couplings in Table 2. The T partial width to η can be calculated from the coupling in Table 2 once the η mass is measured, e.g., in decays of η to dijets. The partial widths to tH, tZ and bW are proportional to λ_T^2; thus the only remaining free parameter to be extracted from the rate measurement in any given final state is λ_T. Measurements of the pattern of branching fractions then provide a nontrivial test of the model. Similarly, in the Littlest Higgs model with two U(1) groups gauged, T can decay into tA_H. Once the A_H mass is measured, a similar analysis can be applied.

3.4.2 Q production and decay

The heavy quarks Q in the SU(3) simple group model can be produced at the LHC via, e.g., $Wd \to U$, $Zu \to U$. The production couplings are given in Table 2; for fixed M_Q, the cross section depends on only one model parameter, δ_ν; in particular the cross section is proportional to $\delta_\nu^2 = v^2/2f^2 t_\beta^2$. The single production cross section for $U + \overline{U}$ is shown in Fig. 4, together with the $U\overline{U}$ pair production cross section from QCD.
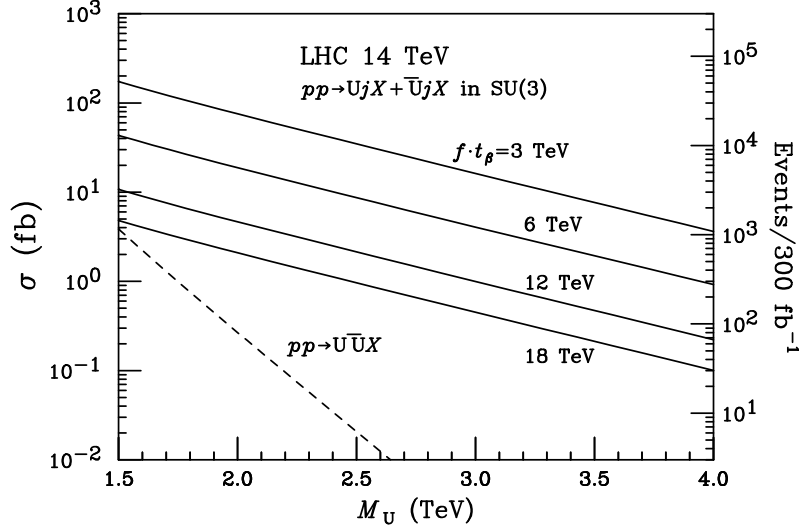
Figure 4: Production cross sections for U in the SU(3) simple group model. The single U production cross section is shown for various values of ft_β (solid lines).

The single U production cross section is quite large compared to single production of T at a comparable mass because T production requires a b quark in the initial state, while U production proceeds from a valence u or d quark. By measuring both M_U and the single U production cross section, as well as f from measurements in the gauge sector (see Sec. 4), one can determine λ_U and t_β from Eqs. (3.4) and (3.5). This measurement of t_β is independent from that in the T sector and can be used as a nontrivial test of the model, as will be discussed further in Sec. 3.5.

Production of the heavy quark partners of the first generation offers an additional powerful handle on the SU(3) simple group model. First, consider single U production in the universal fermion embedding. This proceeds via the subprocesses

$$dW^+ \to U, \qquad uZ \to U; \qquad\qquad \overline{d}W^- \to \overline{U}, \qquad \overline{u}Z \to \overline{U}. \qquad (3.9)$$

At a proton-proton collider such as the LHC, we expect the cross section for U production, from initial-state valence u and d quarks, will be much larger than that for $\overline{U}$, from initial-state sea $\overline{u}$ and $\overline{d}$ antiquarks. In fact, $\overline{U}$ production constitutes less than 10% of the total $U + \overline{U}$ cross section shown in Fig. 4. There will thus be a large asymmetry in the charge of the final lepton in $U, \overline{U}$ decays to $W^\pm$, with many more positively charged leptons.

In the anomaly-free embedding, single D production proceeds via the subprocesses

$$uW^- \to D, \qquad dZ \to D; \qquad\qquad \overline{u}W^+ \to \overline{D}, \qquad \overline{d}Z \to \overline{D}. \qquad (3.10)$$

Because of the parton densities in the proton, the rate for D production via charged current will be somewhat higher than for U, while the rate for D production via neutral current will be somewhat lower than for U, resulting in a comparable total cross section. Again, there will be a large asymmetry in the charge of the final lepton in $D, \overline{D}$ decays to $W^{\mp}$, with many more negatively charged leptons. This allows a simple measurement of the dominant lepton charge in $Q \to q'W(\to \ell\nu)$ decays to distinguish the universal fermion embedding from the anomaly-free fermion embedding. The fermion embedding must be known in order for the model parameters to be extracted from the single-Q production cross section because the embedding determines which parton densities enter the production cross section calculation.
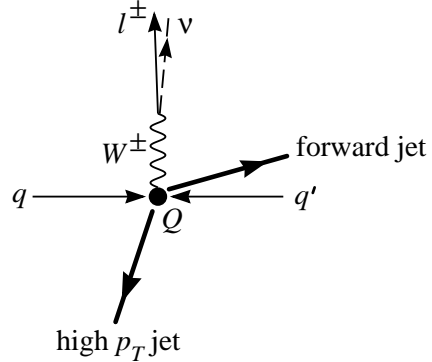
Just as for T, the decay modes of U in the SU(3) simple group model depend on the spectrum of masses. The U quark decays into uH, uZ and dW with partial widths

$$\Gamma(U \to uH) = \Gamma(U \to uZ) = \frac{1}{2}\Gamma(U \to dW) = 5.0 \left(\frac{\text{TeV}}{ft_{\beta}}\right)^2 \left(\frac{M_U}{\text{TeV}}\right)^3 \text{GeV}. \qquad (3.11)$$

U can also decay into $u\eta$; however, the coupling at leading order in v/f is proportional to the up quark Yukawa coupling, so this decay is extremely suppressed and can be neglected. If U is heavy enough, it can also decay into uY and dX with partial widths that depend only on the heavy gauge boson mass $M_{X,Y}$; the UuY and UdX couplings are fixed in terms of the SM gauge coupling g. The heavy gauge boson mass $M_{X,Y}$ can be obtained from the Z' mass measurement (see Sec. 4). The partial widths to uH, uZ and dW can then be extracted together with δ_{ν} from the rate measurement into any final state. The above discussion applies equally to D in the anomaly-free fermion embedding.

The signal kinematics are as follows. U is produced via dW^+ or uZ fusion, yielding a forward jet from which the W or Z was radiated. U then decays into a high-p_T quark and a W boson, with $W \to \ell\nu$. The W is highly boosted, with a momentum of roughly half the U mass, so that the momenta of the neutrino and charged lepton are almost parallel. The decay kinematics are sketched in Fig. 5.

We can take advantage of the large boost of the W boson in U decay to reconstruct the U mass. Normally such a decay involving a neutrino in the final state would allow only the reconstruction of the U transverse mass. However,

Figure 5: Kinematics of $Q = U, D$ production and decay.

because U is very heavy, we can neglect the W mass relative to its momentum and approximate the direction of the neutrino momentum to be parallel to that of the charged lepton. We can then reconstruct the full neutrino momentum and combine it with that of the charged lepton and the high-p_T jet to reconstruct a mass peak for U.

We apply the following cuts to select U production events over the SM W^+jj background. We require a positively-charged electron or muon with

$$|\eta_\ell| < 3, \qquad p_{T\ell} > 20 \text{ GeV}. \qquad (3.12)$$

For the central high-p_T jet we require

$$|\eta_{j_1}| < 3, \qquad p_{Tj_1} > 300 \text{ GeV}. \qquad (3.13)$$

We also require that the forward jet be tagged, with

$$3 < |\eta_{j_2}| < 5, \qquad p_{Tj_2} > 30 \text{ GeV}. \qquad (3.14)$$

Finally we require missing transverse momentum,

$$\not{p}_T > 30 \text{ GeV}. \qquad (3.15)$$

To simulate the detector effects, we smear the energies for the charged lepton and the jets according to a Gaussian form, $\Delta E/E = a/\sqrt{E/\text{GeV}} \oplus b$, with $a = 5\%$, $b = 1\%$ for a charged lepton and $a = 50\%$, $b = 2\%$ for a jet.

The p_T distribution of the highest-p_T jet is shown in the left panel of Fig. 6, together with the W^+jj background. The signal distribution clearly exhibits a Jacobian peak near $M_U/2$. The right panel of Fig. 6 shows the U transverse mass and the fully reconstructed U mass. The U mass is reconstructed from the momenta of ℓ^+ and the highest-p_T jet, as well as the missing momentum assumed to point along the direction of the ℓ^+ momentum. The reconstructed mass variable indeed leads to a sharper peak than the transverse mass.

In Fig. 6 we have included only U production (without the $\overline{U}$ contribution), and folded in the branching fractions of $U \to W^+u$ and $W^+ \to \ell^+\nu$, with $\ell^+ = e^+, \mu^+$. The signal cross section after cuts for $M_U = 3$ TeV and $f\,t_\beta = 3$ TeV is about 0.66 fb, resulting in close to 200 signal events in 300 fb^{-1} of LHC luminosity. The background is well under control. Additional statistics can be gained by considering the decay channels $U \to uZ, uH$.

One can do a similar analysis for single C (S) production, using M_C (M_S) and the production cross section together with f from the gauge sector measurements to determine λ_C (λ_S) and make another independent measurement of t_β. However, because C (S) is produced from inital-state sea quarks c and s, its production rate will be lower, only 10–20% of that of U (D). Further, since the sea quark and antiquark distributions are equal, there will be no asymmetry in the charge of the final lepton in C (S) decays to $W^\pm$. This allows the C (S) resonance to be experimentally distinguished from the U (D) resonance, if enough events can be collected above background.

3.5 Testing the Higgs mass divergence cancellation in the top sector

The key experimental test of the little Higgs models is to verify the cancellation of the Higgs mass quadratic divergence, embodied in the crucial relation of Eq. (3.2). Ideally, one could hope to measure the couplings λ_T and λ_T' directly, without making any assumptions about the model structure. The coupling λ_T controls the T production cross section in Wb
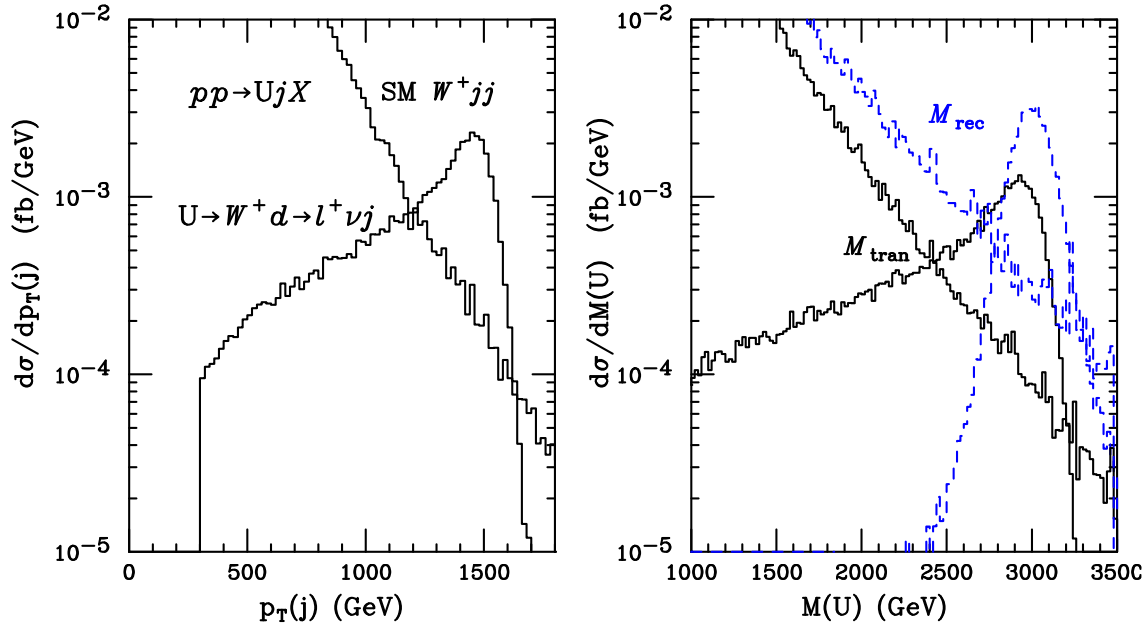
Figure 6: Mass reconstruction of U in $pp \to Uq \to \ell^+ \nu jj$, for $M_U = 3$ TeV and $f\,t_\beta = 3$ TeV. (Left) p_T of the highest-p_T jet in the event. (Right) Transverse mass M_{tran} (solid black histograms) and the full reconstructed mass M_{rec} (dashed blue histograms). Also shown is the background from SM $W^+ jj$.

fusion, where it can be extracted [13, 14] by measuring the single-T production rate and the T mass from signal kinematics. The coupling λ_T' could in principle be extracted from a measurement of the associated TH production cross section. However, a quick estimate [32] indicates that the cross section is too small to be observable at the LHC. Instead, the relation in Eq. (3.2) for the Higgs mass divergence cancellation must be checked within the context of the particular model. Once the model is determined, the relevant independent parameters that control the top sector must be overconstrained to make a nontrivial test of the model.

In the Littlest Higgs model, one can use the model relation $\lambda_T' = \lambda_T M_T / f$ to write the divergence cancellation condition in terms of the four observables $(\lambda_t, \lambda_T, M_T, f)$. Note that only three of these are independent in the Littlest Higgs model; λ_T and M_T can both be written in terms of f, λ_t and x_λ. Combining T-sector measurements of M_T and λ_T with a measurement of f from the heavy gauge boson sector, one can overconstrain the parameters and verify the cancellation of the quadratic divergence.

In the SU(3) simple group model the situation is more complicated because of the ratio of the two vacuum condensates, $f_2 / f_1 = t_\beta$, which appears in the fermion sector of the model. Thus, in addition to the four parameters $(\lambda_t, \lambda_T, M_T, f)$ measurable in the T and heavy gauge boson sectors, one needs a measurement of t_β in order to overconstrain the parameters and verify the relation in Eq. (3.2). Fortunately, t_β can be extracted independently of the λ_T and M_T measurements by measuring the mass and production

cross section of the U or D quarks, since their production couplings are proportional to $1/t_\beta$.

3.6 Comparison with other models

3.6.1 A fourth generation sequential top-prime

The key feature that distinguishes T from a fourth generation sequential top-prime is the fact that it is an SU(2) singlet before mixing with the top quark. This feature allows for the presence of a vectorlike mass term for T and flavor-changing TtH and TtZ couplings in the mass basis, both of which are forbidden by electroweak symmetry in a fourth-generation model. As pointed out in Ref. [15], detecting and measuring the flavor-changing neutral current decays $T \to Zt$ and $T \to Ht$, with equal branching fractions, allows one to rule out the fourth-generation hypothesis and conclude that T is an electroweak singlet, acquiring its coupling to the Higgs via a gauge-invariant TtH term.

3.6.2 The top quark see-saw

In the top quark see-saw model [33, 34], EWSB occurs via the condensation of the top quark in the presence of an extra vectorlike SU(2)-singlet quark, forming a composite Higgs boson. In order to reproduce the correct electroweak scale, the condensate mass must be large, of order 600 GeV. The vectorlike singlet quark joins the top in a see-saw, yielding the physical top mass (adjusted to the experimental value) and a multi-TeV mass for the vectorlike quark. The little Higgs models thus generically contain an extended top sector with the same electroweak quantum numbers as in the top see-saw model, i.e., a (multi-)TeV-scale isosinglet vectorlike quark T with a small mixing with the SM top quark that gives rise to TtZ, TtH and TbW couplings.

The most important difference between the top see-saw model and the little Higgs models is that the top see-saw model makes no prediction for the dimension-5 $HHTT$ coupling λ'_T, although this coupling can be generated radiatively. Thus, the top see-saw model does not in general satisfy the condition for cancellation of the Higgs mass quadratic divergence given in Eq. (3.2).

In the top see-saw model, the TtH coupling λ_T is constrained by the compositeness condition, which requires the wavefunction renormalization of the composite Higgs field to vanish at the compositeness scale M_c. Ignoring the effect of EWSB, the effective Lagrangian of the top see-saw model is [34, 35]

$$\mathcal{L} = Z_h |\mathcal{D}h|^2 + \left[\sqrt{2} y_t \bar{\psi}_L t_R \sqrt{Z_h} h + \sqrt{2} \lambda_T \bar{\psi}_L T_R \sqrt{Z_h} h - M_T \bar{T}_L T_R + \text{h.c.} \right] + V_h, \quad (3.16)$$

where Z_h is the wavefunction renormalization of the composite Higgs field h and V_h is the usual SM Higgs potential. In the large-N_c approximation, this implies [34]

$$\lambda_T^2 = \frac{4\pi^2}{N_c \log(M_c/M_T)} - \frac{m_t^2}{v^2}. \quad (3.17)$$

The compositeness scale M_c should not be too far away from the scale of the heavy states. For $M_c/M_T \sim 10$–100 and $N_c = 3$, we obtain $\lambda_T \sim 5.2$–2.4; in particular, the compositeness

condition generally requires a fairly large value for λ_T. In little Higgs models, on the other hand, λ_T is typically of order one or smaller. In the Littlest Higgs model, $\lambda_T = x_\lambda m_t/v \simeq x_\lambda/\sqrt{2}$, which reaches the typical top quark see-saw values only for $x_\lambda \gtrsim 4$. Large values of x_λ in the Littlest Higgs model tend to push up the T mass, leading to greater fine tuning in the electroweak scale. In the SU(3) simple group model, $\lambda_T = s_\beta c_\beta (x_\lambda - x_\lambda^{-1}) m_t/v$, which is further suppressed by the $s_\beta c_\beta \leq 1/2$ factor in front.

4. The gauge sector

Little Higgs models extend the electroweak gauge group at the TeV scale. The structure of the extended electroweak gauge group determines crucial properties of the little Higgs model, which can be revealed by studying the new gauge bosons at the TeV scale. Therefore, we continue with a study of the heavy gauge boson sectors of little Higgs models.

4.1 Heavy gauge boson masses and parameters

The extra gauge bosons get their masses from the f condensate, which breaks the extended gauge symmetry. For our two prototype models, the gauge boson masses are given in terms of the model parameters by

$$\left.\begin{array}{l} M_{W_H} = M_{Z_H} = gf/2sc = 0.65f/\sin 2\theta \\ M_{A_H} = g s_W f/2\sqrt{5} c_W s' c' = 0.16 f/\sin 2\theta' \end{array}\right\} \text{ in the Littlest Higgs model,}$$

$$\left.\begin{array}{l} M_{Z'} = \sqrt{2} g f/\sqrt{3 - t_W^2} = 0.56f \\ M_X = M_Y = gf/\sqrt{2} = 0.46f = 0.82 M_{Z'} \end{array}\right\} \text{ in the SU(3) simple group model. (4.1)}$$

In the SU(3) simple group model the heavy gauge boson masses are determined by only one free parameter, the scale $f = \sqrt{f_1^2 + f_2^2}$. The Littlest Higgs model has two additional gauge sector parameters, $\tan\theta = s/c = g_2/g_1$ [in the SU(2)^2 →SU(2) breaking sector] and $\tan\theta' = s'/c' = g_2'/g_1'$ [in the U(1)^2 →U(1) breaking sector]. If only one copy of U(1) is gauged [21], the A_H state is not present and the gauge sector of the Littlest Higgs model is controlled by only two free parameters, f and $\tan\theta$. Because the model with only one copy of U(1) gauged is favored by the electroweak precision constraints, and since the U(1) sectors of the product group models are quite model-dependent, we focus in what follows on the heavy SU(2) gauge bosons W_H and Z_H. The W_H and Z_H bosons capture the crucial features of the gauge sector of the Littlest Higgs model and their phenomenology can be applied directly to the other product group models.

4.2 Heavy gauge boson interactions with SM particles

The gauge couplings of the Higgs doublet take the general form

$$\mathcal{L} = \begin{cases} [G_{HHVV} VV + G_{HHV'V'} V'V' + G_{HHVV'} VV'] H^2 \\ [G_{HHV^+V^-} V^+V^- + G_{HHV'^+V'^-} V'^+V'^- + G_{HHV^+V'^-}(V^+V'^- + V^-V'^+)] H^2, \end{cases}$$

$$(4.2)$$

where the top line is for V neutral and the bottom line is for V charged. Here V and V' stand for the SM and heavy gauge bosons, respectively. This Lagrangian leads to two

quadratically divergent diagrams contributing to the Higgs mass: one involving a loop of V, proportional to G_{HHVV}, and the other involving a loop of V', proportional to $G_{HHV'V'}$. The divergence cancellation in the gauge sector can thus be written as

$$\sum_i G_{HHV_iV_i} = 0, \tag{4.3}$$

where the sum runs over all gauge bosons in the model. The couplings in the models under consideration are given in Table 3. In the SU(3) simple group model, the quadratic divergence cancels between the Z and Z' loops and between the W and X loops. In the Littlest Higgs model, the quadratic divergence cancels between the W and W_H loops and there is a partial cancellation between the Z and Z_H loops. Including the A_H loop leads to a complete cancellation of the quadratic divergence from the Z loop. The key test of the little Higgs mechanism in the gauge sector is the experimental verification of Eq. (4.3); we discuss the prospects further in Sec. 4.4.

	Littlest Higgs	SU(3) simple group
G_{HHZZ}	$g^2/8c_W^2$	$g^2/8c_W^2$
$G_{HHW^+W^-}$	$g^2/4$	$g^2/4$
$G_{HHV'V'}$	$G_{HHZ_HZ_H} = -g^2/8$	$G_{HHZ'Z'} = -g^2/8c_W^2$
	$G_{HHW_H^+W_H^-} = -g^2/4$	$G_{HHX^+X^-} = -g^2/4$
$G_{HHVV'}$	$G_{HHZZ_H} = -g^2\cot 2\theta/4c_W$	$G_{HHZZ'} = g^2(1-t_W^2)/4c_W\sqrt{3-t_W^2}$
	$G_{HHW^+W_H^-} = -g^2\cot 2\theta/4$	$G_{HHW^+X^-} = 0$
δ_Z	$-\sin 4\theta\, v^2/8c_Wf^2$	$-(1-t_W^2)\sqrt{3-t_W^2}\,v^2/8c_Wf^2$
δ_W	$c_W\delta_Z$	0
$g_{VVV'}$	$g_{W^+W^-Z_H} = -gc_W\delta_Z$	$g_{W^+W^-Z'} = gc_W\delta_Z$
	$g_{W^+W_H^-Z} = -g\delta_Z$	$g_{W^+X^-Z} = 0$
$g_{VV'V'}$	$g_{W_H^+W_H^-Z} = -gc_W$	$g_{X^+X^-Z} = -g(1-2s_W^2)/2c_W$
		$g_{Y^0\overline{Y}^0Z} = -g/2c_W$
	$g_{W^+W_H^-Z_H} = -g$	$g_{W^+X^-\overline{Y}^0} = g/\sqrt{2}$
$g_{V'V'V'}$	$g_{W_H^+W_H^-Z_H} = 2g\cot 2\theta$	$g_{X^+X^-Z'} = g_{\overline{Y}^0Y^0Z'} = g/\sqrt{2}$

Table 3: Heavy gauge boson parameters and couplings in the Littlest Higgs model and the SU(3) simple group model. The triple gauge coupling Feynman rule for $V_1^\mu(k_1)V_2^\nu(k_2)V_3^\rho(k_3)$ is given in the form $-ig_{V_1V_2V_3}[g^{\mu\nu}(k_1-k_2)^\rho + g^{\nu\rho}(k_2-k_3)^\mu + g^{\rho\mu}(k_3-k_1)^\nu]$, with the convention $g_{W^+W^-Z} = -gc_W$.

After EWSB, the couplings of H^2 to one heavy and one SM gauge boson induce mixing between the heavy and SM gauge bosons:

$$V' = V_0' - \delta_V V_0, \qquad \delta_V = -v^2 G_{HHVV'}/M_{V'}^2, \tag{4.4}$$

where V_0', V_0 stand for the states before EWSB. The mixing parameters δ_V are given in Table 3. This mixing gives rise to triple gauge couplings between one heavy and two SM

gauge bosons, also shown in Table 3. In the SU(3) simple group model, EWSB also splits the X and Y gauge boson masses by a small amount,

$$M_Y - M_X = \frac{gv^2}{4\sqrt{2}f} \simeq 3.9 \left(\frac{\text{TeV}}{M_{Z'}}\right) \text{GeV}. \tag{4.5}$$

In the Littlest Higgs model, the couplings of the heavy gauge bosons to the $SU(2)_L$ fermion currents take the form

$$Z_H^\mu \overline{f} f: \quad ig \cot\theta T_f^3 \gamma^\mu P_L, \qquad\qquad W_H^{+\mu} \overline{u} d: \quad -\frac{ig}{\sqrt{2}} \cot\theta \gamma^\mu P_L, \tag{4.6}$$

where $T_f^3 = 1/2 \ (-1/2)$ for up (down) type fermions. Below the TeV scale, exchange of W_H and Z_H gives rise to four-fermi operators, which are constrained by the electroweak precision data. The experimental constraints are loosened by going to small values of $\cot\theta$, for which the couplings of the heavy gauge bosons are suppressed.

In the SU(3) simple group model, the Z' couples to SM fermions with gauge strength, while the X, Y gauge bosons couple only via the mixing between SM fermions and their TeV-scale partners. The couplings are given in Table 4.

4.3 Heavy gauge boson production and decay

The best way to discover new heavy gauge bosons at the LHC is generally through Drell-Yan production. This is certainly true in the little Higgs models.

In the Littlest Higgs model, the heavy gauge bosons Z_H, W_H couple to pairs of SM fermions through the $SU(2)_L$ current, with coupling strength scaled by $\cot\theta$ compared to the SM $SU(2)_L$ couplings. They thus have large production cross sections, as shown in Fig. 7, controlled by one common free parameter, $\cot\theta$.[5] In addition, because Z_H and W_H form an SU(2) triplet, they are degenerate in mass up to very small EWSB effects. Thus, the measurement of the Z_H mass in dileptons predicts the transverse mass distribution of the W_H in $W_H \to \ell\nu$, and the measurement of the rate for Z_H into dileptons predicts the rate for W_H into leptons, allowing a test of the SU(2) triplet nautre of (W_H, Z_H).

In the SU(3) simple group model, the heavy gauge boson Z' couples to pairs of SM fermions with couplings fixed in terms of the SM gauge couplings and depending only on the (discrete) choice of the fermion embedding, as shown in the left panel of Fig. 7. Unlike the Z_H of the Littlest Higgs model, there is no tunable parameter in the Z' cross section.[6]

---

[5]Note that the electroweak precision data tend to favor small values of $\cot\theta$, which reduces the contribution of W_H, Z_H to four-Fermi operators at low energy. Small $\cot\theta$ lowers the Drell-Yan cross section, reducing the LHC reach for W_H, Z_H discovery.

[6]This parameter independence is the most characteristic feature of the Z' in simple group models with the extended gauge group $SU(3) \times U(1)_X$ [5, 9, 7]. Models with a larger extended gauge group, $SU(N) \times U(1)_X$ with $N > 3$, lose this parameter independence because they contain $N-2$ broken diagonal generators, which mix in general. For example, the $SU(4) \times U(1)_X$ model of Ref. [5] contains two broken diagonal generators, Z_1' (which couples to SM fermion pairs with fixed strength) and Z_2' (which does not couple to fermion pairs). After mixing, the mass eigenstates Z', Z'' share the fermion couplings with the mixing angle as a free parameter. If the fermion couplings of both states can be measured, the parameter independence reappears in the form of a coupling sum rule.

	SU(3) simple group
$Z'\bar{t}t :$	$-\frac{ig}{c_W\sqrt{3-4s_W^2}}[(\frac{1}{2}-\frac{1}{3}s_W^2)P_L+\frac{2}{3}s_W^2 P_R]$
$Z'\bar{b}b :$	$-\frac{ig}{c_W\sqrt{3-4s_W^2}}[(\frac{1}{2}-\frac{1}{3}s_W^2)P_L-\frac{1}{3}s_W^2 P_R]$
$Z'\bar{u}u :$	$-\frac{ig}{c_W\sqrt{3-4s_W^2}}[(-\frac{1}{2}+\frac{2}{3}s_W^2)P_L+\frac{2}{3}s_W^2 P_R]$ (anomaly free)
	$-\frac{ig}{c_W\sqrt{3-4s_W^2}}[(\frac{1}{2}-\frac{1}{3}s_W^2)P_L+\frac{2}{3}s_W^2 P_R]$ (universal)
$Z'\bar{d}d :$	$-\frac{ig}{c_W\sqrt{3-4s_W^2}}[(-\frac{1}{2}+\frac{2}{3}s_W^2)P_L-\frac{1}{3}s_W^2 P_R]$ (anomaly free)
	$-\frac{ig}{c_W\sqrt{3-4s_W^2}}[(\frac{1}{2}-\frac{1}{3}s_W^2)P_L-\frac{1}{3}s_W^2 P_R]$ (universal)
$Z'\bar{e}e :$	$-\frac{ig}{c_W\sqrt{3-4s_W^2}}[(\frac{1}{2}-s_W^2)P_L-s_W^2 P_R]$
$Z'\bar{\nu}\nu :$	$-\frac{ig}{c_W\sqrt{3-4s_W^2}}(\frac{1}{2}-s_W^2)P_L$
$X_\mu^-\bar{b}t :$	$\frac{g}{\sqrt{2}}\delta_t\gamma_\mu P_L$
$X_\mu^-\bar{d}u :$	$\frac{g}{\sqrt{2}}\delta_\nu\gamma_\mu P_L$
$X_\mu^-\bar{e}\nu :$	$\frac{g}{\sqrt{2}}\delta_\nu\gamma_\mu P_L$
$Y_\mu^0\bar{t}t :$	$\frac{g}{\sqrt{2}}\delta_t\gamma_\mu P_L$
$Y_\mu^0\bar{u}u :$	0 (anomaly free)
	$\frac{g}{\sqrt{2}}\delta_\nu\gamma_\mu P_L$ (universal)
$Y_\mu^0\bar{d}d :$	$\frac{g}{\sqrt{2}}\delta_\nu\gamma_\mu P_L$ (anomaly free)
	0 (universal)
$Y_\mu^0\bar{e}e :$	0
$Y_\mu^0\bar{\nu}\nu :$	$\frac{g}{\sqrt{2}}\delta_\nu\gamma_\mu P_L$
$Y_\mu^0 H\eta :$	$\frac{ig}{2\sqrt{2}}(p_\eta-p_H)_\mu$

Table 4: Heavy gauge boson couplings in the SU(3) simple group model. We neglect flavor misalignments. The momenta $p_{\eta,H}$ of the scalars are outgoing.

The heavy gauge bosons X,Y of the SU(3) simple group model have a very different phenomenology, rooted in their identity as the SU(2)$_L$ doublet (X^-,Y^0) of broken off-diagonal generators of SU(3). Because they couple to SM quark pairs only through $q-Q$ mixing as given in Table 4, their production cross sections in Drell-Yan are suppressed by $\delta_\nu^2 \propto v^2/f^2$. This is shown for X in the right panel of Fig. 7. Because of this large cross section difference, $X^\pm$ cannot be mistaken for the charged members of an SU(2) triplet containing Z', providing an easy distinction between simple group and product group models. The $\sim 20\%$ mass splitting between $X^\pm$ and Z' given in Eq. (4.1) also serves to distinguish $X^\pm, Z'$ from an SU(2) triplet.

An important feature of the product group models is the couplings of Z_H, W_H to dibosons, which gives rise to the decays $Z_H \to ZH$, W^+W^- and $W_H \to WH$, WZ. These couplings arise from a $W_H^a W^a hh^\dagger$ term in the Lagrangian [12] and are proportional to $\cot 2\theta$ due to the characteristic collective breaking structure of the gauge couplings in the product group models. The bosonic decay modes are dominated by the longitudinal components of the final-state bosons; their partial widths can be shown by the Goldstone
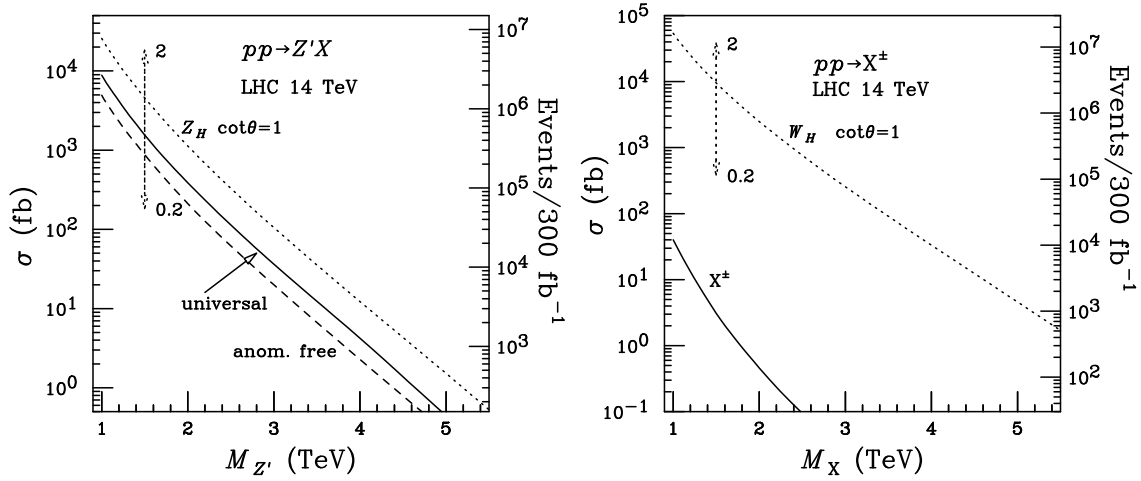
Figure 7:   Cross sections for neutral (left) and charged (right) heavy gauge boson production at the LHC, as a function of the mass of the produced particle. Dotted lines show Z_H (left) and W_H (right) production in the Littlest Higgs model for $\cot\theta = 1$; the variation in cross section for $\cot\theta = 2$ and 0.2 is shown by the dotted arrows. For the SU(3) simple group model, Z' production is shown in the left panel for the universal (solid) and anomaly-free (dashed) fermion embeddings, and $X^\pm$ production is shown in the right panel for $t_\beta = 3$. The $X^\pm$ cross section is proportional to $1/t_\beta^2$.

boson equivalence theorem to obey the relation $\Gamma(Z_H \to ZH) = \Gamma(Z_H \to W^+W^-) = \Gamma(W_H \to WH) = \Gamma(W_H \to WZ) \equiv \Gamma(V_H \to VH)$, where we neglect final-state masses and

$$\Gamma(V_H \to VH) = \frac{g^2 \cot^2 2\theta}{192\pi} M_{V_H} = 0.70 \cot^2 2\theta \left(\frac{M_{V_H}}{\text{TeV}}\right) \text{GeV}. \tag{4.7}$$

Here M_{V_H} is the mass of Z_H or W_H. The measurement of $\cot\theta$ from $Z_H \to \ell^+\ell^-$ thus predicts the rates for decays of both Z_H and W_H into dibosons. The decay branching fractions of Z_H and W_H in the Littlest Higgs model are shown as a function of $\cot\theta$ in Fig. 8. We neglect final-state masses and assume that no decays to A_H are present (namely, $Z_H \to A_H H$ and $W_H \to A_H W$).

In the SU(3) simple group model, the decay partial widths of Z' into pairs of SM bosons, ZH and W^+W^-, are fixed in terms of the Z' mass (neglecting final-state masses) to be

$$\Gamma(Z' \to ZH) = \Gamma(Z' \to W^+W^-) = \frac{g^2(1 - t_W^2)^2}{192\pi(3 - t_W^2)} M_{Z'} = 0.13 \left(\frac{M_{Z'}}{\text{TeV}}\right) \text{GeV}, \tag{4.8}$$

and the decay partial widths into pairs of SM fermions are fixed once the fermion embedding is chosen. As discussed in Sec. 3.4.2, the fermion embedding can be determined at the LHC by detecting the TeV-scale quark partner of the first generation, U or D, decaying into Wq; the charge asymmetry of the final-state W then determines the embedding. Knowledge of the fermion embedding from the fermion sector can be used to compute the Z' couplings
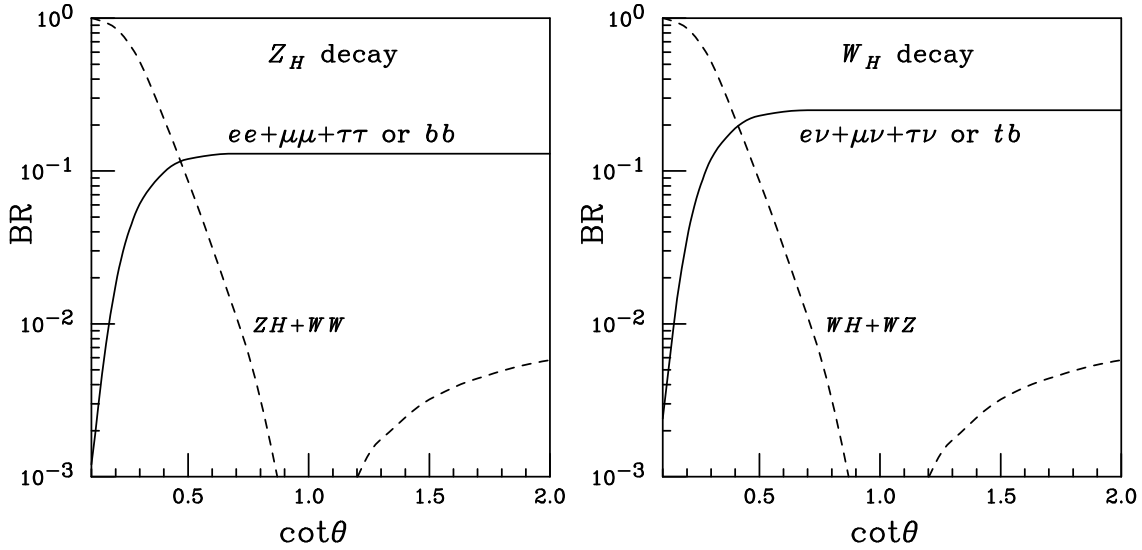
Figure 8: Decay branching fractions of Z_H (left) and W_H (right) in the Littlest Higgs model, as a function of $\cot\theta$. Final-state masses are neglected.

uniquely and perform a cross-check the model. If the TeV-scale fermion partners T and/or Q_m are not too heavy, they can be present in Z' boson decays. If kinematically accessible, decays of Z' to pairs of TeV-scale fermion partners proceed via gauge couplings. This is in contrast to the product group models, in which the TeV-scale top quark partner is mostly electroweak singlet and couples to Z_H only through its electroweak doublet admixture at order v^2/f^2. The Z' can also decay to one SM fermion and one TeV-scale fermion partner; however, the partial widths of these decays are suppressed by $\delta_t^2, \delta_\nu^2 \propto v^2/f^2$ and will be numerically unimportant. Finally, the decay $Z' \to Y^0\eta$ will be kinematically accessible if η is lighter than the Z'–Y^0 mass splitting,

$$M_{Z'} - M_Y = 0.18 M_{Z'} = 180 \left(\frac{M_{Z'}}{\text{TeV}}\right) \text{GeV}. \tag{4.9}$$

The decay branching fractions of Z' in the SU(3) simple group model are given in Table 5, assuming that decays to TeV-scale fermion-partner pairs or to $Y^0\eta$ are kinematically forbidden and neglecting final-state masses.

4.4 Testing the Higgs mass divergence cancellation in the gauge sector

The defining feature of the little Higgs models is the cancellation of the Higgs mass quadratic divergence at one-loop level. Here we investigate this cancellation in the gauge sector, as embodied in Eq. (4.3). Ideally, one could hope to measure directly the couplings $G_{HHV'V'}$ for each heavy gauge boson V' in the model. This could be done by measuring associated production of H with a heavy gauge boson; e.g., $Z'H$ associated production in the SU(3) simple group model. This probes $G_{HHZ'Z'}$ through the diagram involving $q\bar{q} \to Z'^* \to Z'H$, where one Higgs boson has been replaced by its vev in the interaction

Decay mode	Branching fraction			
	SU(3) simple group		Littlest Higgs	
	universal	anomaly-free	$\cot\theta = 1$	$\cot\theta = 0.2$
$ee = \mu\mu = \tau\tau$	3.0%	3.7%	4.2%	0.60%
$\sum_{i=1}^{3} \nu_i \bar\nu_i$	5.2%	6.3%	12.5%	1.8%
$t\bar t$	15%	18%	12.5%	1.8%
$b\bar b$	13%	16%	12.5%	1.8%
$u\bar u = c\bar c$	15%	13%	12.5%	1.8%
$d\bar d = s\bar s$	13%	11%	12.5%	1.8%
$ZH = WW$	0.87%	1.1%	0	43%
Total width	$15\left(\frac{M_{Z'}}{\text{TeV}}\right)$ GeV	$12\left(\frac{M_{Z'}}{\text{TeV}}\right)$ GeV	$34\left(\frac{M_{Z_H}}{\text{TeV}}\right)$ GeV	$9.5\left(\frac{M_{Z_H}}{\text{TeV}}\right)$ GeV

Table 5: Decay branching fractions of Z' in the SU(3) simple group model with universal and anomaly-free fermion embeddings, and of Z_H in the Littlest Higgs model for $\cot\theta = 1$ and 0.2. Final-state masses are neglected.

vertex. Ideally, one will want to measure both the magnitude and the sign of $G_{HHZ'Z'}$, perhaps through its interference with the similar diagram containing an s-channel Z. A detailed study is needed.

In addition to testing the divergence cancellation, the measurement of the $HHV'V'$ couplings also sheds light onto the structure of the model by revealing which heavy gauge bosons are involved in the cancellation of each SM contribution to the Higgs mass quadratic divergence. In the Littlest Higgs model, Z_H cancels the divergence from the SM W^3 boson, W_H^+ and W_H^- cancel the divergence from the SM $W^\pm$ bosons, and A_H (if it is present) cancels the divergence from the SM hypercharge boson. In contrast, in the SU(3) simple group model, Z' cancels the divergences from the SM W^3 boson *and* the hypercharge boson, while X (together with its isospin partner Y) cancels the divergence from the SM $W^\pm$ bosons. Thus the $HHZ'Z'$ coupling strength that is characteristic of the little Higgs divergence cancellation mechanism can vary from model to model. In all product group models with SU(2)^2 →SU(2)$_L$ breaking structure, the value of this coupling will be the same as in the Littlest Higgs model. In simple group models the value of the coupling will be different, and may depend on the model. For example, in the SU(4)×U(1)$_X$ model of Ref. [5], the two broken diagonal generators mix to form mass eigenstates Z' and Z'', which both take part in the divergence cancellation; the sum rule then reads

$$G_{HHZZ} + G_{HHZ'Z'} + G_{HHZ''Z''} = 0. \tag{4.10}$$

A second approach to test the Higgs mass divergence cancellation, first described in Ref. [12], is to measure the couplings of Higgs bosons to one SM gauge boson and one new heavy gauge boson: e.g., $HHW^+W_H^-$, $HHZZ_H$ in the Littlest Higgs model [12]. This approach works only for the product group models, in which these couplings show a characteristic $\cot 2\theta$ dependence which is fixed by the collective breaking structure of the gauge couplings and the nonlinear transformation of the SM Higgs doublet under the

enlarged gauge symmetry. A "Big Higgs" model, in which the Higgs doublet transformed linearly under one of the two SU(2) gauge groups as the fermion doublets do, would have a $HHZZ_H$ coupling proportional to $g\cot\theta$ [if h transformed under SU(2)$_1$] or $g\tan\theta$ [if h transformed under SU(2)$_2$]. These couplings can be probed in the decays $Z_H \to ZH$ and $W_H \to WH$ [12] from Z_H, W_H bosons produced on-shell, and will thus be more straightforward to measure than the $HHV'V'$ couplings discussed above. The $\cot\theta$ dependence of the Z_H production cross section and decay to dileptons and the $\cot 2\theta$ dependence of the Z_H decay to ZH can be probed simultaneously by measuring the rate into dileptons and the rate into ZH [12]; these rates will fall upon the curve shown in Fig. 9 for the Littlest Higgs model.
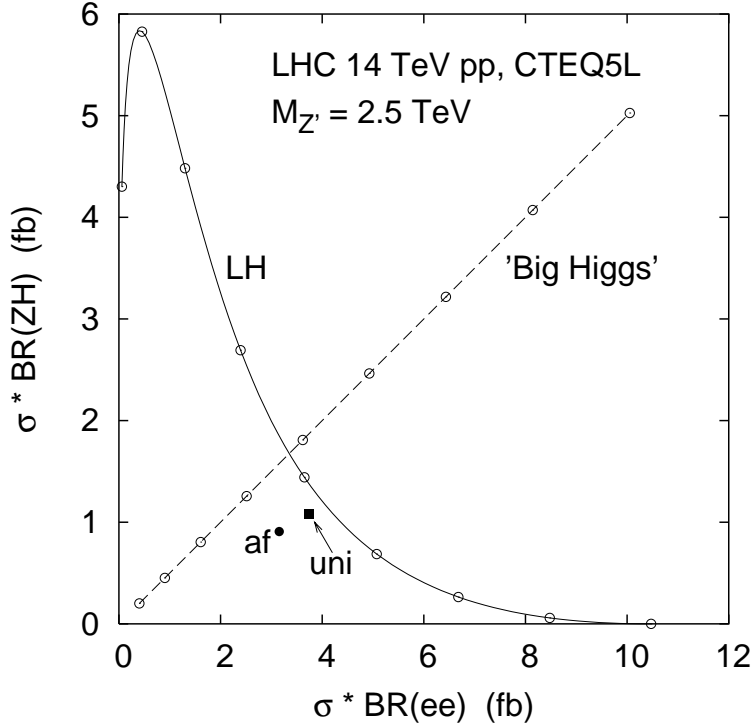
Figure 9: Cross section times branching ratio into ee versus ZH for a 2.5 TeV Z' boson in the Littlest Higgs model ('LH', solid line), the SU(3) simple group model with anomaly-free ('af', filled circle) and universal ('uni', filled square) fermion embeddings, and the "Big Higgs" model of Ref. [12] (dashed line). Open circles on the Littlest Higgs and Big Higgs lines indicate $\cot\theta$ values from 0.2 to 1 (left to right) in steps of 0.1. Branching ratios are computed assuming that only decays into pairs of SM particles are present; we ignore, e.g., $Z_H \to A_H H$ and $Z' \to Y\eta$. We neglect all final-state particle masses except that of the top quark.

In simple group models, the $HHZZ'$ coupling does *not* provide a probe of the Higgs mass divergence cancellation because in these models this coupling is not directly related to the crucial $HHZ'Z'$ vertex that takes part in the cancellation of the Higgs mass quadratic divergence in the gauge sector. In fact, in the SU(3) simple group model, the $HHZZ'$ coupling is fixed by the extended gauge structure and would be the same in any model with the gauge group SU(3)×U(1), whether or not the little Higgs mechanism were realized.

The rates of Z' into dileptons and into ZH in the SU(3) simple group model are predicted uniquely for the universal and anomaly-free fermion embeddings, as shown in Fig. 9. In order to test the cancellation of the quadratic divergence in simple group models, it is thus very important to uncover the gauge structure and fermion embedding of the model. For this purpose, we now turn to a discussion of the determination of the Z' properties in the simple group models.

4.5 Identifying the Z'

In addition to testing the little Higgs *mechanism* in the gauge sector as described in the previous section, one must also identify the *model* to which a newly-discovered Z' boson belongs. This entails identifying the extended gauge structure and determining how the SM fits into it. We examine here some techniques that can be used at the LHC to shed light on the couplings of the Z'. We consider the Z_H of the Littlest Higgs model and the Z' of the SU(3) simple group model, with both the universal and anomaly-free fermion embeddings. As examples of other new physics possibilities, we also consider a sequential Z' with the same couplings to fermions as the SM Z boson, the Z'_ψ and Z'_χ bosons of the E_6 model [36], and Z_R of the left-right symmetric model [37].

4.5.1 Rate in dileptons

A Z' boson will most likely be first discovered in decays to dileptons. The dilepton rate then immediately tells us the production cross section times the leptonic branching ratio, and thus fixes a combination of the Z' couplings to up and down quarks (in the production cross section), the Z' coupling to leptons (in the decay partial width), and the Z' total width (which enters the branching ratio to leptons). While the Z' couplings to up and down quarks enter the production cross section together, multiplied by the appropriate parton densities, it may be possible to separate them experimentally by fitting the shape of the Z' rapidity distribution to high-precision measurements of the up and down quark parton densities [38].

The SU(3) simple group model gives a definite prediction for the $Z' \to \ell^+\ell^-$ rate in each of the fermion embeddings, shown on the horizontal axis of Fig. 9. If extra decay modes of Z' to the heavy fermion partners are kinematically allowed, they will increase the Z' total width and thus decrease the rate into dileptons. Decays of Z' into one SM and one heavy fermion are suppressed by the heavy-light mixing, $\sim v^2/f^2$. Thus only decays into pairs of heavy fermions can contribute significantly; these are likely to be either kinematically inaccessible or heavily suppressed by phase space. In the Littlest Higgs model, the rate of Z_H into dileptons depends on the free parameter $\cot\theta$. Thus, in this channel, the Littlest Higgs model can fake any other Z' model for an appropriate value of $\cot\theta$.

The rate in dileptons is uniquely predicted for the left-right symmetric model Z_R and for a sequential Z' (unless a tunable coupling is introduced by hand). The Z' bosons in the E_6 model can mix, introducing a free parameter in their cross sections; however, the cross section is still constrained within a particular range for a Z' of given mass, and the mixing angle can be extracted from the cross section. A Z' from an extra U(1) gives a rate in dileptons tunable with the U(1) coupling. Therefore, while this rate measurement

gives some valuable information about the Z' couplings, it cannot uniquely determine the model.

4.5.2 Decay branching fractions to other fermion species

In order to probe the Z' couplings to fermions in more detail, one must look for Z' decays into additional fermion species. This opens a window onto the relative couplings of the Z' to particles with different hypercharges. Decays into neutrinos are only accessible through the Z' total width, which in little Higgs models is typically smaller than the detector dilepton mass resolution (see Table 5). We thus consider decays into pairs of quarks. This is a more difficult search than detecting the Z' in dileptons because of the large dijet background at the LHC. However, it may be possible to detect the Z' decaying into top quark pairs, as a peak in the $t\bar{t}$ invariant mass spectrum, or into bottom quark pairs, as a peak in the b-tagged dijet invariant mass spectrum.

Measuring the rate of the Z' into top (bottom) quark pairs and taking the ratio with the rate to dileptons gives the ratio of partial widths into top (bottom) versus electrons, shown in Table 6. In the Littlest Higgs model, this ratio is fixed independent of $\cot\theta$ because the

	Z_H	Z'_{uni}	Z'_{af}	Z'_{seq}	Z'_ψ	Z'_χ	Z_R
BR(tt)/BR(ee)	3.0	4.8	4.8	3.4	3.0	0.6	4.4
BR(bb)/BR(ee)	3.0	4.4	4.4	4.4	3.0	3.0	7.8

Table 6: Ratio of branching fractions into $t\bar{t}$ ($b\bar{b}$) versus e^+e^- for Z' bosons in various models. From left to right: Z_H (Littlest Higgs), Z'_{uni} and Z'_{af} (SU(3) simple group with universal and anomaly-free fermion embeddings, respectively), Z'_{seq} (sequential Z'), Z'_ψ and Z'_χ (E_6 model), and Z_R (left-right symmetric model). Final-state masses are neglected; the top mass dependence can be included by multiplying BR(tt)/BR(ee) by $(1-R)\sqrt{1-4R}$, where $R = m_t^2/M_{Z'}^2$.

$\cot\theta$ dependence enters the couplings to all fermions in the same way. Further, because Z_H couples universally to all fermion doublets, this ratio is just given by the number of color degrees of freedom, $N_c = 3$ (neglecting final-state masses). This ratio is also fixed in the SU(3) simple group model; it is different from the value in the Littlest Higgs model because of the U(1)$_X$ content of the Z', which introduces a dependence on the fermion hypercharge. Note that the ratio of top (bottom) to electron partial widths is the same in the universal and the anomaly-free fermion embeddings, because in both embeddings the leptons and the third generation of quarks all transform as **3**s of SU(3); the difference between the two embeddings appears only in the first two generations of quarks.

Similarly, these ratios are independent of model parameters for a sequential Z', the E_6 Z'_ψ and Z'_χ, and the left-right symmetric Z_R. The E_6 Z'_ψ and Z'_χ mix in general, leading to intermediate values of the partial width raitos. Z'_ψ has the same BR(tt)/BR(ee) and BR(bb)/BR(ee) as the Littlest Higgs Z_H, and Z'_χ has the same BR(bb)/BR(ee), as the Littlest Higgs Z_H. Likewise, the sequential Z' has the same BR(bb)/BR(ee) as the SU(3) simple group model Z'; however, its BR(tt)/BR(ee) is rather different. Of course, the couplings of a Z' from an anomalous extra U(1) can be tuned to duplicate the predictions of any of these models.

4.5.3 Forward-backward asymmetry

The forward-backward asymmetry in $f_i \bar{f}_i \to Z' \to f_f \bar{f}_f$ probes the chiral structure of the Z' couplings to the initial- and final-state fermions. At the partonic level, this asymmetry is defined as

$$A_{FB}^{0,if} = \frac{N_F - N_B}{N_F + N_B} = \frac{3}{4} \mathcal{A}_i \mathcal{A}_f, \tag{4.11}$$

where N_F (N_B) is the number of events with the final-state fermion momentum in the forward (backward) direction defined relative to the initial-state fermion. The asymmetry $\mathcal{A}_f$ is defined in terms of the couplings $g_{L,R}^f$ as

$$\mathcal{A}_f = \frac{(g_L^f)^2 - (g_R^f)^2}{(g_L^f)^2 + (g_R^f)^2}. \tag{4.12}$$

Even though the LHC is a symmetric pp collider, a forward-backward asymmetry can be defined by taking advantage of the fact that the valence quarks in the proton tend to carry a higher momentum fraction x than the sea (anti)quarks [39, 40]. A "hadronic" forward-backward asymmetry can then be defined as

$$A_{FB}^{\text{had}} = \frac{N_F - N_B}{N_F + N_B}, \tag{4.13}$$

where now the forward direction for the final-state fermion is defined relative to the boost direction of the Z' center-of-mass frame. In the narrow-width approximation (neglecting interference between the Z' resonance and the continuum photon and Z exchange), A_{FB}^{had} is given in terms of the partonic asymmetries by

$$A_{FB}^{\text{had}} = \frac{\int dx_1 \sum_{q=u,d} A_{FB}^{0,qf} \left(F_q(x_1) F_{\bar{q}}(x_2) - F_{\bar{q}}(x_1) F_q(x_2) \right) \text{sign}(x_1 - x_2)}{\int dx_1 \sum_{q=u,d,s,c} \left(F_q(x_1) F_{\bar{q}}(x_2) + F_{\bar{q}}(x_1) F_q(x_2) \right)}, \tag{4.14}$$

where $F_q(x_1)$ is the parton distribution function (PDF) for quark q in the proton with momentum fraction x_1, evaluated at $Q^2 = M_{Z'}^2$. The momentum fraction x_2 is related to x_1 by the condition $x_1 x_2 = M_{Z'}^2/s$ in the narrow-width approximation. Only u and d quarks contribute to the numerator since we explicitly take the quark and antiquark PDFs to be identical for the sea quarks; all flavors contribute to the denominator.

Here we consider Z' decays to $e^+ e^-$ only, since it is much easier at LHC to determine the charge of a lepton than the charge of a quark. Decays to $\mu^+ \mu^-$ can be added to double the statistics. The relevant partonic asymmetries and A_{FB}^{had} are listed in Table 7 for the little Higgs models under consideration, as well as a number of other Z' models. The hadronic forward-backward asymmetry A_{FB}^{had} varies with $M_{Z'}$ due to the shape of the PDFs. The Z' mass dependence is shown in Fig. 10 for the models included in Table 7. It is interesting to note that the asymmetries of the E_6 Z' bosons are less than or equal to zero, unlike the rest of the models. The E_6 boson asymmetries remain negative definite for arbitrary mixing between Z'_ψ and Z'_χ: $A_{FB}^{0,ue}$ is always zero and $A_{FB}^{0,de}$ varies between -0.75 and 0 depending on the mixing angle. In Eq. (4.14) we have expressed A_{FB}^{had} as a single number, integrated over rapidity, which depends on both $A_{FB}^{0,ue}$ and $A_{FB}^{0,de}$. It may be possible to

	Z_H	Z'_{uni}	Z'_{af}	Z'_{seq}	Z'_ψ	Z'_χ	Z_R
$\mathcal{A}_e$	1	0.15	0.15	0.15	0	0.8	-0.28
$\mathcal{A}_u$	1	0.77	0.67	0.67	0	0	-0.95
$\mathcal{A}_d$	1	0.94	0.91	0.94	0	-0.8	-0.97
$A_{FB}^{0,ue}$	0.75	0.087	0.076	0.076	0	0	0.20
$A_{FB}^{0,de}$	0.75	0.11	0.10	0.11	0	-0.48	0.20
A_{FB}^{had}	0.44	0.054	0.049	0.049	0	-0.077	0.12

Table 7: Coupling asymmetries before cuts for Z' bosons in the models listed in Table 6. A_{FB}^{had} is calculated for the LHC (pp collisions at 14 TeV) using CTEQ5L PDFs in the narrow width approximation, with $M_{Z'} = 2$ TeV.
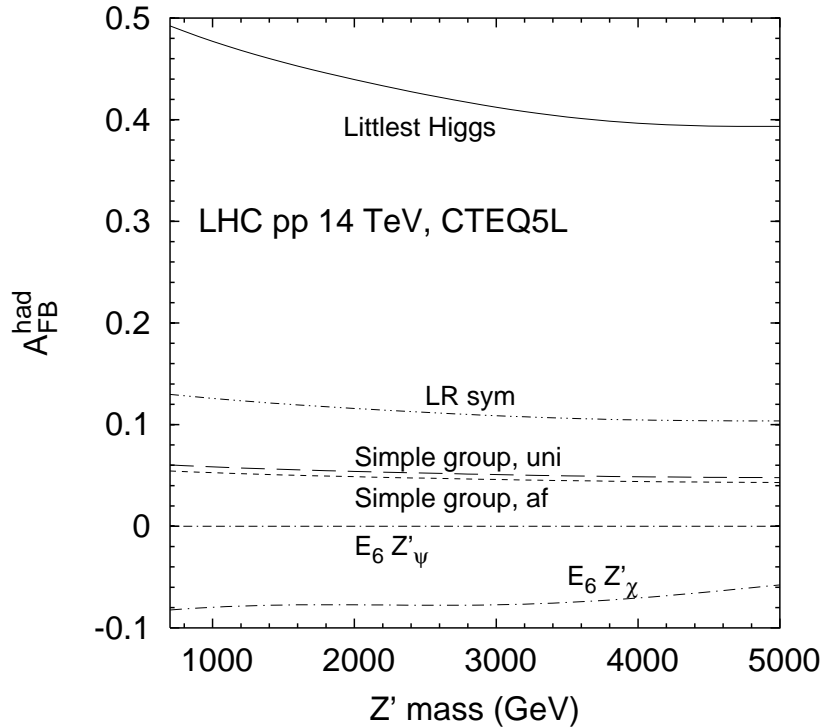
Figure 10: The hadronic forward-backward asymmetry A_{FB}^{had} as a function of $M_{Z'}$ for the models in Table 7. The curve for a sequential Z' is identical to the SU(3) simple group Z' with anomaly-free (af) fermion embedding.

extract these two quantities separately by fitting the asymmetry as a function of the Z' rapidity to high-precision measurements of the up and down quark parton densities [38]; however, this would require a huge amount of luminosity.

In the Littlest Higgs model, a measurement of A_{FB}^{had} would provide a spectacular test of the model because it would confirm that $\mathcal{A}_u = \mathcal{A}_d = \mathcal{A}_e = \pm 1$; that is, that the Z_H couplings to fermions are either purely left-handed or purely right-handed. The sign ambiguity is due to the fact that $A_{FB}^{0,if}$ depends on the product $\mathcal{A}_i \mathcal{A}_f$. Together with measurements of BR(tt)/BR(ee) and/or BR(bb)/BR(ee), which would demonstrate the

universality of the Z_H couplings to fermions, and the discovery of the $W_H^\pm$ degenerate in mass and with a related production rate, this measurement would confirm Z_H as a member of an SU(2) triplet of gauge bosons. In such a case we learn that the SM $SU(2)_L$ gauge symmetry arises from the diagonal breaking of $[SU(2)]^2$, with the SM fermion doublets transforming under one of the two SU(2) gauge groups. A measurement of $A_{FB}^{\rm had}$ will also provide a test of the SU(3) simple group model and the other Z' models considered, since it probes another independent combination of the Z' couplings to fermions.

4.5.4 Bosonic decay modes

Measuring the bosonic decay modes $Z' \to ZH$ and $Z' \to W^+W^-$ probes the transformation properties of the Higgs doublet under the extended gauge symmetry and the mixing of Z and Z' induced by electroweak symmetry breaking. As described in detail in Sec. 4.4, this can shed light on the little Higgs mechanism in the gauge sector, but it also provides useful information about the model structure. Also of interest are bosonic decay modes of the Z' involving non-SM bosons in the final state, such as $Z' \to Y\eta$ in the SU(3) simple group model or $Z_H \to A_H H$ in the Littlest Higgs model. Detecting and measuring the branching fractions of these decay modes provides additional information on the structure of the extended gauge group and the mixings among the new gauge bosons.

5. Other phenomenological features of the SU(3) simple group model

In this section we collect some additional features of the SU(3) simple group model not directly relevant to the simple group/product group classification and the identification of the little Higgs mechanism.

5.1 The heavy leptons

In the SU(3) simple group model, the three lepton doublets of the SM are enlarged into triplets. The model thus contains three heavy neutral states N_m. The scalar interactions of the leptons can be written as

$$\mathcal{L}_Y = i\lambda_{N_m} N_m^c \Phi_2^\dagger L_m + \frac{i\lambda_e^{mn}}{\Lambda} e_m^c \epsilon_{ijk} \Phi_1^i \Phi_2^j L_n^k + \text{h.c.}, \tag{5.1}$$

where $m, n = 1, 2, 3$ are generation indices, $i, j, k = 1, 2, 3$ are SU(3) indices, $L_m = (\nu, e, iN)_m^T$ are the lepton triplets, and N_m^c are right-handed neutral leptons that marry the N_m and get masses of order $f \sim$ TeV. We neglect neutrino masses; a nice extension of the SU(3) simple group model including neutrino masses was presented in Ref. [44].

Equation (5.1) generates masses for N_m,

$$M_{N_m} = \lambda_{N_m} s_\beta f. \tag{5.2}$$

The Lagrangian also contains a term

$$\mathcal{L}_Y \supset -\frac{\lambda_{N_m} c_\beta}{\sqrt{2}} H N_m^c \nu + \text{h.c.} = -\frac{M_{N_m}}{\sqrt{2} f t_\beta} H N_m^c \nu + \text{h.c.} \tag{5.3}$$

for each generation, leading to mixing between the N_m and the SM neutrinos given by $N = N_0 - \delta_\nu \nu_0$, where N_0, ν_0 denote the electroweak eigenstates of each generation and δ_ν was given in Eq. (3.5). This mixing gives rise to the couplings of N to eW and νZ with Feynman rules

$$W_\mu^+ \overline{N} e : \; \frac{ig\delta_\nu}{\sqrt{2}} \gamma_\mu P_L, \qquad\qquad Z_\mu \overline{N} \nu : \; \frac{ig\delta_\nu}{2c_W} \gamma_\mu P_L. \qquad (5.4)$$

Because the N_m carry lepton number, their production at the LHC requires an additional lepton in the final state and can thus proceed only through s-channel gauge boson exchange, e.g., $q\bar{q}' \to W^{+*} \to Ne^+$. Their decays, into νH, eW and νZ, along with eX, νY and $\nu\eta$ if kinematically accessible, will be spectacular. The N_m could also be produced at a linear collider of sufficient energy through t-channel W exchange, $e^+e^- \to \bar{\nu}N$.

5.2 The X and Y gauge bosons

The heavy gauge bosons X^-, Y^0 correspond to the off-diagonal broken generators of SU(3) and thus communicate between the SU(2)$_L$ doublet fermions and the SU(2)$_L$ singlets, with couplings of gauge strength of the form XQq' and YQq as summarized in Table 2. These couplings can play a role in T or Q decay if the corresponding final states are kinematically accessible. They will not play a significant role in single T or Q production because the initial-state couplings of X^-, Y^0 to pairs of SM fermions are suppressed by v/f. While X^-, Y^0 could be produced in association with T or Q, e.g., $b \to TX^-$, these processes have two TeV-mass particles in the final state and will be limited by phase space.

The production cross sections of the X and Y gauge bosons in Drell-Yan are very small. We thus consider other ways of producing these particles. If they are light enough, X and Y can be produced in the decays of the TeV-scale quark partners:

$$T \to X^+ b, \overline{Y}^0 t, \qquad\qquad U_j \to X^+ d_j, \overline{Y}^0 u_j \qquad \text{or} \qquad D_j \to X^- u_j, Y^0 d_j. \qquad (5.5)$$

For example, taking $M_T = 1$ TeV, $M_Y = 0.9$ TeV and $\lambda_T = 1$, we find $(T \to t\overline{Y}^0$ is kinematically forbidden for these masses),

$$\text{BR}(T \to bX^+) \simeq 0.55\%. \qquad (5.6)$$

Similarly, X and Y can be produced through the decays of the heavy lepton partners, $N \to X^+\ell^-, \overline{Y}^0\nu$. The X and Y bosons can also be pair produced by electroweak interactions via the triple gauge couplings in Table 3; however, pair production of these TeV-scale particles will suffer from reduced phase space and off-shell s-channel propagators compared to Drell-Yan production of the Z'.

If they are heavy enough, X and Y can decay to one SM fermion and one TeV-scale fermion partner,

$$\begin{array}{lll} X^+ \to T\overline{b}, U_j \overline{d}_j, N_i\ell^+, & Y^0 \to t\overline{T}, u_j \overline{U}_j, \nu_i \overline{N}_i & \text{(universal)} \\ X^+ \to T\overline{b}, u_j \overline{D}_j, N_i\ell^+, & Y^0 \to t\overline{T}, d_j \overline{D}_j, \nu_i \overline{N}_i & \text{(anomaly free).} \end{array} \qquad (5.7)$$

Neglecting the SM fermion mass, the partial widths for these decays are given by

$$\Gamma(V \to F\bar{f}) = \frac{N_c g^2}{32\pi} \beta^2 \left[1 - \frac{\beta}{3}\right] M_V = 4.2 \, N_c \beta^2 \left[1 - \frac{\beta}{3}\right] \left(\frac{M_V}{\text{TeV}}\right) \text{GeV}, \qquad (5.8)$$

where $N_c = 1$ or 3 is the number of colors and $\beta = (1 - M_F^2/M_V^2)$. This decay mode and the production in Eq. (5.5) are mutually exclusive, depending on the relative masses of X, Y and the TeV-scale fermion partners.

If the decay to one SM fermion and one TeV-scale fermion partner is kinematically inaccessible, X and Y can decay to pairs of SM fermions through their mixings with the TeV-scale fermion partners, with partial widths proportional to $\delta_t^2, \delta_\nu^2 \propto v^2/f^2$. The decays of X are independent of the fermion embedding,

$$X^- \to b\bar{t}, d_j\bar{u}_j, \ell^-\bar{\nu}, \tag{5.9}$$

while the decays of Y depend on the fermion embedding, since Y can decay only to fermions that mix with a heavy partner:

$$Y^0 \to t\bar{t}, u_j\bar{u}_j, \nu\bar{\nu} \quad \text{(universal)}, \qquad Y^0 \to t\bar{t}, d_j\bar{d}_j, \nu\bar{\nu} \quad \text{(anomaly free)}. \tag{5.10}$$

Unfortunately, there are no decays of Y to charged dileptons because N_i mix only with the neutrinos. The decays $Y^0 \to t\bar{t}$, $X^- \to b\bar{t}$ are controlled by δ_t, while the decays to the first two quark generations and to the leptons are controlled by the smaller δ_ν. Thus, decays to third generation quarks will have a somewhat larger partial width. Neglecting final-state masses, the relevant partial widths are

$$\Gamma(X^- \to b\bar{t}) = \Gamma(Y^0 \to t\bar{t}) = \frac{3g^2}{48\pi}\delta_t^2 M_Y = 0.51\lambda_T^2 \left(\frac{\text{TeV}}{M_T}\right)^2 \left(\frac{M_Y}{\text{TeV}}\right) \text{GeV},$$

$$\Gamma(X^- \to jj) = \Gamma(Y^0 \to jj) = 2\frac{3g^2}{48\pi}\delta_\nu^2 M_Y = \frac{0.11}{t_\beta^2}\left(\frac{\text{TeV}}{M_Y}\right) \text{GeV},$$

$$\Gamma(X^- \to \ell\bar{\nu}) = \Gamma(Y^0 \to \nu\bar{\nu}) = 3\frac{g^2}{48\pi}\delta_\nu^2 M_Y = \frac{0.054}{t_\beta^2}\left(\frac{\text{TeV}}{M_Y}\right) \text{GeV}, \tag{5.11}$$

where jj denote jets from quarks of the first two generations and the decays to leptons are summed over all three generations. Finally, Y can decay to $H\eta$ via the coupling in the last row of Table 4,

$$\Gamma(Y^0 \to H\eta) = \Gamma(\overline{Y}^0 \to H\eta) = \frac{g^2 M_Y}{384\pi} = 0.35\left(\frac{M_Y}{\text{TeV}}\right) \text{GeV}. \tag{5.12}$$

5.3 The singlet pseudoscalar η

The scalar sectors of little Higgs models are very model-dependent. For completeness, however, we briefly sketch here the decay modes of the singlet (pseudo-)scalar η in the SU(3) simple group model. A more detailed analysis of the η phenomenology can be found in Ref. [41]. The singlet scalar η, which naturally gets a mass of a couple hundred GeV, can decay to pairs of SM fermions with couplings that depend on the SM fermion masses. These couplings receive contributions from the usual fermion Yukawa couplings, via the expansion of the nonlinear sigma model fields, and from the couplings of η to a SM fermion and its TeV-scale partner combined with the F–f mixing. These couplings are all of order m_f/f, that is, suppressed by v/f relative to the usual fermion Yukawa couplings. The η

can also decay into a Higgs boson and an off-shell Y, which then decays to a pair of SM fermions with couplings suppressed by the F–f mixing. We expect the decays of η into pairs of fermions to dominate, with branching fractions proportional to the fermion masses up to order-one factors related to the contribution from the F–f mixing. The total width of η will be suppressed by v^2/f^2 compared to that of a "bosophobic" Higgs of the same mass; however, this width will be too narrow to measure directly and too wide to give rise to displaced vertices, and thus can only be probed through production cross sections.

6. Conclusions

The little Higgs models represent a new approach to electroweak symmetry breaking that will be accessible at future high-energy colliders. These models stabilize the hierarchy between a relatively low cutoff scale ~ 10 TeV and the electroweak scale by making the Higgs a pseudo-Goldstone boson of a spontaneously broken approximate global symmetry. Implementing such a global symmetry requires enlarging the gauge, fermion and scalar sectors of the SM. Little Higgs models therefore predict new gauge bosons, fermions and scalars at or below the TeV scale, which offer exciting possibilities for beyond-the-SM collider phenomenology at the LHC.

However, many models of physics beyond the SM contain new gauge bosons, fermions, and/or scalars at or below the TeV scale. If such particles are discovered, one will want to know whether they implement the little Higgs mechanism by canceling the one-loop quadratic divergence in the Higgs mass due to the SM gauge bosons, top quark, and Higgs quartic coupling.

We categorized the many little Higgs models into two classes based on the structure of the extended electroweak gauge group:

(a) product group models, in which the SM $SU(2)_L$ gauge group arises from the diagonal breaking of two or more gauge groups, and

(b) simple group models, in which the SM $SU(2)_L$ gauge group arises from the breaking of a single larger gauge group down to an $SU(2)$ subgroup.

As prototypes of each class, we studied the experimental signatures of the Littlest Higgs model and the $SU(3)$ simple group model, respectively.

The "smoking guns" for the little Higgs mechanism – the cancellation of the Higgs mass quadratic divergences between loops of SM particles and loops of the new particles – are quite straightforward and allow one to distinguish models that implement the little Higgs mechanism from other models that have a similar superficial phenomenology. In the top sector, the little Higgs mechanism appears as a sum rule involving the top quark Yukawa coupling, the TtH or TbW coupling λ_T, and the dimension-five $TTHH$ coupling λ'_T. In product group models, the simple structure of the top mass generation mechanism ensures that λ'_T can be expressed in terms of λ_T, M_T and the top Yukawa coupling. The little Higgs mechanism can then be checked by measuring λ_T and M_T, computing the condensate f, and comparing with f from the gauge sector. In simple group models, on the other hand,

the top mass generation mechanism is slightly more complicated and involves two (or more) TeV-scale condensates. This introduces an extra free parameter into the top sector (which can be chosen as the ratio of the two condensates, $f_2/f_1 \equiv t_\beta$), so that all three parameters λ_T, λ'_T, and M_T must be measured in the top sector. We have not found a way to measure λ'_T directly at the LHC. Instead, the required third parameter can be measured from the production rate of the TeV-scale quarks associated with the first two generations in the simple group models. These measurements of the extended top sector and the TeV-scale quark partners of the first two generations, if present, thus allow one to test the little Higgs mechanism in the top sector, distinguish the structure of the top quark mass generation mechanism, and extract the model parameters that control the fermion sector. We showed explicitly how these measurements allow one to distinguish the top sector of a little Higgs model from a fourth-generation top-prime and from a top see-saw model.

In the gauge sector, the little Higgs mechanism appears as a sum rule involving the Higgs boson coupling to pairs of SM vector bosons and to pairs of the new TeV-scale vector bosons. The couplings involved in the sum rule can be directly measured via $q\bar{q} \to V'^* \to V'H$ associated production. Measurement of these couplings allows one to test which new particles are responsible for canceling each of the SM contributions to the Higgs mass-squared quadratic divergence. In product group models, the test of the little Higgs mechanism is particularly simple because of the collective breaking structure of the Higgs couplings to gauge bosons: it is enough to measure the $Z_H Z H$ ($W_H W H$) couplings, which are accessible through $Z_H \to ZH$ ($W_H \to WH$) decays. The simple group models have a different collective breaking structure in the gauge sector, however, so that a direct measurement of the $V'V'H$ couplings is necessary. Additional measurements in the gauge sector will shed light on the structure of the extended electroweak gauge group. We showed explicitly how measurements of the properties of a Z' allow one to distinguish the Z' states present in little Higgs models from the Z's in the E_6 and left-right symmetric models and from a sequential Z'.

The scalar sector is very model dependent. It depends on the global symmetry structure; therefore the classification of models into product group and simple group does not give a useful classification of the scalar sector phenomenology.

Acknowledgments

A. Survey of little Higgs models

A.1 Product group models

The majority of little Higgs models are product group models. In addition to the Littlest Higgs, these include the theory space models (the Big Moose [1] and the Minimal Moose [2]), the SU(6)/Sp(6) model of Ref. [4], and two extensions of the Littlest Higgs with built-in custodial SU(2) symmetry [6, 8]. There are also product group models with T-parity in the literature [17, 18, 19, 20]; however, we do not address them here in any detail. In general, the phenomenology of models with T-parity is quite different from that discussed here; however, the top partner is typically T-parity even so that its phenomenology can be taken over directly from the Littlest Higgs case.

We start with the theory space models. The Minimal Moose [2] consists of two sites (where the gauge groups live) connected by four link fields (scalar fields transforming under the gauge groups at either end of the link). The electroweak gauge symmetry at one site is SU(2)×U(1), while at the other it is SU(3) [or alternatively, a second copy of SU(2)×U(1); electroweak precision constraints [42] favor this second possibility]. The diagonal breaking of the gauge symmetry down to $SU(2)_L \times U(1)_Y$ leaves a set of SU(3) gauge bosons [alternatively the broken SU(2)×U(1) gauge bosons] at the TeV scale. The top quark mass is generated by an interaction of the same form as Eq. (2.1), leaving a heavy charge 2/3 electroweak singlet quark at the TeV scale. The scalar spectrum consists of two Higgs doublets, a complex triplet and a complex singlet at the weak scale, with an additional Higgs doublet, triplet, and singlet at the TeV scale. The Big Moose [1] is an extended version of this structure, with a longer chain of gauge groups connected by link fields that break down to the diagonal SU(2)×U(1), leaving a larger number of broken gauge generators at the TeV scale. Many different theory space structures yield the little Higgs mechanism, with only mild topological constraints on the shape of the theory space [43]. In particular, the theory space can be chosen such that the low-energy theory contains only two Higgs doublets, giving the extra light scalars of the Minimal Moose masses at the TeV scale [43]. Theory space models always contain at least two light Higgs doublets.

The SU(6)/Sp(6) model [4] is similar to the Littlest Higgs, but starting with a global SU(6) symmetry broken down to Sp(6) at the TeV scale by an antisymmetric condensate. A subgroup [SU(2)×U(1)]^2 of the global symmetry is gauged; the gauge symmetry is broken down to $SU(2)_L \times U(1)_Y$ by the condensate, leaving a set of SU(2)×U(1) gauge bosons at the TeV scale. The top quark mass is generated in exact analogy to Eq. (2.1), leaving a heavy charge 2/3 electroweak singlet quark at the TeV scale. The scalar spectrum consists of two light Higgs doublets, plus a complex singlet at the TeV scale.

The extensions of the Littlest Higgs with built-in custodial SU(2) symmetry [6, 8] were constructed in order to avoid some of the electroweak precision constraints on the Littlest Higgs model [25, 26, 21]. The first such extension is a hybrid of the Littlest Higgs and the Minimal Moose with an SO(5)×[SU(2)×U(1)] gauge symmetry [6]. It contains two light Higgs doublets, plus additional scalars at the TeV scale due to the enlarged global symmetry. It also contains extra TeV-scale gauge bosons from the enlarged gauge symmetry. The second such extension expands the global symmetry group to SO(9), spontaneously

broken down to SO(5)×SO(4) [8]. This model contains only a single light Higgs doublet, with three scalar triplets and a singlet at the TeV scale. The gauge symmetry is [SU(2)$_L$×SU(2)$_R$]×[SU(2)×U(1)], broken down to the SM electroweak gauge group by the symmetry breaking condensate. The model thus contains extra TeV-scale gauge bosons compared to the Littlest Higgs. The top sectors of both extensions are identical to that of the Littlest Higgs.

The product group models all share two features. First, the models all contain a set of SU(2) gauge bosons at the TeV scale, obtained from the diagonal breaking of two gauge groups down to SU(2)$_L$. Some models contain additional TeV-scale gauge bosons as well, from the breaking of more than two SU(2) gauge groups or from the breaking of gauge groups larger than SU(2). Second, the models all generate the top quark mass from a Lagrangian involving two terms, only one of which couples to the scalar sector of the model. This results in an extended top quark sector of the same form as in the Littlest Higgs model. These two features distinguish the product group models from the simple group models, which we consider next.

A.2 Simple group models

In addition to the SU(3) simple group model, there are two other simple group models in the literature to date: the SU(4) simple group model [5] and the SU(9)/SU(8) model of Ref. [7]. These two models depart from the SU(3) simple group model in different directions.

The SU(4) simple group model [5] is a straightforward extension of the SU(3) model to the electroweak gauge group SU(4)×U(1)$_X$. It was introduced because the simplest version of the SU(3) model generates a Higgs quartic coupling only at one-loop level through the Coleman-Weinberg potential, leading to a too-light Higgs boson [5]. This problem can be fixed by adding an extra term to the scalar Lagrangian [9], which explicitly breaks a global U(1) symmetry in the model (and has the added benefit of giving mass to the η pseudoscalar, which would otherwise be a Nambu-Goldstone boson). The SU(4) model, on the other hand, generates a Higgs quartic coupling at tree-level, so the Higgs mass is easily large enough.

In the SU(4) simple group model the isospin doublets of the SM are all extended to quadruplets under SU(4). A total of four scalar quadruplets are needed to break SU(4)×U(1)$_X$ down to SU(2)$_L$×U(1)$_Y$, which leads to extra light scalars so that the low-energy theory contains two light Higgs doublets and two real singlets, plus three complex singlets which get masses of order $f \sim$ TeV. The potential generated for the two Higgs doublets is not the most general possible, yielding interesting relations among the Higgs masses and couplings; in fact, the potential for the two Higgs doublets is of the same form as the one in the SU(6)/Sp(6) product group model. There are now four symmetry breaking vevs, $f_{1,...,4}$. The fermion sector contains two heavy quark-partners and two heavy lepton-partners for each generation. Only one of the heavy quark-partners in each generation mixes with the corresponding SM quark. Like in the SU(3) model, the fermions can be embedded in a universal (but anomalous) way into SU(4) or in an anomaly-free way [22]. Again, the anomaly-free embedding only works if the number of fermion generations is a

multiple of three. The heavy gauge sector contains the broken generators of SU(4)→SU(2), namely two neutral gauge bosons Z' and Z'' (which mix in general), two complex SU(2) doublets (Y^0, X^-), $(Y^{0\prime}, X^{-\prime})$, and a complex SU(2) singlet $Y^{0\prime\prime}$. The phenomenology of the first Z' and the first doublet (Y^0, X^-) are similar to those of the SU(3) model.

The SU(9)/SU(8) model of Ref. [7] contains exactly the same gauge group and fermion sector as the SU(3) simple group model. Thus the gauge and fermion sectors contain the same particle content and interactions as in the SU(3) simple group model. The only difference is the global symmetry structure, which leads to a different scalar sector. The global symmetry group is SU(9), broken down to SU(8) by a vacuum condensate with two independent vevs, $f_{1,2}$. The Higgs quartic coupling in this model is generated at tree level by Lagrangian terms that explicitly break the SU(9) global symmetry. The scalar sector contains two light Higgs doublets, plus two complex singlets that get masses of order $f \sim$ TeV. As in the SU(4) model, the potential generated for the two Higgs doublets is far from the most general possible, yielding interesting relations among the Higgs masses and couplings.

The simple group models share two features which distinguish them from the product group models. First, the models all contain an SU(N)×U(1) gauge symmetry that is broken down to SU(2)$_L$×U(1)$_Y$, yielding the TeV-scale gauge bosons. The gauge couplings of the expanded SU(N)×U(1) symmetry are thus fixed in terms of the known SM gauge couplings. The gauge structure also forbids mixing between the SM $W^\pm$ bosons and the TeV-scale gauge bosons, in contrast to the product group models. Second, the top quark mass is generated from a Lagrangian involving two terms, which couple the top quark to two different nonlinear sigma model fields. This structure introduces an additional parameter into the top sector, which complicates the phenomenology and allows the heavy top-partner to be made lighter relative to the TeV-scale gauge bosons than in the product group models, thereby reducing the fine-tuning.

B. The SU(3) simple group model

In this Appendix we collect some technical details of the SU(3) simple group model of Refs. [5, 9] and derive the interaction Lagrangian in the mass basis.

The SU(3) simple group model [5, 9] is constructed by enlarging the SM SU(2)$_L$×U(1)$_Y$ gauge group to SU(3)×U(1)$_X$. This requires enlarging the SU(2) doublets of the SM to SU(3) triplets and adding the additional SU(3) gauge bosons. The SU(3)×U(1)$_X$ gauge symmetry is broken down to the SM electroweak gauge group by two complex scalar fields $\Phi_{1,2}$, which are triplets under the SU(3) with aligned vevs $f_{1,2}$, both of order a TeV. We start with a scalar potential for $\Phi_{1,2}$ which has a [SU(3)×U(1)]^2 global symmetry. After $\Phi_{1,2}$ acquire vevs, the global symmetry is spontaneously broken down to [SU(2)×U(1)]^2. At the same time, the global symmetry is broken explicitly down to its diagonal SU(3)×U(1) subgroup by the gauge interactions. The scalar fields are parameterized as a nonlinear

sigma model with

$$\Theta = \frac{1}{f}\left[\begin{pmatrix} 0 & 0 & h \\ 0 & 0 & \\ h^\dagger & 0 \end{pmatrix} + \frac{\eta}{\sqrt{2}}\begin{pmatrix} 1 & 0 & 0 \\ 0 & 1 & 0 \\ 0 & 0 & 1 \end{pmatrix}\right], \qquad h = \begin{pmatrix} h^0 \\ h^- \end{pmatrix}, \qquad (B.1)$$

and

$$\Phi_1 = e^{i\Theta f_2/f_1}\begin{pmatrix} 0 \\ 0 \\ f_1 \end{pmatrix} = fc_\beta\left[\begin{pmatrix} 0 \\ 0 \\ 1 \end{pmatrix} + \frac{it_\beta}{f}\begin{pmatrix} h \\ \eta/\sqrt{2} \end{pmatrix} - \frac{t_\beta^2}{2f^2}\begin{pmatrix} \sqrt{2}\eta h \\ h^\dagger h + \eta^2/2 \end{pmatrix} + \cdots\right], (B.2)$$

$$\Phi_2 = e^{-i\Theta f_1/f_2}\begin{pmatrix} 0 \\ 0 \\ f_2 \end{pmatrix} = fs_\beta\left[\begin{pmatrix} 0 \\ 0 \\ 1 \end{pmatrix} - \frac{i}{t_\beta f}\begin{pmatrix} h \\ \eta/\sqrt{2} \end{pmatrix} - \frac{1}{2t_\beta^2 f^2}\begin{pmatrix} \sqrt{2}\eta h \\ h^\dagger h + \eta^2/2 \end{pmatrix} + \cdots\right].$$

We define $f^2 \equiv f_1^2 + f_2^2$ and $t_\beta \equiv \tan\beta = f_2/f_1$. Under the $SU(2)_L$ SM gauge group, h transforms as a doublet and will be identified as the SM Higgs doublet with a vev $v \equiv \sqrt{2}\langle h^0 \rangle = 246$ GeV, while η is a real singlet which also remains light. We have chosen η proportional to the unit matrix because this state remains unmixed with the unphysical (eaten) Goldstone bosons after EWSB.[7] We do not write down the Goldstone bosons that are eaten by the broken gauge generators.

The $SU(3)$ gauge bosons can be written in matrix form as

$$A^a T^a = \frac{A^3}{2}\begin{pmatrix} 1 & & \\ & -1 & \\ & & 0 \end{pmatrix} + \frac{A^8}{2\sqrt{3}}\begin{pmatrix} 1 & & \\ & 1 & \\ & & -2 \end{pmatrix} + \frac{1}{\sqrt{2}}\begin{pmatrix} & W^+ & Y^0 \\ W^- & & X^- \\ \overline{Y}^0 & X^+ & \end{pmatrix}. \qquad (B.3)$$

The Φ vevs break the $SU(3)\times U(1)_X$ gauge symmetry down to the SM $SU(2)_L\times U(1)_Y$ via the covariant derivative term

$$\mathcal{L}_\Phi = \left|\left(\partial_\mu + igA_\mu^a T^a - \frac{ig_x}{3}B_\mu^x\right)\Phi_i\right|^2, \qquad (B.4)$$

where the $SU(3)$ gauge coupling g is equal to the SM $SU(2)_L$ gauge coupling and the $U(1)_X$ gauge coupling g_x is fixed in terms of g and the weak mixing angle $t_W \equiv \tan\theta_W$ by

$$g_x = \frac{gt_W}{\sqrt{1 - t_W^2/3}}. \qquad (B.5)$$

The broken gauge generators get masses of order $f \sim$ TeV and consist of a Z' boson (a linear combination of A^8 and B^x) and a complex $SU(2)_L$ doublet (Y^0, X^-).

B.1 Gauge and Higgs sectors

Before EWSB, the X and Y gauge bosons and a linear combination Z' of the A^8 and B^x gauge bosons get masses from the f vevs. The linear combination Z' that becomes massive is

$$Z_0' = \frac{\sqrt{3}gA^8 + g_x B^x}{\sqrt{3g^2 + g_x^2}} = \frac{1}{\sqrt{3}}\left(\sqrt{3 - t_W^2}A^8 + t_W B^x\right). \qquad (B.6)$$

---

[7]We thank Dave Rainwater for enlightening discussions on this point.

We denote states and masses before EWSB with the subscript zero. The orthogonal combination of A^8 and B^x becomes the hypercharge gauge boson B,

$$B = \frac{-g_x A^8 + \sqrt{3}g B^x}{\sqrt{3g^2 + g_x^2}} = \frac{1}{\sqrt{3}}\left(-t_W A^8 + \sqrt{3 - t_W^2} B^x\right). \tag{B.7}$$

Hypercharge is given by

$$Y = -\frac{1}{\sqrt{3}}T^8 + Q_x, \qquad T^8 = \frac{1}{2\sqrt{3}}\mathrm{diag}(1,1,-2), \tag{B.8}$$

where $Q_x = -1/3$ for the scalar fields Φ_i. We also have the relations

$$A^3 = c_W Z_0 + s_W A, \qquad A^8 = \sqrt{1 - t_W^2/3}\, Z_0' + \frac{s_W^2}{\sqrt{3}c_W}Z_0 - \frac{s_W}{\sqrt{3}}A$$

$$B^x = \frac{t_W}{\sqrt{3}}Z_0' - s_W\sqrt{1 - t_W^2/3}\, Z_0 + c_W\sqrt{1 - t_W^2/3}\, A, \tag{B.9}$$

where A is the photon.

For use in precision corrections, we give the W and Z boson masses and their couplings to the Higgs at next-to-leading order in v^2/f^2 in Table 8. The WWH and ZZH couplings can be written in the form

$$\mathcal{L} = 2\frac{M_W^2}{v}y_W W^+ W^- H + \frac{M_Z^2}{v}y_Z ZZH, \tag{B.10}$$

with coefficients $y_{W,Z}$ given in Table 8.

M_W	$\frac{gv}{2}\left[1 - \frac{v^2}{12f^2}\left(\frac{s_\beta^4}{c_\beta^2} + \frac{c_\beta^4}{s_\beta^2}\right)\right]$
M_Z	$\frac{gv}{2c_W}\left[1 - \frac{v^2}{12f^2}\left(\frac{s_\beta^4}{c_\beta^2} + \frac{c_\beta^4}{s_\beta^2}\right) + \frac{v^2}{16f^2}(1 - t_W^2)^2\right]$
$W_\mu^+ W_\nu^- H$:	$\frac{ig^2 v}{2}\left[1 - \frac{v^2}{3f^2}\left(\frac{s_\beta^4}{c_\beta^2} + \frac{c_\beta^4}{s_\beta^2}\right)\right]g_{\mu\nu}$
$W_\mu^+ W_\nu^- HH$:	$\frac{ig^2}{2}\left[1 - \frac{v^2}{f^2}\left(\frac{s_\beta^4}{c_\beta^2} + \frac{c_\beta^4}{s_\beta^2}\right)\right]g_{\mu\nu}$
$Z_\mu Z_\nu H$:	$\frac{ig^2 v}{2c_W^2}\left[1 - \frac{v^2}{3f^2}\left(\frac{s_\beta^4}{c_\beta^2} + \frac{c_\beta^4}{s_\beta^2}\right) - \frac{v^2}{4f^2}(1 - t_W^2)^2\right]g_{\mu\nu}$
$Z_\mu Z_\nu HH$:	$\frac{ig^2}{2c_W^2}\left[1 - \frac{v^2}{f^2}\left(\frac{s_\beta^4}{c_\beta^2} + \frac{c_\beta^4}{s_\beta^2}\right) - \frac{v^2}{4f^2}(1 - t_W^2)^2\right]g_{\mu\nu}$
y_W	$1 + \frac{v^2}{f^2}\left[-\frac{1}{6}\left(\frac{s_\beta^4}{c_\beta^2} + \frac{c_\beta^4}{s_\beta^2}\right)\right]$
y_Z	$1 + \frac{v^2}{f^2}\left[-\frac{1}{6}\left(\frac{s_\beta^4}{c_\beta^2} + \frac{c_\beta^4}{s_\beta^2}\right) - \frac{3}{8}(1 - t_W^2)^2\right]$

Table 8: W and Z boson masses and their couplings to the Higgs at next-to-leading order in v^2/f^2 in the SU(3) simple group model.

B.2 Fermion sector

Because the model contains a gauged SU(3), SM fermions that are doublets under SU(2) must be expanded into triplets under the SU(3). In addition, new SU(3)-singlet fermions must be introduced to cancel the hypercharge anomalies and to marry and give mass to the new third components of the SU(3)-triplet fermions.

The most straightforward way to construct a fermion sector for the SU(3) simple group model is to expand all the SU(2) doublets of the SM into SU(3) triplets, adding additional SU(3)-singlet right-handed fermions as needed, as was done in Ref. [5]. We call this embedding "universal", since the three generations have identical quantum numbers. The quarks and leptons of each generation are put into $\mathbf{3}$ representations of SU(3):

$$Q_m^T = (u, d, iU)_m, \qquad iu_m^c, id_m^c, iU_m^c \qquad \text{(universal)}$$
$$L_m^T = (\nu, e, iN)_m, \qquad ie_m^c, iN_m^c, \qquad \text{(B.11)}$$

where m is the generation index. We do not include a right-handed neutrino at this stage, leaving the neutrinos massless. Neutrino masses could be incorporated, e.g., through a see-saw mechanism in the UV completion of the little Higgs model [5] or within the little Higgs theory itself [44]; however, this is beyond the scope of our current work. The Q_x charges of the fermions are given in Table 9.

	Universal embedding						
fermion	$Q_{1,2}$	Q_3	u_m^c, T^c, U_m^c	d_m^c	L_m	N_m^c	e_m^c
Q_x charge	1/3	1/3	$-2/3$	1/3	$-1/3$	0	1
SU(3) rep	$\mathbf{3}$	$\mathbf{3}$	$\mathbf{1}$	$\mathbf{1}$	$\mathbf{3}$	$\mathbf{1}$	$\mathbf{1}$
	Anomaly-free embedding						
fermion	$Q_{1,2}$	Q_3	u_m^c, T^c	d_m^c, D^c, S^c	L_m	N_m^c	e_m^c
Q_x charge	0	1/3	$-2/3$	1/3	$-1/3$	0	1
SU(3) rep	$\bar{\mathbf{3}}$	$\mathbf{3}$	$\mathbf{1}$	$\mathbf{1}$	$\mathbf{3}$	$\mathbf{1}$	$\mathbf{1}$

Table 9: The Q_x charges and SU(3) representations of the fermions in the universal and anomaly-free embeddings.

It was pointed out by Kong [22] that such a universal fermion sector leads to SU(3) and U(1)$_x$ gauge anomalies, although the SM SU(2) and U(1)$_Y$ gauge groups remain anomaly-free. These anomalies are not necessarily a problem because the little Higgs model is only an effective theory valid up to an energy scale $\Lambda \sim 4\pi f$. Additional fermions can be added at the scale Λ to cancel the SU(3) and U(1)$_x$ gauge anomalies without affecting the phenomenology at the f scale. Alternatively, one can construct a fermion sector that is anomaly-free already at the f scale and yet contains no more degrees of freedom than the universal embedding, as proposed by Kong [22]. This can be done by putting the first two generations of quarks in $\bar{\mathbf{3}}$ representations of SU(3), while the third quark generation and all three lepton generations are in $\mathbf{3}$s of SU(3). We call this embedding "anomaly-free". It is fascinating to note that with this fermion content, the anomalies do not cancel within a single generation, as in the SM, but rather three generations (or a multiple thereof) are

required to cancel the anomalies. The anomaly cancellation pattern of this fermion content has been previously pointed out in 3-3-1 models [23] outside of the little Higgs context.

The quarks of the third generation and three generations of leptons are put into **3** representations of SU(3), exactly as in the universal embedding. The first two generations of quarks are put into **3̄** representations of SU(3):

$$Q_1^T = (d, -u, iD), \qquad id^c, iu^c, iD^c \qquad \text{(anomaly free)}$$
$$Q_2^T = (s, -c, iS), \qquad is^c, ic^c, iS^c, \qquad\qquad \text{(B.12)}$$

where the minus signs in front of u and c are there because the **2̄** of SU(2) is $(d, -u)$ [which is equivalent to the **2**, (u, d)]. Notice that the heavy vector-like quarks of the first two generations have electric charge $-1/3$, in contrast to the charge $+2/3$ heavy quark of the third generation. The Q_x charges of the fermions are given in Table 9.

B.2.1 Lepton masses and mixing

The lepton sector is identical in both the universal and anomaly-free embeddings. The lepton masses are generated by the Lagrangian in Eq. (5.1), where we have chosen the flavor basis to correspond to the mass basis for the heavy neutrino partners N_m. The N_m masses are then given by Eq. (5.2). The dimension-5 operator in Eq. (5.1) normalized by the cutoff scale Λ gives masses to the charged leptons via the 3×3 Yukawa matrix λ_e^{mn}, which also generates a CKM-like mixing matrix V_{im}^ℓ between the charged lepton mass eigenstates e_i and the heavy neutrino partners N_m. This mixing matrix appears in the $X^- \bar{e}_i N_m$ couplings,

$$\mathcal{L} \supset -\frac{g}{\sqrt{2}} V_{im}^\ell X_\mu^- \bar{e}_i \gamma^\mu P_L N_m. \qquad (\text{B.13})$$

These couplings can lead to lepton flavor violating processes, such as $\mu \to e\gamma$, via loops of N_m and X^-. As in the quark sector of the SM, this lepton flavor violation will be GIM-suppressed and will vanish in the limit that V_{im}^ℓ is diagonal, so that the N_m mass eigenstates are aligned with the charged lepton mass eigenstates. The lepton flavor violation will also vanish in the limit that the N_m are degenerate. The experimental limits on lepton flavor violation therefore put stringent constraints on the λ_{N_m} couplings and/or on the structure of the λ_e^{mn} matrix.

After EWSB, the h vev induces mixing between N_{m0} and the corresponding neutrino ν_{m0} at order v/f, where as usual we use a subscript 0 to denote the SU(3) eigenstates and no subscript to denote the mass eigenstates after EWSB. Because of the structure of the N_m mass term in Eq. (5.1), N_m mixes only with the neutrino in the same SU(3) triplet, with a mixing angle δ_ν given in Eq. (3.5) that is the same for all three generations. Note that $t_\beta > 1$ suppresses δ_ν. The SU(3) eigenstates N_{m0} and ν_{i0} are given in terms of the mass eigenstates N_m and the SM neutrinos in the charged lepton mass basis $(\nu_i = \nu_e, \nu_\mu, \nu_\tau)$ by

$$N_{m0} = N_m + \delta_\nu V_{mi}^{\ell\dagger} \nu_i, \qquad \nu_{i0} = \left(1 - \frac{1}{2}\delta_\nu^2\right)\nu_i - \delta_\nu V_{im}^\ell N_m, \qquad (\text{B.14})$$

where we have kept the δ_ν^2 term in the neutrino mixing because it will modify the well-measured couplings of neutrinos to the W and Z bosons at order v^2/f^2. In particular,

the Fermi constant G_F is measured in muon decay. The four-Fermi effective interaction Lagrangian is

$$\mathcal{L} = -2\sqrt{2}G_F J^{+\mu}J^-_\mu = -\frac{g^2}{2M_W^2}J^{+\mu}J^-_\mu\left(1-\delta_\nu^2\right). \tag{B.15}$$

Plugging in M_W^2 (from Table 8) and δ_ν, we have,

$$\frac{1}{G_F} = \sqrt{2}v^2\left\{1+\frac{v^2}{f^2}\left[-\frac{1}{6}\left(\frac{s_\beta^4}{c_\beta^2}+\frac{c_\beta^4}{s_\beta^2}\right)+\frac{1}{2t_\beta^2}\right]\right\}. \tag{B.16}$$

The couplings of the scalars H and η to lepton pairs are given in Table 10. The couplings of charged leptons to H get a multiplicative correction factor y_ℓ relative to the SM Yukawa couplings in terms of the lepton mass due to the nonlinear sigma model expansion.

$H\overline{e}_ie_i$:	$-\frac{im_{e_i}}{v}y_\ell$
$H\overline{N}_m\nu_i$:	$-\frac{ic_\beta}{\sqrt{2}}\lambda_{N_m}V_{mi}^{\ell\dagger}P_L$
$H\overline{N}_mN_m$:	$\mathcal{O}(v^2/f^2)$
$\eta\overline{e}_ie_i$:	$\frac{\sqrt{2}m_{e_i}}{f}\cot2\beta\gamma_5$
$\eta\overline{N}_mN_m$:	$-\frac{c_\beta}{\sqrt{2}}\lambda_{N_m}\gamma_5$
y_ℓ	$1-\frac{v^2}{6f^2}\left(3+\frac{s_\beta^4}{c_\beta^2}+\frac{c_\beta^4}{s_\beta^2}\right)$

Table 10: Couplings of H and η to lepton pairs.

B.2.2 Lepton couplings to gauge bosons

The fermion couplings to gauge bosons are given by the fermion kinetic term,

$$\mathcal{L} = \bar{\psi}i\mathcal{D}_\mu\gamma^\mu\psi, \qquad \mathcal{D} = \partial + igA^aT^a + ig_xQ_xB^x, \tag{B.17}$$

with the Q_x charges given in Table 9. The generators T^a of the fundamental **3** representation of SU(3) are given in Eq. (B.3).

The couplings of the Z' to lepton pairs were given in Table 4. The couplings of the heavy off-diagonal gauge bosons $X^\mp$, Y^0 and $\overline{Y}^0$ to leptons were given in Table 2, neglecting flavor misalignment between the charged leptons and the N_m. Allowing for the possibility of flavor misalignment, we have

$$\mathcal{L}_{X,Y} = -\frac{g}{\sqrt{2}}\left[iX^-_\mu\bar{e}_i\gamma^\mu\left(V_{im}^\ell N_m + \delta_\nu\nu_i\right) + iY^0_\mu\bar{\nu}_i\gamma^\mu\left(V_{im}^\ell N_m + \delta_\nu\nu_i\right) + \text{h.c.}\right], \tag{B.18}$$

where all fermion fields are left-handed and we have taken the neutrinos in the charged lepton mass basis, $\nu_i = \nu_e, \nu_\mu, \nu_\tau$; N_m are the heavy neutral leptons in their mass basis. The couplings of $W^\pm$ to lepton pairs, keeping terms of order v^2/f^2 in interactions involving only SM particles and terms of order v/f in interactions involving one or more heavy particles, are

$$\mathcal{L}_W = -\frac{gW^+_\mu}{\sqrt{2}}\left[\left(1-\frac{1}{2}\delta_\nu^2\right)\overline{\nu}_i\gamma^\mu e_i - \delta_\nu V_{mi}^{\ell\dagger}\overline{N}_m\gamma^\mu e_i + \text{h.c.}\right]. \tag{B.19}$$

The couplings of the Z boson to leptons, including the corrections from mixing between Z and Z' and mixing between the heavy neutral leptons and the SM neutrinos, are

$$\mathcal{L}_Z = -Z_\mu\frac{g}{c_W}\left\{\left(J_3^\mu - s_W^2J_Q^\mu\right) - \frac{1}{2}\delta_\nu^2\overline{\nu}_i\gamma^\mu\nu_i - \frac{1}{2}\left[\delta_\nu V_{im}^{\ell*}\overline{N}_m\gamma^\mu\nu_i + \text{h.c.}\right]\right.$$

$$\left. + \frac{\delta_Z}{\sqrt{3-4s_W^2}}\left[\left(\frac{1}{2}-s_W^2\right)\left(\overline{\nu}_i\gamma^\mu\nu_i + \overline{e}_i\gamma^\mu e_i\right) + s_W^2\overline{e}_i^c\gamma^\mu e_i^c + \left(-1+s_W^2\right)\overline{N}_i\gamma^\mu N_i\right]\right\}, \tag{B.20}$$

where the leading-order coupling is given in terms of the standard fermion currents

$$J_3^\mu = \overline{f}\gamma^\mu T^3 f, \qquad\qquad J_Q^\mu = \overline{f}\gamma^\mu Q_f f - \overline{f}^c\gamma^\mu Q_{f^c} f^c. \tag{B.21}$$

The couplings of the photon to fermions are given by the electromagnetic current as usual, $\mathcal{L}_A = -A_\mu e J_Q^\mu$.

B.2.3 Quark masses and mixing: anomaly-free embedding

The quark sector is more complicated than the lepton sector because of the anomaly-free embedding structure. The relevant Lagrangian terms for the third generation and for the first two generations are

$$\mathcal{L}_3 = \lambda_1^t i u_1^c \Phi_1^\dagger Q_3 + \lambda_2^t i u_2^c \Phi_2^\dagger Q_3 + \frac{\lambda_b^m}{\Lambda} i d_m^c \epsilon_{ijk}\Phi_1^i \Phi_2^j Q_3^k + \text{h.c.}$$

$$\mathcal{L}_{1,2} = \lambda_1^{dn} i d_1^{nc} Q_n^T \Phi_1 + \lambda_2^{dn} i d_2^{nc} Q_n^T \Phi_2 + \frac{\lambda_u^{mn}}{\Lambda} i u_m^c \epsilon_{ijk}\Phi_1^{*i}\Phi_2^{*j}Q_n^k + \text{h.c.}, \tag{B.22}$$

where $n = 1, 2$; $i, j, k = 1, 2, 3$ are SU(3) indexes; u_1^c and u_2^c are linear combinations of t^c and T^c [see Eqs. (B.23) and (B.25) below]; b_m^c runs over all the down-type conjugate quarks $(d^c, s^c, b^c, D^c, S^c)$; d_1^{nc} and d_2^{nc} are linear combinations of d^c and D^c for $n = 1$ and of s^c and S^c for $n = 2$ [see Eqs. (B.26) and (B.28) below]; and u_m^c runs over all the up-type conjugate quarks (u^c, c^c, t^c, T^c).

The f vevs generate mass terms for three heavy quarks. The state

$$T^c = \frac{\lambda_1^t c_\beta u_1^c + \lambda_2^t s_\beta u_2^c}{\sqrt{\lambda_1^{t2}c_\beta^2 + \lambda_2^{t2}s_\beta^2}} \tag{B.23}$$

marries T, giving it a mass of

$$M_T = f\sqrt{\lambda_1^{t2}c_\beta^2 + \lambda_2^{t2}s_\beta^2} \tag{B.24}$$

and leaving the orthogonal combination of u_1^c and u_2^c massless:

$$t^c = \frac{-\lambda_2^t s_\beta u_1^c + \lambda_1^t c_\beta u_2^c}{\sqrt{\lambda_1^{t2}c_\beta^2 + \lambda_2^{t2}s_\beta^2}}. \tag{B.25}$$

The states (here we denote $\lambda_{1,2}^{dn}$ by $\lambda_{1,2}^d$ for $n = 1$ and by $\lambda_{1,2}^s$ for $n = 2$)

$$D^c = \frac{\lambda_1^d c_\beta d_1^{1c} + \lambda_2^d s_\beta d_2^{1c}}{\sqrt{\lambda_1^{d2}c_\beta^2 + \lambda_2^{d2}s_\beta^2}}, \qquad\qquad S^c = \frac{\lambda_1^s c_\beta d_1^{2c} + \lambda_2^s s_\beta d_2^{2c}}{\sqrt{\lambda_1^{s2}c_\beta^2 + \lambda_2^{s2}s_\beta^2}} \tag{B.26}$$

marry D and S, respectively, giving them masses of

$$M_D = f\sqrt{\lambda_1^{d2}c_\beta^2 + \lambda_2^{d2}s_\beta^2}, \qquad\qquad M_S = f\sqrt{\lambda_1^{s2}c_\beta^2 + \lambda_2^{s2}s_\beta^2}, \tag{B.27}$$

and leaving the orthogonal combinations massless:

$$d^c = \frac{-\lambda_2^d s_\beta d_1^{1c} + \lambda_1^d c_\beta d_2^{1c}}{\sqrt{\lambda_1^{d2}c_\beta^2 + \lambda_2^{d2}s_\beta^2}}, \qquad\qquad s^c = \frac{-\lambda_2^s s_\beta d_1^{2c} + \lambda_1^s c_\beta d_2^{2c}}{\sqrt{\lambda_1^{s2}c_\beta^2 + \lambda_2^{s2}s_\beta^2}}. \tag{B.28}$$

After EWSB, the quark mass terms are

$$\mathcal{L}_{\text{up mass}} = -M_T T^c T + \frac{v}{\sqrt{2}} \frac{s_\beta c_\beta (\lambda_1^{t2} - \lambda_2^{t2})}{\sqrt{\lambda_1^{t2} c_\beta^2 + \lambda_2^{t2} s_\beta^2}} T^c t - \frac{v}{\sqrt{2}} \frac{\lambda_1^t \lambda_2^t}{\sqrt{\lambda_1^{t2} c_\beta^2 + \lambda_2^{t2} s_\beta^2}} t^c t$$

$$+ \frac{v}{\sqrt{2}} \frac{f}{\Lambda} \lambda_u^{mn} u_m^c u_n + \text{h.c.} \tag{B.29}$$

$$\mathcal{L}_{\text{down mass}} = -M_D D^c D - \frac{v}{\sqrt{2}} \frac{s_\beta c_\beta (\lambda_1^{d2} - \lambda_2^{d2})}{\sqrt{\lambda_1^{d2} c_\beta^2 + \lambda_2^{d2} s_\beta^2}} D^c d + \frac{v}{\sqrt{2}} \frac{\lambda_1^d \lambda_2^d}{\sqrt{\lambda_1^{d2} c_\beta^2 + \lambda_2^{d2} s_\beta^2}} d^c d$$

$$- M_S S^c S - \frac{v}{\sqrt{2}} \frac{s_\beta c_\beta (\lambda_1^{s2} - \lambda_2^{s2})}{\sqrt{\lambda_1^{s2} c_\beta^2 + \lambda_2^{s2} s_\beta^2}} S^c s + \frac{v}{\sqrt{2}} \frac{\lambda_1^s \lambda_2^s}{\sqrt{\lambda_1^{s2} c_\beta^2 + \lambda_2^{s2} s_\beta^2}} s^c s$$

$$+ \frac{v}{\sqrt{2}} \frac{f}{\Lambda} \lambda_b^m d_m^c b + \text{h.c.} \tag{B.30}$$

where $u_n = u, c$; $u_m^c = u^c, c^c, t^c, T^c$; and $d_m^c = d^c, s^c, b^c, D^c, S^c$.

The couplings λ_u^{mn} and λ_b^m cause a misalignment between the mass eigenstates in the up and down sectors, leading to the CKM matrix. They also cause an analogous misalignment between the SM quark mass eigenstates and the heavy quarks D, S, and T, leading to an analogous matrix. We choose the "flavor basis" to be the mass basis for D, S, T. Two unitary matrices are needed to rotate the left-handed up- and down-type quarks from the flavor basis (primed fields) into the mass basis (unprimed fields):

$$V^u \begin{pmatrix} u' \\ c' \\ t' \end{pmatrix} = \begin{pmatrix} u \\ c \\ t \end{pmatrix}, \qquad V^d \begin{pmatrix} d' \\ s' \\ b' \end{pmatrix} = \begin{pmatrix} d \\ s \\ b \end{pmatrix}. \tag{B.31}$$

The CKM matrix is then given by

$$V^{\text{CKM}} = V^u V^{d\dagger}. \tag{B.32}$$

These matrices appear in the quark gauge couplings; see Sec. B.2.4 for details. Note that, in contrast to the SM, there are *two* physically meaningful mixing matrices.

Electroweak symmetry breaking also induces mixing between the heavy left-handed quarks D, S, T and the SM quarks. In the up-quark sector, the terms in Eq. (B.29) involving T^c lead to mixing between T and u, c, t that violates the SU(3) symmetry. As usual we use the subscript 0 to denote SU(3) states; fields with no subscript denote the mass eigenstates after the mixing induced by EWSB. We can rewrite the SU(3) state T_0 in terms of the mass eigenstate T and the SM fermions in the interaction basis (primed fields) as

$$T_0 = T + \delta_{u_i} u_i', \tag{B.33}$$

with $i = 1, 2, 3$, where

$$\delta_u = \frac{v}{\sqrt{2}\Lambda} \frac{\lambda_u^{T^c u}}{\sqrt{\lambda_1^{t2} c_\beta^2 + \lambda_2^{t2} s_\beta^2}}, \qquad \delta_c = \frac{v}{\sqrt{2}\Lambda} \frac{\lambda_u^{T^c c}}{\sqrt{\lambda_1^{t2} c_\beta^2 + \lambda_2^{t2} s_\beta^2}}, \qquad \delta_t = \frac{v}{\sqrt{2}f} \frac{s_\beta c_\beta (\lambda_1^{t2} - \lambda_2^{t2})}{(\lambda_1^{t2} c_\beta^2 + \lambda_2^{t2} s_\beta^2)}.$$

$$\tag{B.34}$$

One can choose the couplings $\lambda_u^{T^c u}$ and $\lambda_u^{T^c c}$ to be small in order to suppress the mixing effects in the first and second generations. In the mass basis (unprimed fields) this becomes

$$T_0 = T + \Delta_{u_i} u_i, \qquad \Delta_{u_i} = V_{ij}^{u*} \delta_{u_j} \simeq V_{i3}^{u*} \delta_t, \qquad (\text{B.35})$$

where in the last approximate equality we neglect $\lambda_u^{T^c u}$ and $\lambda_u^{T^c c}$. After mixing, the up quarks in the mass basis become

$$u_{i0} = \left(1 - \frac{1}{2} |\Delta_{u_i}|^2 \right) u_i - \Delta_{u_i} T, \qquad (\text{B.36})$$

where we have kept the $|\Delta_{u_i}|^2$ term (which is of order v^2/f^2) because it will modify the well-measured couplings of quarks to the W boson.

Similarly, in the down-quark sector, the terms in Eq. (B.30) involving D^c (S^c) lead to mixing between D and d, b (S and s, b). As in the up sector, we can rewrite the SU(3) states D_0 and S_0 in terms of the mass eigenstates D and S and the SM fermions in the interaction basis (primed fields) as

$$D_0 = D + \delta_{Dd_i} d_i', \qquad S_0 = S + \delta_{Sd_i} d_i', \qquad (\text{B.37})$$

with $i = 1, 2, 3$, where

$$\delta_{Dd} = \frac{-v}{\sqrt{2} f} \frac{s_\beta c_\beta (\lambda_1^{d2} - \lambda_2^{d2})}{(\lambda_1^{d2} c_\beta^2 + \lambda_2^{d2} s_\beta^2)}, \qquad \delta_{Ds} = 0, \qquad \delta_{Db} = \frac{v}{\sqrt{2}\Lambda} \frac{\lambda_b^{D^c}}{\sqrt{\lambda_1^{d2} c_\beta^2 + \lambda_2^{d2} s_\beta^2}},$$

$$\delta_{Sd} = 0, \qquad \delta_{Ss} = \frac{-v}{\sqrt{2} f} \frac{s_\beta c_\beta (\lambda_1^{s2} - \lambda_2^{s2})}{(\lambda_1^{s2} c_\beta^2 + \lambda_2^{s2} s_\beta^2)}, \qquad \delta_{Sb} = \frac{v}{\sqrt{2}\Lambda} \frac{\lambda_b^{S^c}}{\sqrt{\lambda_1^{s2} c_\beta^2 + \lambda_2^{s2} s_\beta^2}}. \qquad (\text{B.38})$$

The zero mixings, $\delta_{Ds} = \delta_{Sd} = 0$, are a consequence of the collective breaking mass generation for d and s in the D, S mass basis. One can choose $\lambda_b^{D^c}$ and $\lambda_b^{S^c}$ to be small in order to suppress the mixing effects in the b quark sector. From Eq. (B.30), the small mass of the d (s) quark requires one of the couplings $\lambda_{1,2}^d$ ($\lambda_{1,2}^s$) to be very small. We choose the small coupling to be λ_1^d (λ_1^s) so that the mixing effects in the down-quark sector are suppressed in the same $t_\beta > 1$ limit as the mixing effects in the neutrino sector. We then have,

$$\delta_{Dd} \simeq \delta_{Ss} \simeq \frac{v}{\sqrt{2} t_\beta f} = -\delta_\nu. \qquad (\text{B.39})$$

In the mass basis (unprimed fields), the D and S states become

$$D_0 = D + \Delta_{Dd_i} d_i, \qquad \Delta_{Dd_i} = V_{ij}^{d*} \delta_{Dd_j} \simeq -V_{i1}^{d*} \delta_\nu,$$
$$S_0 = S + \Delta_{Sd_i} d_i, \qquad \Delta_{Sd_i} = V_{ij}^{d*} \delta_{Sd_j} \simeq -V_{i2}^{d*} \delta_\nu, \qquad (\text{B.40})$$

where in the last approximate equalities we neglect $\lambda_b^{D^c}$ and $\lambda_b^{S^c}$. After mixing, the down quarks in the mass basis become

$$d_{i0} = \left(1 - \frac{1}{2} |\Delta_{Dd_i}|^2 - \frac{1}{2} |\Delta_{Sd_i}|^2 \right) d_i - \Delta_{Dd_i} D - \Delta_{Sd_i} S, \qquad (\text{B.41})$$

where we again have kept the $|\Delta_{Dd_i}|^2$ and $|\Delta_{Sd_i}|^2$ terms, which are of order v^2/f^2.

We now write the couplings of the scalars, H and η, to quark pairs, taking into account corrections from the expansion of the nonlinear sigma model and the mixing between the SM quarks and the heavy quarks. The different treatment of the third quark generation in the anomaly-free fermion embedding [Eq. (B.22)] leads to flavor-changing couplings of quarks to H (at order v^2/f^2) and to η (at order v/f). The full parameter dependence of the flavor changing couplings depends on the exact form of the up and down quark mass matrices, which determine the quark mixing in the left- and right-handed sectors. A detailed exploration of the quark mass matrices is beyond the scope of this work. Instead, we write down the scalar couplings ignoring the mixing of the right-handed top quark t^c with the first two generations.

We begin with the couplings of T quark pairs. T couples to η with a coupling of order one and to H with a coupling of order v/f:

$$\mathcal{L}_{T^cT} \simeq (HT^cT)\frac{v}{f}\left[(\lambda_1^{t2}s_\beta^2 + \lambda_2^{t2}c_\beta^2)\frac{f}{2M_T} - s_\beta^2 c_\beta^2(\lambda_1^{t2} - \lambda_2^{t2})^2\frac{f^3}{2M_T^3}\right]$$
$$+(i\eta T^cT)s_\beta c_\beta(\lambda_1^{t2} - \lambda_2^{t2})\frac{f}{\sqrt{2}M_T} + \text{h.c.,} \tag{B.42}$$

where we have neglected terms involving $\lambda_u^{T^cu}$ and $\lambda_u^{T^cc}$. Similarly, D and S quark pairs couple to η with a coupling of order one:

$$\mathcal{L}_{D_m^cD_m} \simeq \frac{c_\beta}{\sqrt{2}}\lambda_2^d(i\eta D^cD) + \frac{c_\beta}{\sqrt{2}}\lambda_2^s(i\eta S^cS) + \text{h.c.,} \tag{B.43}$$

where we have neglected terms involving $\lambda_b^{D^c}$ and $\lambda_b^{S^c}$ and taken $\lambda_1^{d,s} \ll \lambda_2^{d,s}$ [if the top quark mass were neglected, Eq. (B.42) would also reduce to this simple form]. One would naively expect an $HD_m^cD_m$ coupling at order v/f coming from replacing one Higgs field by its vev in the nonlinear sigma model expansion term $HHD_m^cD_m$; however, this term is exactly canceled by the contribution from $HD_m^cd_m$ after $d-D$ mixing if the down and strange quark masses are neglected.

The leading-order couplings of scalars to one T quark and one SM up-type quark are

$$\mathcal{L} \simeq (HT^cu_i)\left[s_\beta c_\beta(\lambda_1^{t2} - \lambda_2^{t2})\frac{f}{\sqrt{2}M_T}V_{i3}^{u*}\right] - (i\eta t^cT)\left[\frac{\lambda_1^t\lambda_2^tf}{\sqrt{2}M_T}\right] + \text{h.c.,} \tag{B.44}$$

where we again neglect terms involving $\lambda_u^{T^cu}$ and $\lambda_u^{T^cc}$ and in the last term ignore the mixing of the right-handed top quark t^c with the first two generations. The last term can be written in terms of SM quark masses and mixing angles via the relation (again ignoring right-handed quark mixing)

$$\frac{\lambda_1^t\lambda_2^tf}{\sqrt{2}M_T} = \sum_j \frac{m_{u_j}}{v}V_{j3}^{u*} \simeq \frac{m_t}{v}V_{33}^{u*}, \tag{B.45}$$

where we have used $m_u, m_c \ll m_t$. The couplings in Eq. (B.44) will lead to the decays $T \to tH$ and $T \to t\eta$.

The couplings of scalars to D, S and one SM down-type quark are

$$\mathcal{L} \simeq \frac{c_\beta}{\sqrt{2}} \lambda_2^d V_{i1}^{d*} (HD^c d_i) + \frac{c_\beta}{\sqrt{2}} \lambda_2^s V_{i2}^{d*} (HS^c d_i) + \text{h.c.,} \tag{B.46}$$

where we have neglected terms involving $\lambda_b^{D^c}$ and $\lambda_b^{S^c}$ and ignored couplings of η proportional to the down or strange quark masses. These couplings will lead to the decays $D, S \to d_i H$.

The couplings of scalars to a pair of SM up-type quarks (again ignoring right-handed quark mixing) are

$$\mathcal{L} = (Hu_i^c u_j) \left\{ \delta_{ij} \frac{-m_{u_i}}{v} \left[1 - \frac{v^2}{6f^2} \left(3 + \frac{s_\beta^4}{c_\beta^2} + \frac{c_\beta^4}{s_\beta^2} \right) \right] + \delta_{i3} \frac{m_t}{2\sqrt{2}f} V_{33}^{u*} \Delta_{u_j} \left(\frac{c_\beta^2 - s_\beta^2}{s_\beta c_\beta} \right) \right.$$

$$\left. - \delta_{i3} V_{j3}^{u*} \frac{v m_t}{2f^2} V_{33}^{u*} + \delta_{u_i^c} \Delta_{u_j} \frac{M_T}{v} \right\}$$

$$+ (i\eta u_i^c u_j) \left[\delta_{ij} \frac{m_{u_i}}{\sqrt{2}f} \left(\frac{s_\beta^2 - c_\beta^2}{s_\beta c_\beta} \right) + \delta_{i3} \Delta_{u_j} \frac{m_t}{v} V_{33}^{u*} \right] + \text{h.c.} \tag{B.47}$$

Note the flavor-changing couplings involving t^c from terms containing a δ_{i3}. Here we have introduced the notation $\delta_{u_i^c}$ for the mixings between u_i^c and T^c, which occur at order v^2/f^2. They are given explicitly by

$$\delta_{u^c} = -\frac{v}{M_T} \frac{f}{\sqrt{2}\Lambda} \left(\delta_u \lambda_u^{u^c u'} + \delta_c \lambda_u^{u^c c'} \right), \qquad \delta_{c^c} = -\frac{v}{M_T} \frac{f}{\sqrt{2}\Lambda} \left(\delta_u \lambda_u^{c^c u'} + \delta_c \lambda_u^{c^c c'} \right),$$

$$\delta_{t^c} = \frac{v}{M_T} \left\{ \frac{m_t}{v} V_{33}^{u*} \left[\Delta_t + \frac{v}{2\sqrt{2}f} \left(\frac{c_\beta^2 - s_\beta^2}{s_\beta c_\beta} \right) \right] - \frac{f}{\sqrt{2}\Lambda} \left(\delta_u \lambda_u^{t^c u'} + \delta_c \lambda_u^{t^c c'} \right) \right\}, \tag{B.48}$$

where $T^c = T_0^c - \delta_{u_i^c} u_{i0}^c$.

The couplings of scalars to a pair of SM down-type quarks (again ignoring right-handed quark mixing) are

$$\mathcal{L} = (Hd_i^c d_j) \left\{ \delta_{ij} \frac{-m_{d_i}}{v} \left[1 - \frac{v^2}{6f^2} \left(3 + \frac{s_\beta^4}{c_\beta^2} + \frac{c_\beta^4}{s_\beta^2} \right) \right] + \frac{v^2}{2f^2} \left[-\delta_{i1} \frac{m_d}{v} V_{11}^{d*} V_{j1}^{d*} - \delta_{i2} \frac{m_s}{v} V_{22}^{d*} V_{j2}^{d*} \right] \right.$$

$$+ \frac{v}{2\sqrt{2}f} \left(\frac{c_\beta^2 - s_\beta^2}{s_\beta c_\beta} \right) \left[-\delta_{i1} \Delta_{Dd_j} \frac{m_d}{v} V_{11}^{d*} - \delta_{i2} \Delta_{Sd_j} \frac{m_s}{v} V_{22}^{d*} \right]$$

$$\left. + \delta_{Dd_i^c} \Delta_{Dd_j} \frac{M_D}{v} + \delta_{Sd_i^c} \Delta_{Sd_j} \frac{M_S}{v} \right\}$$

$$+ (i\eta d_i^c d_j) \left[\delta_{ij} \frac{-m_{d_i}}{\sqrt{2}f} \left(\frac{s_\beta^2 - c_\beta^2}{s_\beta c_\beta} \right) + \delta_{i1} \Delta_{Dd_j} \frac{m_d}{v} V_{11}^{d*} + \delta_{i2} \Delta_{Sd_j} \frac{m_s}{v} V_{22}^{d*} \right] + \text{h.c.,} \tag{B.49}$$

where we have used (neglecting right-handed quark mixing)

$$\frac{\lambda_1^d \lambda_2^d f}{\sqrt{2} M_D} = -\frac{m_d}{v} V_{11}^{d*}, \qquad\qquad \frac{\lambda_1^s \lambda_2^s f}{\sqrt{2} M_S} = -\frac{m_s}{v} V_{22}^{d*}. \tag{B.50}$$

Note the flavor-changing couplings involving d^c (s^c) from terms containing a δ_{i1} (δ_{i2}). We also introduce the notation $\delta_{Dd_i^c}$, $\delta_{Sd_i^c}$ for the mixings between d_i^c and D^c, S^c, respectively, which occur at order v^2/f^2. They are given explicitly by

$$\delta_{Dd^c} = -\frac{v}{M_D}\left\{-\frac{m_d}{v}V_{11}^{d*}\left[\delta_{Dd} - \frac{v}{2\sqrt{2}f}\left(\frac{c_\beta^2 - s_\beta^2}{s_\beta c_\beta}\right)\right] + \frac{f}{\sqrt{2}\Lambda}\delta_{Db}\lambda_b^{dc}\right\},$$

$$\delta_{Ds^c} = -\frac{v}{M_D}\frac{f}{\sqrt{2}\Lambda}\delta_{Db}\lambda_b^{sc}, \qquad \delta_{Db^c} = -\frac{v}{M_D}\frac{f}{\sqrt{2}\Lambda}\delta_{Db}\lambda_b^{bc},$$

$$\delta_{Ss^c} = -\frac{v}{M_S}\left\{-\frac{m_s}{v}V_{22}^{d}\left[\delta_{Ss} - \frac{v}{2\sqrt{2}f}\left(\frac{c_\beta^2 - s_\beta^2}{s_\beta c_\beta}\right)\right] + \frac{f}{\sqrt{2}\Lambda}\delta_{Sb}\lambda_b^{sc}\right\},$$

$$\delta_{Sd^c} = -\frac{v}{M_S}\frac{f}{\sqrt{2}\Lambda}\delta_{Sb}\lambda_b^{dc}, \qquad \delta_{Sb^c} = -\frac{v}{M_S}\frac{f}{\sqrt{2}\Lambda}\delta_{Sb}\lambda_b^{bc}, \tag{B.51}$$

where $D^c = D_0^c - \delta_{Dd_i^c}d_{i0}^c$ and $S^c = S_0^c - \delta_{Sd_i^c}d_{i0}^c$.

B.2.4 Quark couplings to gauge bosons: anomaly-free embedding

The couplings of the heavy off-diagonal gauge bosons $X^\mp$, Y^0 and $\overline{Y}^0$ to quarks in the anomaly-free embedding were given in Table 4, neglecting flavor misalignment and CKM mixing. Allowing for the flavor misalignment, we have[8]

$$\begin{aligned}\mathcal{L}_{X,Y} = -\frac{g}{\sqrt{2}}&\left\{iX_\mu^- \bar{d}_i\gamma^\mu\left[V_{i3}^d T + \left(\Delta_{u_j}V_{i3}^d + \Delta_{Dd_i}^* V_{j1}^{u*} + \Delta_{Sd_i}^* V_{j2}^{u*}\right)u_j\right]\right.\\&+iX_\mu^+ \bar{u}_i\gamma^\mu V_{ij}^u D_j + iY_\mu^0 \bar{u}_i\gamma^\mu\left(V_{i3}^u T + \Delta_{u_k}V_{i3}^u u_k\right)\\&\left.+i\overline{Y}_\mu^0 \bar{d}_i\gamma^\mu\left[V_{ij}^d D_j + \left(\Delta_{Dd_k}V_{i1}^d + \Delta_{Sd_k}V_{i2}^d\right)d_k\right] + \text{h.c.}\right\}.\end{aligned} \tag{B.52}$$

The couplings of $W^\pm$ to quark pairs, keeping terms of order v^2/f^2 in interactions involving only SM particles and terms of order v/f in interactions involving one or more heavy particles, are

$$\begin{aligned}\mathcal{L}_W = -\frac{gW_\mu^+}{\sqrt{2}}&\left[\left(1 - \frac{1}{2}|\Delta_{u_i}|^2 - \frac{1}{2}|\Delta_{Dd_j}|^2 - \frac{1}{2}|\Delta_{Sd_j}|^2\right)V_{ij}^{\text{CKM}}\bar{u}_i\gamma^\mu d_j\right.\\&\left.-V_{ij}^{\text{CKM}}\Delta_{u_i}^* \overline{T}\gamma^\mu d_j - V_{ij}^{\text{CKM}}\Delta_{Dd_j}\bar{u}_i\gamma^\mu D - V_{ij}^{\text{CKM}}\Delta_{Sd_j}\bar{u}_i\gamma^\mu S + \text{h.c.}\right].\end{aligned} \tag{B.53}$$

The couplings of the Z' boson to quarks were also given in Table 4, neglecting flavor misalignment and CKM mixing. Allowing for the flavor misalignment, we find flavor-changing couplings for the left-handed quarks involving $V_{i3}^u V_{3j}^{u\dagger}$ in the up sector and $V_{i3}^d V_{3j}^{d\dagger}$ in the down sector:

$$\begin{aligned}\mathcal{L}_{Z'} \supset -\frac{g}{c_W}\frac{Z_\mu'}{\sqrt{3 - 4s_W^2}}&\left[\left(-\frac{1}{2} + \frac{2}{3}s_W^2\right)\left(\bar{u}_i\gamma^\mu u_i + \bar{d}_i\gamma^\mu d_i\right)\right.\\&\left.+\left(1 - s_W^2\right)\left(V_{i3}^u V_{3j}^{u\dagger}\bar{u}_i\gamma^\mu u_j + V_{i3}^d V_{3j}^{d\dagger}\bar{d}_i\gamma^\mu d_j\right)\right].\end{aligned} \tag{B.54}$$

---

[8]The SU(3) generators for the quarks of the first two generations, in the antifundamental $\bar{\mathbf{3}}$ representation, are given by $-T^{a*}$.

The couplings of the Z boson to quarks, including the corrections from mixing between Z and Z' and mixing between the TeV-scale quarks and their SM partners, are

$$
\begin{aligned}
\mathcal{L}_Z = -Z_\mu \frac{g}{c_W} \Bigg\{ & \left(J_3^\mu - s_W^2 J_Q^\mu \right) + \frac{1}{2} \left[-|\Delta_{u_i}|^2 \bar{u}_i \gamma^\mu u_i + \left(|\Delta_{Dd_i}|^2 + |\Delta_{Sd_i}|^2 \right) \bar{d}_i \gamma^\mu d_i \right] \\
& + \frac{\delta_Z}{\sqrt{3 - 4s_W^2}} \left[\left(-\frac{1}{2} + \frac{2}{3} s_W^2 \right) \left(\bar{u}_i \gamma^\mu u_i + \bar{d}_i \gamma^\mu d_i \right) - \frac{2}{3} s_W^2 \bar{u}_i^c \gamma^\mu u_i^c + \frac{1}{3} s_W^2 \bar{d}_i^c \gamma^\mu d_i^c \right. \\
& \left. + \left(1 - s_W^2 \right) \left(V_{i3}^u V_{3j}^{u\dagger} \bar{u}_i \gamma^\mu u_j + V_{i3}^d V_{3j}^{d\dagger} \bar{d}_i \gamma^\mu d_j \right) \right] \\
& + \frac{1}{2} \left[-\Delta_{u_i} \overline{T} \gamma^\mu u_i + \Delta_{Dd_i} \overline{D} \gamma^\mu d_i + \Delta_{Sd_i} \overline{S} \gamma^\mu d_i + \text{h.c.} \right] \Bigg\},
\end{aligned} \tag{B.55}
$$

where the leading-order coupling is given in terms of the standard fermion currents defined in Eq. (B.21). The Z boson couples to pairs of heavy quarks at order one through the electromagnetic current J_Q. Note the flavor-changing couplings induced by $Z - Z'$ mixing. The couplings of photons to fermions are given by the electromagnetic current as usual.

B.2.5 Constraints from flavor physics: anomaly-free embedding

The flavor-changing couplings of Z' to quark pairs can feed into low-energy observables, leading to potentially large flavor-changing neutral currents. The contributions of the anomaly-free fermion embedding to mixing in the neutral K, D, B, and B_s systems and the rare decays $B_{d,s} \to \mu^+ \mu^-$ and $B \to K \mu^+ \mu^-$ were summarized in Ref. [45] in the context of 3-3-1 models without the little Higgs mechanism. If the quark mixing matrices take a Fritzsch-like structure [46], $V_{ij}^{u,d} = \sqrt{m_j/m_i}$ ($i \geq j$), then the strongest bound on the Z' mass comes from B–$\bar{B}$ mixing [47] and requires $M_{Z'} > 10.5$ TeV [45]. The next-most-stringent constraint comes from B_s–$\bar{B}_s$ mixing [45] and requires $M_{Z'} > 5.0$ TeV. Clearly, the down quark mixing matrix must be more diagonal than the Fritzsch-like structure, in order to suppress flavor-changing effects in the down quark sector. In fact, one can choose $V_{i3}^d = \delta_{i3}$, so that the d couplings are flavor-diagonal; this *eliminates* flavor-changing effects in the down quark sector. The flavor-changing effects are then pushed into the up sector. The u and d couplings to Z' can never both be flavor-diagonal because they are related by the CKM matrix [Eq. (B.32)].

B.2.6 Quark masses and mixing: universal embedding

In the universal embedding, the quark Yukawa Lagrangian is given for all three generations by

$$
\mathcal{L} = \lambda_1^{un} i u_1^{nc} \Phi_1^\dagger Q_n + \lambda_2^{un} i u_2^{nc} \Phi_2^\dagger Q_n + \frac{\lambda_d^{mn}}{\Lambda} i d_m^c \epsilon_{ijk} \Phi_1^i \Phi_2^j Q_n^k + \text{h.c.}, \tag{B.56}
$$

where $m, n = 1, 2, 3$ are generation indexes; $i, j, k = 1, 2, 3$ are SU(3) indexes; d_m^c runs over all the down-type conjugate quarks (d^c, s^c, b^c); and $u_{1,2}^{nc}$ are linear combinations of the up-type conjugate quarks as given in Eqs. (B.59) and (B.61) below.

The physics of the down quark sector in the universal embedding is exactly analogous to that of the charged leptons. The down quark Higgs couplings are given by

$$\mathcal{L} = -\frac{m_{d_i}}{v} y_d (H d_i^c d_i) + \text{h.c.}, \qquad y_d = 1 - \frac{v^2}{6f^2} \left(3 + \frac{c_\beta^4}{s_\beta^2} + \frac{s_\beta^4}{c_\beta^2} \right), \qquad (\text{B.57})$$

and their couplings to η are given by

$$\mathcal{L} = -\frac{m_{d_i}}{v} \frac{v}{4\sqrt{2}f} \left(\frac{c_\beta^2 - s_\beta^2}{s_\beta c_\beta} \right) (i\eta d_i^c d_i) + \text{h.c.} \qquad (\text{B.58})$$

In the up sector, the f vevs generate mass terms for the three heavy quarks with charge $+2/3$. The three states

$$U_n^c = \frac{\lambda_1^{un} c_\beta u_1^{nc} + \lambda_2^{un} s_\beta u_2^{nc}}{\sqrt{(\lambda_1^{un})^2 c_\beta^2 + (\lambda_2^{un})^2 s_\beta^2}}, \qquad (\text{B.59})$$

marry the three U_n states, giving them masses of

$$M_{U_n} = f\sqrt{(\lambda_1^{un})^2 c_\beta^2 + (\lambda_2^{un})^2 s_\beta^2} \qquad (\text{B.60})$$

and leaving the orthogonal combinations of u_1^{nc} and u_2^{nc} massless:

$$u_n^c = \frac{-\lambda_2^{un} s_\beta u_1^{nc} + \lambda_1^{un} c_\beta u_2^{nc}}{\sqrt{(\lambda_1^{un})^2 c_\beta^2 + (\lambda_2^{un})^2 s_\beta^2}}. \qquad (\text{B.61})$$

Note that the Yukawa Lagrangian in Eq. (B.56) does *not* generate a misalignment between the SM up quark mass eigenstates and the heavy quarks. Such a misalignment could be generated by adding an additional dimension-5 operator,

$$\frac{\lambda_u^{mn}}{\Lambda} i u_m^c \epsilon_{ijk} \Phi_1^{*i} \Phi_2^{*j} Q_n^k + \text{h.c.}, \qquad (\text{B.62})$$

to generate off-diagonal entries in the up quark mass matrix. We ignore this possibility here. The usual CKM matrix is generated by the off-diagonal entries in the down quark mass matrix, controlled by λ_d^{mn}.

After EWSB, the up quark mass terms are

$$\mathcal{L}_{\text{up mass}} = -M_{U_n} U_n^c U_n + \frac{v}{\sqrt{2}} \frac{s_\beta c_\beta [(\lambda_1^{un})^2 - (\lambda_2^{un})^2]}{\sqrt{(\lambda_1^{un})^2 c_\beta^2 + (\lambda_2^{un})^2 s_\beta^2}} U_n^c u_n$$

$$-\frac{v}{\sqrt{2}} \frac{\lambda_1^{un} \lambda_2^{un}}{\sqrt{(\lambda_1^{un})^2 c_\beta^2 + (\lambda_2^{un})^2 s_\beta^2}} u_n^c u_n + \text{h.c.} \qquad (\text{B.63})$$

These terms lead to mixing between the heavy quarks and their corresponding SM quark partners. As usual, we use the subscript 0 to denote SU(3) states; fields with no subscript denote the mass eigenstates after the mixing induced by EWSB. We can rewrite the SU(3) state U_{m0} in terms of the mass eigenstate U_m and the SM fermion u_m as

$$U_{m0} = U_m + \delta_{u_m} u_m, \qquad u_{m0} = \left(1 - \frac{1}{2}\delta_{u_m}^2 \right) u_m - \delta_{u_m} U_m, \qquad (\text{B.64})$$

where

$$\delta_{u_m} = \frac{v}{\sqrt{2}f} \frac{s_\beta c_\beta[(\lambda_1^{um})^2 - (\lambda_2^{um})^2]}{[(\lambda_1^{um})^2 c_\beta^2 + (\lambda_2^{um})^2 s_\beta^2]}. \tag{B.65}$$

The masses of the SM up-type quarks are given to leading order by

$$\frac{\lambda_1^{um} \lambda_2^{um} f}{\sqrt{2} M_{U_m}} = \frac{m_{u_m}}{v}. \tag{B.66}$$

The small mass of the u (c) quark requires one of the couplings $\lambda_{1,2}^{u1}$ ($\lambda_{1,2}^{u2}$) to be very small. We choose the small coupling to be λ_1^{u1} (λ_1^{u2}) so that the mixing effects in the up-quark sector are suppressed in the same $t_\beta > 1$ limit as the mixing effects in the neutrino sector. We then have,

$$M_U = f\lambda_U s_\beta, \qquad M_C = f\lambda_C s_\beta, \qquad M_T = f\sqrt{\lambda_1^2 c_\beta^2 + \lambda_2^2 s_\beta^2}, \tag{B.67}$$

where we define $\lambda_U = \lambda_2^{u1}$, $\lambda_C = \lambda_2^{u2}$, $\lambda_1 = \lambda_1^{u3}$, and $\lambda_2 = \lambda_2^{u3}$. For the mixing angles we also have

$$\delta_u = \delta_c = \frac{-v}{\sqrt{2} t_\beta f} = \delta_\nu, \qquad \delta_t = \frac{vf}{\sqrt{2} M_T^2} s_\beta c_\beta(\lambda_1^2 - \lambda_2^2). \tag{B.68}$$

We now write the up quark couplings to scalars. The couplings of heavy quark-partner pairs are given by

$$\mathcal{L} = -(i\eta U^c U)\frac{c_\beta}{\sqrt{2}}\lambda_U - (i\eta C^c C)\frac{c_\beta}{\sqrt{2}}\lambda_C + (i\eta T^c T)s_\beta c_\beta(\lambda_1^2 - \lambda_2^2)\frac{f}{\sqrt{2} M_T}$$
$$+ (HT^c T)\frac{v}{f}\left[(\lambda_1^2 s_\beta^2 + \lambda_2^2 c_\beta^2)\frac{f}{2M_T} - s_\beta^2 c_\beta^2(\lambda_1^2 - \lambda_2^2)^2\frac{f^3}{2M_T^3}\right] + \text{h.c.} \tag{B.69}$$

One would naively expect an $HU_m^c U_m$ coupling for the first two generations at order v/f coming from replacing one Higgs field by its vev in the $HHU_m^c U_m$ term that is generated by the expansion of the nonlinear sigma model; however, this term is exactly canceled by the contribution from $HU_m^c u_m$ after $u - U$ mixing in the first two generations if the up and charm quark masses are neglected.

The leading-order couplings of the scalars to one heavy quark partner and one SM up-type quark are

$$\mathcal{L} = -(HU^c u)\frac{c_\beta \lambda_U}{\sqrt{2}} - (HC^c c)\frac{c_\beta \lambda_C}{\sqrt{2}} + (HT^c t)(\lambda_1^2 - \lambda_2^2)\frac{s_\beta c_\beta f}{\sqrt{2} M_T} - (i\eta t^c T)\frac{m_t}{v} + \text{h.c.}, \tag{B.70}$$

where in the η couplings we neglect m_u and m_c in the couplings of the first two generations and neglect the v/f suppressed coupling of the third generation. These couplings will lead to the decays $U_m \to u_m H$ and $T \to t\eta$.

The couplings of scalars to a pair of SM up-type quarks are

$$\mathcal{L} = (Hu_i^c u_i)\left\{\frac{-m_{u_i}}{v}\left[1 - \frac{v^2}{6f^2}\left(\frac{s_\beta^4}{c_\beta^2} + \frac{c_\beta^4}{s_\beta^2}\right) - \delta_{u_i}\frac{v}{2\sqrt{2}f}\left(\frac{c_\beta^2 - s_\beta^2}{s_\beta c_\beta}\right)\right] + \frac{M_{U_i}}{v}\delta_{u_i}\delta_{u_i^c}\right\}$$
$$+ (i\eta u_i^c u_i)\frac{m_{u_i}}{v}\left[\frac{v}{\sqrt{2}f}\left(\frac{s_\beta^2 - c_\beta^2}{s_\beta c_\beta}\right) + \delta_{u_i}\right] + \text{h.c.}, \tag{B.71}$$

where the mixing between u_i^c and U_i^c at order v^2/f^2 is given by $U_i^c = U_{i0}^c - \delta_{u_i^c} u_{i0}^c$, with

$$\delta_{u_i^c} = \frac{m_{u_i}}{M_{U_i}} \left[\delta_{u_i} + \frac{v}{2\sqrt{2}f} \left(\frac{c_\beta^2 - s_\beta^2}{s_\beta c_\beta} \right) \right]. \tag{B.72}$$

B.2.7 Quark couplings to gauge bosons: universal embedding

The couplings of the Z' boson to quarks in the universal embedding were given in Table 4. These couplings are purely flavor-diagonal in the universal fermion embedding. The couplings of the heavy off-diagonal gauge bosons X^- and Y^0 to quarks in the universal embedding were also given in Table 4, neglecting CKM mixing. Keeping the full CKM dependence, we have

$$\mathcal{L}_{X,Y} = -\frac{g}{\sqrt{2}} \left[iX_\mu^- \bar{d}_i \gamma^\mu \left(V_{ji}^{\text{CKM}*} U_j + \delta_{u_j} V_{ji}^{\text{CKM}*} u_j \right) + iY_\mu^0 \bar{u}_i \gamma^\mu \left(U_i + \delta_{u_i} u_i \right) + \text{h.c.} \right]. \tag{B.73}$$

The couplings of $W^\pm$ to quark pairs, keeping terms of order v^2/f^2 in interactions involving only SM particles and terms of order v/f in interactions involving one or more heavy particles, are

$$\mathcal{L}_W = -\frac{gW_\mu^+}{\sqrt{2}} \left[\left(1 - \frac{1}{2} \delta_{u_i}^2 \right) V_{ij}^{\text{CKM}} \bar{u}_i \gamma^\mu d_j - \delta_{u_i} V_{ij}^{\text{CKM}} \bar{U}_i \gamma^\mu d_j + \text{h.c.} \right]. \tag{B.74}$$

The couplings of the Z boson to quarks, including the corrections from mixing between Z and Z' and mixing between the TeV-scale quarks and their SM partners, are

$$\mathcal{L}_Z = -\frac{gZ_\mu}{c_W} \left\{ \left(J_3^\mu - s_W^2 J_Q^\mu \right) - \frac{1}{2} \delta_{u_i}^2 \bar{u}_i \gamma^\mu u_i - \frac{1}{2} \left[\delta_{u_i} \overline{U}_i \gamma^\mu u_i + \text{h.c.} \right] \right. \tag{B.75}$$

$$\left. + \frac{\delta_Z}{\sqrt{3 - 4s_W^2}} \left[\left(\frac{1}{2} - \frac{1}{3} s_W^2 \right) \left(\bar{u}_i \gamma^\mu u_i + \bar{d}_i \gamma^\mu d_i \right) - \frac{2}{3} s_W^2 \bar{u}_i^c \gamma^\mu u_i^c + \frac{1}{3} s_W^2 \bar{d}_i^c \gamma^\mu d_i^c \right] \right\},$$

where the leading-order coupling is given in terms of the usual fermion currents J_3 and J_Q defined in Eq. (B.21). The Z boson couples to pairs of heavy quarks U_i at order one through the electromagnetic current J_Q. The couplings of photons to fermions are given by the electromagnetic current as usual.

B.3 Higgs potential

In this section we describe the generation of the Higgs potential.[9] Additional details can be found in Refs. [9, 41]. We start with the Coleman-Weinberg potential that is generated by loops of gauge bosons and fermions in the running down from the cutoff scale Λ. Above the global symmetry breaking scale f, only operators that are symmetric under the global $[\text{SU}(3)\times\text{U}(1)]^2$ symmetry are generated by the running. The three allowed operators up to dimension four are

$$\Phi_1^\dagger \Phi_1, \qquad \Phi_2^\dagger \Phi_2, \qquad |\Phi_1^\dagger \Phi_2|^2. \tag{B.76}$$

---

[9]We thank Martin Schmaltz for very helpful discussions.

The first two of these operators are just constants and do not involve the Goldstone bosons. We therefore focus on the third operator. Expanding it in terms of the Goldstone bosons to fourth order gives

$$|\Phi_1^\dagger \Phi_2|^2 = f^4 s_\beta^2 c_\beta^2 - f^2 h^\dagger h + \frac{1}{3 s_\beta^2 c_\beta^2}(h^\dagger h)^2 + \frac{3}{32 s_\beta^2 c_\beta^2} h^\dagger h \eta^2 + \mathcal{O}(\phi^6). \tag{B.77}$$

Running below the global symmetry breaking scale f can give contributions to the Coleman-Weinberg potential that are not proportional to $|\Phi_1^\dagger \Phi_2|^2$. These contributions will contain logs of the ratios of masses-squared of f-scale particles and the corresponding SM particles. They will therefore be calculable, i.e., independent of cutoff-scale physics.

The Coleman-Weinberg potential from the X^-, Y^0 and W^+ gauge bosons is,

$$\begin{aligned} V_2 &= \frac{3}{64\pi^2} g^4 \log(\Lambda^2/M_X^2) f^2 (h^\dagger h) \\ V_4 &= \frac{3}{64\pi^2} g^4 \log(\Lambda^2/M_X^2) \left[-\frac{1}{3 s_\beta^2 c_\beta^2}(h^\dagger h)^2 - \frac{3}{32 s_\beta^2 c_\beta^2}(h^\dagger h)\eta^2 \right] \\ &\quad - \frac{3}{128\pi^2} g^4 \log(M_X^2/M_W^2)(h^\dagger h)^2. \end{aligned} \tag{B.78}$$

Here V_2 and the first line of V_4 come from running between Λ and M_X and are proportional to $|\Phi_1^\dagger \Phi_2|^2$, while the second line of V_4 comes from running between M_X and M_W. The running below M_X contributes only a term involving $(h^\dagger h)^2$. It does not contribute any terms involving η since there is no coupling of W boson pairs to $h\eta$.

The Coleman-Weinberg potential from the Z' and Z gauge bosons is,

$$\begin{aligned} V_2 &= \frac{3}{32\pi^2} g^4 \frac{1+t_W^2}{3-t_W^2} \log(\Lambda^2/M_{Z'}^2) f^2 (h^\dagger h) \\ V_4 &= \frac{3}{32\pi^2} g^4 \frac{1+t_W^2}{3-t_W^2} \log(\Lambda^2/M_{Z'}^2) \left[-\frac{1}{3 s_\beta^2 c_\beta^2}(h^\dagger h)^2 - \frac{3}{32 s_\beta^2 c_\beta^2}(h^\dagger h)\eta^2 \right] \\ &\quad - \frac{3}{256\pi^2} g^4 (1+t_W^2)^2 \log(M_{Z'}^2/M_Z^2)(h^\dagger h)^2. \end{aligned} \tag{B.79}$$

Again, V_2 and the first line of V_4 come from running between Λ and $M_{Z'}$ and are proportional to $|\Phi_1^\dagger \Phi_2|^2$, while the second line of V_4 comes from running between $M_{Z'}$ and M_Z. The running below $M_{Z'}$ contributes only a term involving $(h^\dagger h)^2$. It does not contribute any terms involving η since there is no coupling of Z boson pairs to $h\eta$.

The Coleman-Weinberg potential from the fermions can in principle come from loops of any fermion with an order-one Yukawa coupling. However, due to the feature of collective breaking in the model, the order-one Yukawa couplings that give mass to the neutrino partners and the quark partners of the first two generations do not contribute to the terms of the Coleman-Weinberg potential involving the Goldstone bosons (neglecting the tiny Yukawa couplings of the quarks of the first two generations). The only significant contribution is then due to the top quark and its partner T. In what follows we neglect the mixing between quark generations. The Coleman-Weinberg potential from the top quark

and its partner T is,

$$V_2 = -\frac{3}{8\pi^2}\lambda_t^2 M_T^2 \log(\Lambda^2/M_T^2)(h^\dagger h)$$

$$V_4 = -\frac{3}{8\pi^2}\lambda_t^2\frac{M_T^2}{f^2}\log(\Lambda^2/M_T^2)\left[-\frac{1}{3s_\beta^2 c_\beta^2}(h^\dagger h)^2 - \frac{3}{32s_\beta^2 c_\beta^2}(h^\dagger h)\eta^2\right]$$

$$+\frac{3}{16\pi^2}\lambda_t^4\log(M_T^2/m_t^2)(h^\dagger h)^2, \tag{B.80}$$

where $\lambda_t \equiv \lambda_1^t\lambda_2^t f/M_T \simeq \sqrt{2}m_t/v$. Again, V_2 and the first line of V_4 come from running between Λ and M_T and are proportional to $|\Phi_1^\dagger\Phi_2|^2$, while the second line of V_4 comes from running between M_T and m_t. The running below M_T contributes only a term involving $(h^\dagger h)^2$. It does not contribute any terms involving η since there is no coupling of top quark pairs to $h\eta$ or η^2.

Collecting terms, we can write the Coleman-Weinberg potential as follows:

$$V = -m^2 h^\dagger h + \lambda(h^\dagger h)^2 + \lambda' h^\dagger h\eta^2, \tag{B.81}$$

where

$$m^2 = \frac{3}{8\pi^2}\left[\lambda_t^2 M_T^2\log(\Lambda^2/M_T^2) - \frac{g^2}{4}M_X^2\log(\Lambda^2/M_X^2) - \frac{g^2}{8}(1+t_W^2)M_{Z'}^2\log(\Lambda^2/M_{Z'}^2)\right]$$

$$\lambda = \frac{1}{3s_\beta^2 c_\beta^2}\frac{m^2}{f^2} + \frac{3}{16\pi^2}\left[\lambda_t^4\log(M_T^2/m_t^2) - \frac{g^4}{8}\log(M_X^2/M_W^2) - \frac{g^4}{16}(1+t_W^2)^2\log(M_{Z'}^2/M_Z^2)\right]$$

$$\lambda' = \frac{3}{32s_\beta^2 c_\beta^2}\frac{m^2}{f^2}. \tag{B.82}$$

In the expression for m^2, in principle the cutoff Λ in the term generated by quark loops can be different from the cutoff Λ in the two terms generated by gauge boson loops, because the physics that cuts off the quark loops can be different from the physics that cuts off the gauge boson loops. After EWSB, η gets a small positive mass-squared of order $m_H^2 v^2/f^2$ from the λ' term. The Higgs vev and mass are given by

$$v^2 = m^2/\lambda = (246\text{ GeV})^2, \qquad m_H^2 = 2m^2 = 2\lambda v^2. \tag{B.83}$$

It turns out that this m_H is *too small*, because the quartic coupling λ is not big enough compared to m^2.

Following Ref. [9], this problem can be fixed by adding a new operator, $\Phi_1^\dagger\Phi_2 + \text{h.c.}$, to the scalar potential with a coefficient $-\mu^2$ set by hand. This operator breaks the global $SU(3)^2$ down to the diagonal $SU(3)$ while preserving the gauged $SU(3)$. Expanding this operator to fourth order in the Goldstone bosons gives

$$\Phi_1^\dagger\Phi_2 + \text{h.c.} = 2f^2 s_\beta c_\beta + \frac{1}{f^2 s_\beta c_\beta}\left[-f^2(h^\dagger h) - \frac{f^2\eta^2}{2} + \frac{(h^\dagger h)^2}{12s_\beta^2 c_\beta^2} + \frac{3(h^\dagger h)\eta^2}{32s_\beta^2 c_\beta^2} + \frac{\eta^4}{48s_\beta^2 c_\beta^2}\right]. \tag{B.84}$$

Because the $(h^\dagger h)$ and $(h^\dagger h)^2$ terms in this operator have different relative coefficients than in the original operator $|\Phi_1^\dagger\Phi_2|^2$, it can be used to cancel off part of the $m^2 h^\dagger h$ term

without canceling too much of the $\lambda(h^\dagger h)^2$ term. Adding the term $-\mu^2(\Phi_1^\dagger\Phi_2 + \text{h.c.})$ to the potential gives

$$V = -m_{\text{new}}^2 h^\dagger h + \frac{1}{2}m_\eta^2\eta^2 + \lambda_{\text{new}}(h^\dagger h)^2 + \lambda_{\text{new}}' h^\dagger h\eta^2 + \lambda_{\text{new}}''\eta^4, \qquad \text{(B.85)}$$

where

$$m_{\text{new}}^2 = m^2 - \frac{\mu^2}{s_\beta c_\beta}, \qquad\qquad m_\eta^2 = \frac{\mu^2}{s_\beta c_\beta},$$

$$\lambda_{\text{new}} = \frac{1}{3s_\beta^2 c_\beta^2}\frac{m_{\text{new}}^2}{f^2} + \frac{1}{4s_\beta^3 c_\beta^3}\frac{\mu^2}{f^2}$$

$$+ \frac{3}{16\pi^2}\left[\lambda_t^4\log(M_T^2/m_t^2) - \frac{g^4}{8}\log(m_X^2/m_W^2) - \frac{g^4}{16}(1 + t_W^2)^2\log(m_{Z'}^2/m_Z^2)\right],$$

$$\lambda_{\text{new}}' = \frac{3}{32s_\beta^2 c_\beta^2}\frac{m_{\text{new}}^2}{f^2}, \qquad\qquad \lambda_{\text{new}}'' = -\frac{1}{48s_\beta^3 c_\beta^3}\frac{\mu^2}{f^2}. \qquad \text{(B.86)}$$

Note that this term has also given rise to a mass-squared term for η and an η^4 coupling. The η mass m_η is now of order μ, parametrically larger than the η mass term generated by EWSB.

References

[1] N. Arkani-Hamed, A. G. Cohen and H. Georgi, Phys. Lett. B **513**, 232 (2001) [arXiv:hep-ph/0105239].

[2] N. Arkani-Hamed, A. G. Cohen, E. Katz, A. E. Nelson, T. Gregoire and J. G. Wacker, JHEP **0208**, 021 (2002) [arXiv:hep-ph/0206020].

[3] N. Arkani-Hamed, A. G. Cohen, E. Katz and A. E. Nelson, JHEP **0207**, 034 (2002) [arXiv:hep-ph/0206021].

[4] I. Low, W. Skiba and D. Smith, Phys. Rev. D **66**, 072001 (2002) [arXiv:hep-ph/0207243].

[5] D. E. Kaplan and M. Schmaltz, JHEP **0310**, 039 (2003) [arXiv:hep-ph/0302049].

[6] S. Chang and J. G. Wacker, Phys. Rev. D **69**, 035002 (2004) [arXiv:hep-ph/0303001].

[7] W. Skiba and J. Terning, Phys. Rev. D **68**, 075001 (2003) [arXiv:hep-ph/0305302].

[8] S. Chang, JHEP **0312**, 057 (2003) [arXiv:hep-ph/0306034].

[9] M. Schmaltz, JHEP **0408**, 056 (2004) [arXiv:hep-ph/0407143].

[10] S. Chang and H. J. He, Phys. Lett. B **586**, 95 (2004) [arXiv:hep-ph/0311177].

[11] A. E. Nelson, arXiv:hep-ph/0304036; E. Katz, J. y. Lee, A. E. Nelson and D. G. E. Walker, JHEP **0510**, 088 (2005) [arXiv:hep-ph/0312287]; M. Piai, A. Pierce and J. Wacker, arXiv:hep-ph/0405242; D. E. Kaplan, M. Schmaltz and W. Skiba, Phys. Rev. D **70**, 075009 (2004) [arXiv:hep-ph/0405257]; P. Batra and D. E. Kaplan, JHEP **0503**, 028 (2005) [arXiv:hep-ph/0412267]; J. Thaler and I. Yavin, JHEP **0508**, 022 (2005) [arXiv:hep-ph/0501036].

[12] G. Burdman, M. Perelstein and A. Pierce, Phys. Rev. Lett. **90**, 241802 (2003) [Erratum-ibid. **92**, 049903 (2004)] [arXiv:hep-ph/0212228].

[13] T. Han, H. E. Logan, B. McElrath and L. T. Wang, Phys. Rev. D **67**, 095004 (2003) [arXiv:hep-ph/0301040].

[14] M. Perelstein, M. E. Peskin and A. Pierce, Phys. Rev. D **69**, 075002 (2004) [arXiv:hep-ph/0310039].

[15] G. Azuelos *et al.*, Eur. Phys. J. C **39S2**, 13 (2005) [arXiv:hep-ph/0402037].

[16] J. E. Garcia [ATLAS Collaboration], arXiv:hep-ph/0405156.

[17] H. C. Cheng and I. Low, JHEP **0309**, 051 (2003) [arXiv:hep-ph/0308199];

[18] I. Low, JHEP **0410**, 067 (2004) [arXiv:hep-ph/0409025].

[19] H. C. Cheng and I. Low, JHEP **0408**, 061 (2004) [arXiv:hep-ph/0405243].

[20] J. Hubisz and P. Meade, Phys. Rev. D **71**, 035016 (2005) [arXiv:hep-ph/0411264].

[21] C. Csaki, J. Hubisz, G. D. Kribs, P. Meade and J. Terning, Phys. Rev. D **68**, 035009 (2003) [arXiv:hep-ph/0303236].

[22] O. C. W. Kong, arXiv:hep-ph/0307250; J. Korean Phys. Soc. **45**, S404 (2004) [arXiv:hep-ph/0312060].

[23] M. Singer, J. W. F. Valle and J. Schechter, Phys. Rev. D **22**, 738 (1980); R. Foot, H. N. Long and T. A. Tran, Phys. Rev. D **50**, 34 (1994) [arXiv:hep-ph/9402243].

[24] R. A. Diaz, R. Martinez and F. Ochoa, Phys. Rev. D **72**, 035018 (2005) [arXiv:hep-ph/0411263].

[25] C. Csaki, J. Hubisz, G. D. Kribs, P. Meade and J. Terning, Phys. Rev. D **67**, 115002 (2003) [arXiv:hep-ph/0211124].

[26] J. L. Hewett, F. J. Petriello and T. G. Rizzo, JHEP **0310**, 062 (2003) [arXiv:hep-ph/0211218].

[27] M. C. Chen and S. Dawson, Phys. Rev. D **70**, 015003 (2004) [arXiv:hep-ph/0311032].

[28] R. Barbieri, A. Pomarol, R. Rattazzi and A. Strumia, Nucl. Phys. B **703**, 127 (2004) [arXiv:hep-ph/0405040].

[29] G. Marandella, C. Schappacher and A. Strumia, Phys. Rev. D **72**, 035014 (2005) [arXiv:hep-ph/0502096].

[30] Z. Han and W. Skiba, Phys. Rev. D **72**, 035005 (2005) [arXiv:hep-ph/0506206].

[31] W. Skiba, private communication.

[32] J. F. Gunion, H. E. Logan, B. McElrath and D. Rainwater, unpublished.

[33] B. A. Dobrescu and C. T. Hill, Phys. Rev. Lett. **81**, 2634 (1998) [arXiv:hep-ph/9712319].

[34] R. S. Chivukula, B. A. Dobrescu, H. Georgi and C. T. Hill, Phys. Rev. D **59**, 075003 (1999) [arXiv:hep-ph/9809470].

[35] H. Collins, A. K. Grant and H. Georgi, Phys. Rev. D **61**, 055002 (2000) [arXiv:hep-ph/9908330]; H. J. He, C. T. Hill and T. M. P. Tait, Phys. Rev. D **65**, 055006 (2002) [arXiv:hep-ph/0108041].

[36] F. Gursey, P. Ramond and P. Sikivie, Phys. Lett. B **60**, 177 (1976); F. Gursey and M. Serdaroglu, Lett. Nuovo Cim. **21**, 28 (1978); J. L. Hewett and T. G. Rizzo, Phys. Rept. **183**, 193 (1989) and references therein.

[37] J. C. Pati and A. Salam, Phys. Rev. D **10**, 275 (1974); R. N. Mohapatra and J. C. Pati, Phys. Rev. D **11**, 566 (1975); G. Senjanovic and R. N. Mohapatra, Phys. Rev. D **12**, 1502 (1975); R. E. Marshak and R. N. Mohapatra, Phys. Lett. B **91**, 222 (1980).

[38] M. Dittmar, A. S. Nicollerat and A. Djouadi, Phys. Lett. B **583**, 111 (2004) [arXiv:hep-ph/0307020].

[39] P. Langacker, R. W. Robinett and J. L. Rosner, Phys. Rev. D **30**, 1470 (1984); V. D. Barger, N. G. Deshpande, J. L. Rosner and K. Whisnant, Phys. Rev. D **35**, 2893 (1987); J. L. Rosner, Phys. Rev. D **54**, 1078 (1996) [arXiv:hep-ph/9512299].

[40] M. Dittmar, Phys. Rev. D **55**, 161 (1997) [arXiv:hep-ex/9606002].

[41] W. Kilian, D. Rainwater and J. Reuter, Phys. Rev. D **71**, 015008 (2005) [arXiv:hep-ph/0411213].

[42] C. Kilic and R. Mahbubani, JHEP **0407**, 013 (2004) [arXiv:hep-ph/0312053].

[43] T. Gregoire and J. G. Wacker, JHEP **0208**, 019 (2002) [arXiv:hep-ph/0206023].

[44] F. del Aguila, M. Masip and J. L. Padilla, Phys. Lett. B **627**, 131 (2005) [arXiv:hep-ph/0506063].

[45] J. A. Rodriguez and M. Sher, Phys. Rev. D **70**, 117702 (2004) [arXiv:hep-ph/0407248].

[46] D. Gomez Dumm, F. Pisano and V. Pleitez, Mod. Phys. Lett. A **9**, 1609 (1994).

[47] H. N. Long and V. T. Van, J. Phys. G **25**, 2319 (1999) [arXiv:hep-ph/9909302].